LONG-RANGE NEURAL SYNCHRONIZATION IN ATTENTION AND PERCEPTUAL CONSCIOUSNESS

by

Sam McLeod Doesburg

H.B.Sc., University of Toronto, 2002

A THESIS SUBMITTED IN PARTIAL FULFILLMENT OF THE REQUIREMENTS FOR THE DEGREE OF

DOCTOR OF PHILOSOPHY

in

The Faculty of Graduate Studies

(Neuroscience)

THE UNIVERSITY OF BRITISH COLUMBIA

(Vancouver)

April 2008

ABSTRACT

Cognition is dynamic and complex, requiring specific sets of brain areas to cooperate for specific tasks. Neural synchronization is a proposed mechanism for transient functional integration of specific neural populations, enabling feature flexible binding and dynamic assignment of functional connectivity in the brain according to task demands. This thesis addresses the role of neural synchronization in selective attention and perceptual consciousness. The goals of this thesis are to test the hypothesis that synchronization between brain regions is relevant to network dynamics in selective attention and for perceptual organization, and to elucidate the function of synchronization in different frequency ranges.

Using a selective visuospatial cuing paradigm it is shown that deploying attention to one visual hemifield yields transient long-distance gamma-band synchronization between contralateral visual cortex and other, widespread, brain regions. This is interpreted as a mechanism for establishing anticipatory biasing of communication in the cortex. Long-distance gamma synchrony, moreover, is periodically 'refreshed' at a theta rate, possibly serving to maintain this gamma network. While local alpha-band activity was found to be greater ipsilateral to the attended visual hemifield, alpha-band synchronization between primary visual cortex and higher visual areas was greater contralateral to attended locations. This suggests that local alpha synchrony is relevant for inhibition, while long-range alpha synchronization enacts functional coupling.

The onset of a new conscious percept during binocular rivalry coincides with large-scale gamma-band synchronization which recurs at a theta rate. This suggests that gamma synchronization integrates features into a unified conscious percept while the theta cycle maintains that network. Using an audiovisual speech integration paradigm it is shown that large-scale gamma synchronization is greater when incongruence is detected between auditory and visual streams. This highlights an important distinction: neural synchronization reflects neural integration, not perceptual integration. Perceptual integration typically requires neural integration (feature binding), however, in this case detection of audiovisual mismatches requires cooperation within a distributed network, whereas audiovisual speech integration is largely accomplished in superior temporal cortex.

These studies indicate that long-distance gamma synchronization establishes neural integration, the theta cycle maintains gamma synchronous networks, and local and long-range alpha synchrony reflect sustained inhibition and functional coupling mechanisms, respectively.

TABLE OF CONTENTS

ABSTRACT.....ii
TABLE OF CONTENTS.....iii
LIST OF TABLES.....vi
LIST OF FIGURES.....vii
ACKNOWLEDGEMENTS.....ix
DEDICATION.....x
CO-AUTHORSHIP STATEMENT.....xi

CHAPTER 1: INTRODCTION.....1

1.1 Neural Synchronization and Integration: an Historical Review.....1
1.2 Thesis Overview.....10
1.3 References.....19

CHAPTER 2: LARGE-SCALE GAMMA-BAND PHASE SYNCHRONIZATION AND SELECTIVE ATTENTION.....25

2.1 Abstract.....25
2.2 Introduction.....26
2.3 Methods.....29
2.3.1 Subjects and Task.....29
2.3.2 Synchrony Analysis.....32
2.3.3 ERP Analysis.....36
2.4 Results.....38
2.4.1 Phase Synchronization.....38
2.4.2 Event-Related Potentials.....44
2.5 Discussion.....48
2.5.1 General Discussion.....48
2.5.2 Gamma-Band Phase Synchronization.....49
2.5.3 Alpha-Band Amplitude Reduction.....53
Beta-Band Attention Network.....56
2.6 Appendix: Volume Conduction.....57
2.7 Supplementary Material A: Synchronization at Other Frequencies..63
2.7.1 Introduction.....63
2.6.2 Part a) Lateralized Gamma Synchronization at Frequencies near 39 Hz.....65
2.6.3 Part b) Synchronization in Other Frequency Ranges 68
2.6.4 Part c) Long-range Desynchronization Occurring After Cue Onset.....70
2.6.5 Part d) SCD Topography.....71
2.8 Supplementary Material B: Individual PLV Data.....73
2.9 Supplementary Material C: ERP Results for Subjects used in PLV Analysis.....79
2.10 References.....83

CHAPTER 3A: LONG-DISTANCE ALPHA-BAND MEG SYNCHRONIZATION ANDSELECTIVE ATTENTION.....91

3.1 Abstract.....91
3.2 Introduction.....91
3.3 Methods.....93
3.4 Results.....94
3.5 Discussion.....98

CHAPTER 3B: LONG-DISTANCE PHASE SYNCHRONIZATION BETWEEN ALPHA-BAND SOURCES.....100

3.6 Abstract.....100
3.7 Introduction.....100
3.8 Method.....102
3.8.1 Task.....102
3.8.2 MEG Recording and SAM Source Analysis.....102
3.8.3 Synchronization Analysis.....103
3.9 Results.....104
3.10 Discussion.....108
3.11 References.....110

CHAPTER 4: ANTICIPATORY HEMISPHERIC BIASING IN ATTENTION: OCCIPITAL-PARIETAL ALPHA-BAND SYNCHRONIZATION.....112

4.1 Abstract.....112
4.2 Introduction.....113
4.3 Method.....115
4.3.1 Data Set.....115
4.3.2 Phase Synchronization Analysis.....116
4.4 Results.....119
4.5 Discussion.....123
4.6 References.....125

CHAPTER 5: INCREASED GAMMA-BAND SYNCHRONY PRECEDES SWITCHING OF CONSCIOUS PERCEPTUAL OBJECTS IN BINOCULAR RIVALRY.....127

5.1 Abstract.....127
5.2 Introduction.....129
5.3 Methods.....129
5.4 Results.....132
5.5 Discussion.....138
5.6 Conclusion.....140
5.7 Acknowledgements.....140

5.8 References.....141

CHAPTER 6: ASYNCHRONY FROM SYNCHRONY: LONG-RANGE GAMMA-BAND NEURAL SYNCHRONY ACCOMANIES PERCEPTION OF AUDIOVISUAL SPEECH ASYNCHRONY.....144

6.1 Abstract.....144
6.2 Introduction.....144
6.3 Methods.....148
6.4 Results.....156
6.5 Discussion.....163
6.6 Conclusion.....169
6.7 Supplementary Material D Synchronization at Other Frequencies.....170
6.8 References.....173

CHAPTER 7: CONCLUSION.....178

7.1 A Summary of the Thesis.....178
7.2 Implications, Limitations, and Future Directions.....182
7.3 References.....186

APPENDIX: UBC RESEARCH ETHICS BOARD APPROVAL.....188

LIST OF TABLES

Supplementary Materials C Table: ERP Data.....82

Table 6.1: Number of Epochs in Each Condition.....153

LIST OF FIGURES

Figure 2.1 Stimulus display for selective visuospatial attention task.....31

Figure 2.2 Lateralization of large-scale gamma-band phase synchronization in selective attention.....40

Figure 2.3 Alpha and gamma band amplitude in selective attention.....42

Figure 2.4 ERPs and visuospatial attention.....45

Supplementary Material A Figures: Synchronization at other frequencies.....65

Supplementary Material B Figures: Individual PLV data.....75

Supplementary Material C Figures: ERP Data.....81

Figure 3.1 Lateralization of long-range synchronization in selective attention.....96

Figure 3.2 Topography of lateralized of long-range alpha-band synchronization in selective attention.....97

Figure 3.3 Neural generators of alpha-band activation during attention maintenance and long-range network synchronization.....105

Figure 3.4 Time-frequency graphs of occipital-parietal synchronization.....107

Figure 4.1 Time-frequency graphs of lateralized occipital-parietal synchronization.....121

Figure 5.1 Distribution of lengths of ocular dominance.....133

Figure 5.2 Time-frequency graphs time-locked to perceptual switching.....135

Figure 5.3 Topography of long-range synchronization time-locked to perceptual switching.....136

Figure 6.1 The audiovisual behavioural paradigm.....150

Figure 6.2 Time-frequency graphs of global long-range synchronization accompanying congruent and incongruent audiovisual perception.....158

Figure 6.3 **Topography of long-distance synchronization.....159**

Figure 6.4 **Topography and time-frequency graphs for congruent and incongruent audiovisual perception.....162**

Supplementary Material D Figures: Synchronization at Other Frequencies.....170

ACKNOWLEDGEMENTS

I would like to thank my supervisor, Lawrence Ward, for his continual mentorship and guidance throughout this process. Special thanks to Stephanie Thai for all her help in performing experiments, and for helping me maintain organization and focus from day to day in the laboratory. I would also like to thank other lab members who have been particularly helpful to the conduct and completion of my research including Keiichi Kitajo, Alexa Roggeveen, Lauren Emberson and Alan Rahi. I also have much appreciation for the help of members of other laboratories who have helped in the combination of phase synchronization analysis with source analysis. Specifically, I would like to thank Anthony Herdman and Jessica Green. I would also like to extend my thanks to the members of my supervisory committee for their insightful comments (Nicholas Swindale, Martin McKeown and Robert Douglas). And of course, I would like to thank my family for their continuous support throughout my education.

DEDICATION

This work is dedicated to Stephanie Thai. Stephanie I love you, and you are the most important person in my life. The companionship you have given me through these years has been integral to my success and confidence. You have been an essential source of happiness and have helped greatly in getting me through these difficult and stressful times. Thank you Stephanie.

CO-AUTHORSHIP STATEMENT

I was primarily responsible for all aspects of each study in this thesis including experimental design, data collection, statistical analysis and interpretation of the results, and preparation of manuscripts for publication.

Lawrence M. Ward appears as a co-author on all of the works presented here. His role was supervisory only. His contributions included providing laboratory space and equipment, access to subjects, obtaining ethics approval and research funding, consultation on experimental design, analysis of results, preparation of data for publication, and editing of manuscripts submitted for publication.

Chapter four presents results stemming from a reanalysis of data collected at the Human Electrophysiology Laboratory at Simon Fraser University (Director: Dr. J.J. McDonald). Chapter four describes new results owing to a new analysis of the data performed by myself.

CHAPTER 1: INTRODUCTION

1.1 Neural Synchronization and Integration: an Historical Review

Cognition requires cooperation between neural populations within and across brain areas. Such cooperation, moreover, must be dynamic in order to accommodate the demands of particular tasks, and to organize features of various percepts. It is clear that many routine cognitive acts require the coordination of activity between specific brain areas. For example, consider what typically occurs when one discovers that they have misplaced their keys. First, a cluttered table or desk top might be subjected to a serial visual search as objects are examined in turn. This requires activation of, and functional integration within, a task dependant network of brain areas including frontal areas such as prefrontal cortex and frontal eye fields, intraparietal cortex and inferior temporal regions relevant for visual attention control and object recognition (Corbetta and Schulman 2002; Gazzaniga et al. 2002). If that search yields no fruit, one might shift one's attention to recalling the events of the night before in search of some record of the missing keys' fate. This requires that a new assembly of neural regions become active and functionally coupled as attention is disengaged from the visual search and directed towards recent memory. This task involves coordinated activity in the prefrontal cortex, hippocampus and parahippocampal cortical areas (Fell et al. 2001; Gazanniga et al. 2002). The attention search network, moreover, must be disintegrated as neural populations involved in that task are freed up for new duties (in this case prefrontal cortex). It remains an unsolved problem how brain region achieve such transient functional coupling, and subsequent decoupling. Neural synchronization has been proposed as a mechanism for

selective functional integration of neural populations and as a means for perceptual binding (see Engel and Singer 2001; Varela et al. 2001 for reviews).

Proper appreciation of the hypothesis that neural synchrony is a mechanism for cognitive brain dynamics begins with an understanding of its relationship with the idea's forbearer, connectionism. Historically, connectionism refers to the notion that a cognitive representation or process is implemented in the brain by the pattern of connections that exists between multiple neurons. Localizationalism, conversely, believes that mental representations and processes can be explained according to the activity of specified and spatially restricted populations of neurons. In the early twentieth century Karl Lashley set out to determine, through an extensive set of lesion studies, whether the neural trace of a memory (the engram) was located in a particular place in the brain. The results of this extensive set of studies indicated that an engram was not stored in a single brain locus, but was distributed throughout associative cortex (see Thompson 1976 for review). The concept of distributed memory culminated in the seminal theory of Donald Hebb that recurrent coactivation of a set of neurons would strengthen synaptic connectivity between those neurons, effectively embedding memories and learned behaviours in a network of distributed cells (Hebb 1949). In this view, remembering or expressing a learned behaviour would result from the reactivation of the distributed assembly of neurons in which the memory or learned behaviour was stored. Recent decades have borne out Hebb's hypotheses that recurrent coactivation of connected neurons can lead to the strengthening of synaptic connections, and that precise temporal relationships are critical to plasticity in the brain, evidenced by long-term potentiation and spike timing dependant plasticity, respectively (Maren and Baudry 1995; Martin et

al. 2000). By attributing the formation of memory representations to the precisely timed coactivation of neurons, Hebbian theory paved the way for the view that all cognitive representations might be encoded by distributed networks of coactivated neurons. The connectionist viewpoint, accordingly, has expanded its purview beyond memory, becoming an encompassing theory for explaining the organization of mental processes and perceptions in the brain (Bressler and Tognoli 2006; Varela et al. 2001).

Connectionism, by developing the notion that mental activity is the result of the activation of one out of a multitude of distributed ensembles, brought us to the threshold of cognitive dynamics. Conceiving of memories and mental processes as arising from the activities of a set of overlapping networks of interconnected nerve cells, however, raises the question of how an organized, directed mind might realistically arise from such an arrangement. If a neuron, or neural group, can participate in one assembly at one time and yet be part of another distinct assembly at a different time, what determines which neurons participate in a given assembly at any given point? To put this in psychological terms, consider William James' discussion of the stream of consciousness, which has a centre and a fringe, and within which certain contents may become 'hot', then subsequently 'cold' as they wax and wane with respect to the focal point of the mind (James 1890). How is one, out a potential many, ensemble of neurons selectively activated, and temporarily integrated, according to the requirements of given mental operation?

It has been proposed that neurons that oscillate synchronously become transiently functionally integrated and that this mechanism accounts for the brain's ability to

dynamically assign connectivity at the time scale relevant for cognitive activity and sensory awareness (Engel and Singer 2001; Varela et al. 2001). In this view, neurons whose oscillations are synchronous communicate more effectively as bursts of action potentials are consistently received during the depolarized phase of the receiving neuron's ongoing membrane potential fluctuation (Fries 2005).

Extrapolation from Hebb's theory to large-scale network dynamics implemented by neural coherence would predict a ubiquitous relationship between memory processing and neural synchronization. The evidence is indeed broad in scope. Learning an association between a visual stimulus and a finger shock, for instance, is correlated with increased gamma-band coherence between primary visual cortex and somatosensory cortex contralateral to the shocked hand (Miltner et al. 1999). This suggests that synchronization is relevant for the formation of new connections between distant brain regions which underlie associative learning. Recognition of a familiar visual object, relative to the presentation of a unfamiliar object, is correlated with both increased gamma-band activation (reflective of local synchronization) and increased long-distance gamma-band phase locking (reflective of synchronization between brain regions) in the electroencephalogram (Gruber et al. 2002). The application of source localization techniques to these object recognition effects has revealed that gamma-band phase synchronization occurs between multiple sources of gamma-band activation, and that the observed synchronization is correlated with causal influence (measured by partial directed coherence) between the gamma sources (Supp et al. 2007). Synchronization in the gamma frequency range has also been observed between hippocampus and parahippocamapal areas, as well as between CA1 and CA3 regions of the hippocampus

during memory processing (Fell et al. 2001; Montgomery and Buzsáki 2007). The retention of visual information in working memory, moreover, is also coupled with increased synchronization between electrodes over frontal and parietal cortex (Sarnthein et al. 1998). These complementary lines of evidence support the notion that neural synchronization, particularly within the gamma frequency range, produces a lasting representational trace in an assembly of neurons, and that memory and learned behaviour relies on the reactivation of such neural assemblies.

Transient synchronization in the gamma-band is not only relevant for learning and memory, but may also be a mechanism for the binding of features into a percept. Gamma-band synchronization between cortical columns in cat primary visual cortex covaries with global stimulus properties and segregation of the visual scene (Engel et al 1991; Gray et al. 1989). Moreover, organization of an ambiguous visual stimulus into a coherent percept is accompanied by large-scale gamma-band phase synchronization between electroencephalogram (EEG) electrodes, indicating this mechanism is also active in binding perceptual features across brain areas (Rodriguez et al. 1999). An obvious appeal of this approach to perceptual representation is its congruence with our understanding of memory processes. Specifically, when one regards an object and it is held in perceptual consciousness a synchronously oscillating neural assembly is activated to bind the features of the object into an integrated percept (Tallon-Baudry and Bertrand 1999). According to Hebbian principles, the connectivity within this network of neurons is strengthened by this coactivation (Hebb, 1949). When the same object is encountered again this assembly becomes reignited, accounting for the long-distance gamma-band synchronization effects observed during the recognition of familiar objects (Gruber et al.

2002). Further support for the notion that neural synchronization plays a general role for transient integration in the brain comes from the observation that when attention is devoted to a stimulus, gamma-band coherence is greater between electrodes implanted in the primary sensory cortex relevant to the processing of that stimulus (eg. Fries et al. 2001). The role of neural synchronization in perceptual binding and attention will be returned to in greater detail in subsequent chapters.

If diverse processes including memory, perceptual binding, perceptual scene segregation and attention all rely on synchronization within distributed cell assemblies, one might ponder how organized, directed and coherent patterns of behaviour and mental life could emerge from this apparent morass of overlapping and oft simultaneously active processes. Clearly, this requires that out of this forest of brain network activations there must be, at any point in time, a centre of gravity within that network. Returning again to the language of William James, there must be parts of the mind which are 'hot' at one time, and become 'cold' at another (James 1890). In other words there must be a stream of consciousness, the contents of which can be shifted according to the mind's momentary circumstance and needs. It has been suggested that the three essential properties of consciousness are that it is: (i) integrated; features are bound in consciousness, (ii) selective; some information is chosen for conscious inclusion while other information is not, and (iii) dynamic; the contents of consciousness may change from one moment to the next (Tononi 2005). It has furthermore been suggested that perceptual consciousness results from transient synchronization of neural populations representing the various features of the percept into a large-scale synchronously oscillating assembly of neurons, and that the largest integrated neural assembly defines

the contents of consciousness at any given moment (Engel and Singer 2001; Tononi 2005). The clearest evidence for this comes from studies showing that when rivaling stimuli are flickered at different rates during binocular rivalry (in which incongruent visual images are presented to each eye, leading to the alternating perception of one or the other of the stimuli) both local and long-distance synchronization at the flicker frequency of the currently perceived image is substantially increased relative to that of the suppressed image (Cosmeli et al. 2004; Srinivasan et al. 1999).

The view that large-scale synchronously oscillating constellations of neural assemblies are the substrate of perceptual consciousness is predicated on several empirical observations. Waking and rapid eye movement sleep, the central nervous system states associated with consciousness, are the only states in which fast oscillations in the beta and gamma bands find distinct expression (Nunez 1995). Moreover, it should be noted that these fast oscillations achieve much greater spatial segregation in the cortex than do slower oscillations. Theoretically this is an important feature of fast brain oscillations as it is required for selective activation of relevant neural populations. For example, while cortical stimulation in the alpha frequency range propagates diffusely and nonspecifically, gamma-band stimulation leads to increasingly segregated activation due to the dependence of the cortical gamma cycle on interneuron bursting, driven by action potential bursts in thalamocortical projections (Llinás et al. 1998). This property would be required for oscillatory synchronization to bind particular features, but not others, into a percept, or to integrate certain neural populations, but not others, into a task-dependant assembly. It should furthermore be noted that disruption of thalamocortical coherence, under which conditions cortical gamma cycling cannot be maintained, leads to

unconsciousness. This can be observed in slow wave sleep (relative to REM and wakefulness) and during general anesthesia (Alkire and Miller 2005; Llinás and Paré 1991). Such data suggest that coherent corticothalamic activity, which is required to maintain cortical gamma-band oscillations, is necessary for consciousness (Seth et al. 2005). In this view, the oscillatory dynamics of the conscious brain provide the neural platform for the selective and dynamic integration of neural populations at a brain wide scale, establishing the substrate of conscious experience (Varela et al. 2001).

The viewpoint set out here maintains that transient neural synchrony is a fundamental, perhaps ubiquitous, organizing principle for activity in the central nervous system. Were this true, it would be expected that task dependent synchronization would be evident in diverse neural systems and that disruption of synchronization in the brain could have severe consequences which could be observed across a wide set of brain functions. In support of this general interpretation of neural synchrony it should be noted that task-dependent oscillatory synchronization is also observed within the motor system, expressed as corticomusular and corticospinal coherence (Schnitzler et al 2003; Salinius and Hari, 2003). Moreover, task demands also modulate long-distance synchronization patterns between visual and motor cortex during tasks requiring visuomotor integration (Roelfsema et al. 1997). A plethora of evidence supports the view that disruption of normal brain synchronization leads to functional disconnection in the brain and may account for the symptoms of a diverse set of pathological conditions including schizophrenia, autism, dyslexia and Parkinson's disease (see Llinás et al. 2005; Schnitzler et al. 2006; Uhlhaas and Singer 2006 for reviews).

It is becoming increasingly clear that neural synchrony plays a role in assigning dynamic functional connectivity in the brain, and that oscillations in particular frequency ranges are associated with specific roles (this latter point will be returned to in greater detail in subsequent chapters). Much recent evidence, however, suggests that the relationship of neural oscillations to cognitive processing is more complex than is imagined in much of the current theory. For example, it is becoming apparent that oscillatory synchrony within a particular bandwidth can play an entirely different role depending on the scale at which the synchronization occurs. For the purposes of this manuscript, local synchronization refers to synchronization within a cortical region (a Brodmann area), while long-range/long-distance synchronization refers to synchronization between cortical regions. The term large-scale synchronization is used in reference to long-distance synchronization within a network likely to include more than two brain areas. A wealth of longstanding evidence indicates that the local alpha oscillations are relevant to the inhibition of processing within a cortical area (see Klimesch et al. 2007 for review). Synchronization between distant cortical areas at an alpha rate, however, has been observed under task conditions in which those areas would be required to cooperate (see Palva and Palva 2007 for review). Unfortunately, even this type of distinction leaves cloudy waters. Intracranial EEG (iEEG) reveals that visual perception and attention modulate gamma-band activity differently across distinct task-relevant cortical regions (Lachaux et al. 2005; Tallon-Baudry et al. 2005). Such results entail that entirely general statements about the roles of oscillatory synchronizations in a particular frequency range at certain scales, such as 'local gamma amplitude increases index active processing, while long-distance synchronization at a gamma rate reflects

integration,' may not be true, at least not in all cases. Forward looking investigations have sought to disambiguate such problems by looking for systematic relationships between oscillations in different bandwidths, and between different neural scales. It has been revealed using human iEEG, for example, that during cognitive processing gamma oscillations are phase locked to the theta cycle in the neocortex (Canolty et al. 2006). Furthermore, it has been reported that the gamma rhythm may act as preprocessing for beta oscillations, in that an initial phase, wherein gamma oscillations are expressed in both the local field potential and in the firing rate of single cells, is followed a secondary phase in which the local field potential still expresses a gamma rhythm but individual cells respond at a beta rate which is locked to the population gamma cycle (individual neurons do not fire on every cycle) (Olufsen 2003). Although still sufficient for the generation of experimental hypotheses, it is becoming increasingly clear that simply dealing with oscillations in one frequency band at one scale is insufficient to explain brain function as it is relevant to complex processes such as attention, perception, memory and consciousness. An emerging challenge for explaining how brain synchronization contributes to cognitive processing will be understanding how neural oscillations of different rates interact across various spatial and temporal scales of measurement.

1.2 Thesis Overview

The present work expands our understanding of the relationship between neural synchronization and functional brain integration in cognition by examining large-scale synchronization in selective visual attention and perceptual consciousness. These two

arenas were chosen for evaluation of the hypothesis that neural synchrony mediates cognitive integration because perceptual consciousness is an *integrated* state (features are bound into a visual representation) and because attention is an *integrative* process (attention promotes feature binding). Given the complexities of our emerging understanding of brain oscillations and cognitive function, emphasis was placed on (i) determining the extent and nature of the relationship between cognitive integration and functional integration across brain areas, (ii) bringing clarity to the understanding of interaction of synchronous brain oscillations across multiple frequency ranges and across local and long-distance scales, and (iii) reconciling and interpreting the increasingly complex and apparently incohesive body of evidence detailing the role of synchronization at different scales and frequencies in cognition.

Chapter 2, originally published by Doesburg et al. (2008), provides evidence that when attention is deployed to a location in one visual hemifield, long-range gamma-band phase synchronization is observed between electrodes over contralateral visual cortex and other, widespread, brain regions. This effect is interpreted as indexing the establishment of a network of functionally integrated brain regions that promotes information appearing at the attended location for transfer to processing in other cortical regions. Specifically, this result is taken to indicate functional coupling between primary visual cortex representing attended locations and brain regions related to higher cognitive processes. This result also provides a mechanism to explain why the contents of attention are more effectively integrated with other information both within and between modalities. The observed large-scale gamma-band synchronization was accompanied by oscillatory changes in other frequency bands at both local and long-distance scales. Most notably,

the time courses of local alpha amplitude changes appear to be coordinated with gamma-band synchronization effects. After the attention network has been established via long-distance gamma-band phase synchronization, lateralized local alpha activity appears which is sustained until target onset, suggesting alpha oscillations are relevant for maintaining selective attention at a location.

If synchronization between brain regions produces the enhanced processing and propensity for integration attended information is known to receive, however, it stands to reason that brain regions representing an attended location should remain synchronized with areas responsible for higher processing throughout the period in which attention is maintained. To observe this effect we instructed subjects to perform a spatial attention cuing task while magnetoencephalographic (MEG) data were recorded. The MEG is less sensitive to volume conduction than the EEG, is sensitive to neural generators at different orientations, and is differentially sensitive to particular frequency bands, allowing the detection of effects not visible in EEG recordings. Chapter 3A describes the results of this experiment, originally published by Doesburg and Ward (2007), which demonstrate that long-distance alpha-band synchronization is greater between sensors over visual cortex contralateral to the cued location and those located about the rest of the head. This synchronization was maintained until target onset and showed a striking time course correspondence with the large-scale gamma and local alpha effects described in Chapter 2. These results, taken together, suggest that long-distance gamma band synchronization is relevant for establishing the attentional network, whereas local and long-range alpha oscillatory mechanisms work in concert to maintain attentional deployment.

Additionally, Chapter 3B describes a supplementary analysis of the MEG data in which synthetic aperture magnetometry (SAM) beamformer was used to localize sources of changes in alpha oscillatory power in specific brain regions. This analysis revealed four reliable recurrent sources: bilateral activations in primary visual cortex and bilateral activations in posterior parietal cortex. Interestingly, although alpha power was greater in primary visual cortex ipsilateral to the cued visual hemifield, alpha-band phase synchronization was greater between primary and parietal sources contralateral to the locus of attention. These data are consistent with the sensor analyses presented in Chapters 2 and 3A, and suggest that whereas local alpha activation is indicative of inhibition, long distance synchronization is relevant for integration. Evidence of lateralized long-range gamma-band phase synchronization was also observed, similar to that reported in Chapter 2.

Chapter 4 presents an analysis of long-distance phase synchronization between electrical source activations that were reconstructed from EEG scalp data recorded from subjects engaged in a visual attention cueing experiment. These data were recorded, and the source imaging was performed, at the Human Electrophysiology Laboratory at Simon Fraser University. BESA beamformer analysis was employed to reconstruct sources of theta-band activity (4-7 Hz) in the interval between an attentional cue and the onset of an expected target. The purpose of the analysis reported here was to investigate whether the long-distance synchronization effects described in the preceding chapters are also visible between sources of EEG activation observed in a network of cortical regions relevant for endogenous attention control. Analysis of phase locking between these sources of theta-band activation revealed increased alpha-band synchronization between primary visual

cortex and parietal cortex contralateral to the attended visual hemifield during the time period preceding target onset. This result demonstrates that alpha-band synchronization observed in our earlier studies was not likely to have arisen from volume conduction. Moreover, this analysis strengthens our interpretation that long-range alpha-band synchronization functions to promote the enhanced processing of stimuli appearing at attended locations since this synchronization, reflective of increased communication, occurs between primary visual cortex representing the attended location and brain areas associated with attention control.

It has been hypothesized that perceptual consciousness results from a large-scale network of neurons synchronously oscillating in the gamma band which serves to integrate features of the perceptual objects populating experience (Engel and Singer 2001; Varela et al. 2001). According to such a view, the onset of a new visual percept requires the activation of many spatially separated neural populations, which code various features, and their integration into a large-scale assembly. We hypothesized that this network integration would be achieved by long-distance gamma-band synchronization. To test this, EEG was recorded while subjects were presented with incongruent visual stimuli to each eye (this condition leads to conscious perception of one or the other images at any given time, and which stimulus is dominant alternates periodically). Chapter 5 describes this experiment, originally published by Doesburg, Kitajo and Ward (2005), which evidences that the onset of a new visual percept coincides with globally increased long-distance gamma-band phase synchronization between electrodes. The observed gamma-band synchronization is short lived, yet is periodically 'refreshed' at a theta rate. This evidence suggests that large-scale gamma band

synchronization is relevant for the organization of a new visual percept, and that a theta-band carrier frequency serves to maintain such a percept by periodically reintegrating such gamma-synchronous neural ensembles.

It has been demonstrated, previously as well as in the work presented here, that neural synchronization may serve to functionally integrate neural populations. In the context of perceptual processes in the brain, this synchronization often functions to organize a coherent percept, as observed in visual scene segmentation, attention and the emergence of a percept in binocular rivalry or ambiguous stimuli (Doesburg et al. 2005; Engel et al. 1991; Gray et al. 1989; Rodriguez et al. 1999). What is not clear, however, is whether this phenomenon is ubiquitous. Although the binding of features in complex stimuli generally requires communication between multiple spatially separated neural populations, it is not clear if perceptual coherence can be equated to increased synchronization in all cases. Organization of the perceptual scene requires two types of processes: (i) determination of which features are to be grouped into a perceptual object and which are not, and (ii) binding of the features of a perceptual object to produce and unified and coherent percept. What is sometimes underappreciated is that the first type of process requires active parsing of information. The mismatch negativity, elicited from the auditory cortex when stimuli deviate from an expected pattern and thus may originate from a new environmental source, is an example of an active process relevant to segregation of the perceptual scene rather than its integration (Picton et al. 2000). It is entirely plausible to suspect that processes relevant to higher order aspects of perceptual scene segregation, for example those indicating incongruence between auditory and visual inputs, may require the coordinated activity of a network of brain areas.

According to the integration by synchronization hypothesis, this would entail transient coherence between oscillations in brain areas required to identify a mismatch between auditory and visual streams. It might also be predicted, conversely, that an integrated audiovisual percept would be accompanied by increased long-range neural synchronization given the substantial evidence that feature binding is accomplished by synchronization between neural populations representing various aspects of the perceived object.

Chapter 6 provides evidence that the detection of asynchrony between the auditory and visual streams of speech stimuli, leading to a perception in which the auditory speech stream is perceived as incongruent with the visual stream, is accompanied by increased large-scale gamma-band phase synchronization between EEG electrodes. This result, originally published by Doesburg et al. (2008), is interpreted as an indication that the parsing of auditory and visual speech streams into separate perceptual objects is an active process requiring coordinated activity within a distributed network of cortical regions. The observed long-distance gamma-band synchronization, in this view, reflects functional coupling in this network. Previous evidence is reviewed indicating that audiovisual speech integration, conversely, may be accomplished principally by structures in the superior temporal lobe rather than in a distributed network. The results of this study illustrate an important distinction: neural synchronization is a mechanism for functional integration of neural populations, not a mechanism for perceptual integration and feature binding *per se*. In many cases integrated perception is indeed positively correlated with increased neural synchronization, relative to nonintegrated perception, within and across brain areas. This

is not surprising given that the matching of various features requires active cooperation across cortical regions. The study presented here, however, demonstrates that this is not always the case, as certain perceptual tasks require more coordination of activity across distributed brain areas to determine that perceptual streams should be segregated than is required to integrate percepts that are congruent. In this case this is because processes relevant for audiovisual speech integration are relatively localized while those relevant for the detection of asynchrony between auditory and visual speech streams are more distributed.

The results of the experiments presented here, taken together, indicate that long-distance neural synchronization is relevant for the transient functional coupling of neural populations for the organization of a percept, and for the configuration of transient connectivity in the brain for the deployment and maintenance of attention. Moreover, these results underscore a number of specific roles for neural synchrony in particular frequency ranges and illustrate how oscillatory synchronization interacts across frequency ranges and scales. Synchronization of gamma rhythms across cortical regions serves to establish a new constellation of active and communicating brain areas. This can be observed in the emergence of a new percept during binocular rivalry, when a new anticipatory network is established when attention is deployed to a particular location, and when a distributed network is activated for the detection of audiovisual incongruence in speech. A consistent relationship between long-distance gamma-band synchronization and the theta cycle is also observed. Long-range gamma synchronizations are short lived, typically terminating after approximately 75 ms (about 3 gamma-rate cycles at 25 ms/cycle for 40 Hz oscillations). When a particular network state is maintained, such as

when a particular percept is being maintained or when selective attention is continuously engaged at a particular location, we see that these large-scale gamma-oscillatory neural assemblies are periodically 'refreshed' at a theta rate (4 -7 Hz). Such observations are consistent with the idea that the theta cycle is acting as a carrier frequency to maintain gamma synchronization over longer distances, or that it is a clocking mechanism for the organization of gamma brain rhythms (von Stein and Sarnthien 2000; Canolty et al. 2006). Theta and gamma band oscillations at both local and long-distance scales both seem to reflect active and integrated processing. The observations reported here, however, suggest that in the case of alpha oscillations there is a dissociation between the functional meaning of synchronization in this frequency range across local and long-distance scales. Consistent with most previous research, the work presented here supports the theory increased local alpha-band activation is reflective of inhibition or inactivity within a cortical area. Analysis of alpha synchronization between brain regions, however, suggests that it is relevant for transient functional coupling. The time-course of such alpha synchronizations suggests that they are intimately related to theta and gamma band oscillatory dynamics. Whereas it appears that high frequency oscillatory synchronization is required to establish a functional brain network, alpha synchronization works in tandem with the theta-modulated-gamma mechanism to maintain that network. In short, the studies presented here elucidate how oscillatory synchronization contributes to selective attention and the organization of perceptual consciousness.

1.3 References

Alkire MT, Miller J. General anesthesia and the neural correlates of consciousness Prog Brain Res (2005) 150:229–244.

Bressler ST, Tognoli E. Operational principles of neurocognitive networks. Int J Psychophysiol (2006) 60(2):139–148.

Canolty RT, Edwards E, Dalal SS, Soltani M, et al. High gamma power is phase-locked to theta oscillations in human neocortex. Science (2006) 313:1626–1628.

Corbetta M, Shulman GL. Control of goal-directed and stimulus-driven attention in the brain. Nat Rev Neurosci (2002) 3(3):201-215.

Cosmeli D, David O, Lachaux JP, Martinerie J, Garnero L, Renault B et al. Waves of consciousness: ongoing cortical patterns during binocular rivalry. Neuroimage (2004) 23:128–140.

Doesburg SM, Emberson LL, Rahi A, Cameron D, Ward LM. Asynchrony from synchrony: long-range gamma-band neural synchrony accompanies perception of audiovisual speech asynchrony. Exp Brain Res (2008) 185(1):11–20.

Doesburg SM, Kitajo K, Ward LM. Increased gamma-band synchrony precedes switching of conscious perceptual objects in binocular rivalry. Neuroreport (2005) 16(11):386–396.

Doesburg SM, Roggeveen AB, Kitajo K, Ward LM. Large-scale gamma-band phase synchronization and selective attention. Cer Cortex (2008) 18(2):386–396.

Doesburg SM, Ward LM. Long-distance alpha-band MEG synchronization maintains selective visual attention. International Congress Series 1300 (2007) 551-544.

Engel AK, König P, Singer W. Direct physiological evidence for scene segmentation by temporal coding. Proc Natl Acad Sci USA (1991) 88:9136–9140.

Engel AK, Singer W. Temporal binging and the neural correlates of sensory awareness. Trends Cogn Sci (2001) 5:16–25.

Fell J, Klaver P, Lehnertz K, Grunwald T, Schaller C, Elger CE, Fernández G. Human memory formation is accompanied by rhinal-hippocampal coupling and decoupling. Nature Neuroscience (2001) 4:1259–1264.

Fries P. A mechanism for cognitive dynamics: neuronal communication through neuronal coherence. Trends Cogn Sci (2005) 9:474–479.

Fries P, Reynolds JH, Rorie AE, Desimone R. Modulation of oscillatory neuronal synchronization by selective visual attention. Science (2001) 291:1506–1507.

Gazzaniga MS, Ivry RB, Mangun GR. Cognitive neuroscience. (2002) 2nd edition. New York: WW Norton.

Gray CM, König P, Engel AK, Singer W. Oscillatory responses in cat visual cortex exhibit inter-columnar synchronization which reflects global stimulus properties. Nature (1989) 338:334–337.

Gruber T, Müller MM, Keil A. Modulation of induced gamma band responses in a perceptual learning task in the human EEG. J Cogn Neurosci (2002) 14(5):732–744.

Hebb DO. The organization of behavior. Lawrence Earlbaum Associates. New York. (1949).

James W. The principles of psychology. Harvard University Press. New York. (1890). 1328 p.

Klimesch W, Sauseng P, Hanslmayr S. EEG alpha oscillations: the inhibition timing hypothesis. Brian Res Rev (2007) 53(1):63–88.

Lachaux JP, George N, Tallon-Baudry C, Martinerie J, et al. The many faces of the gamma band response to complex visual stimuli. Neuroimage (2005) 25:491–501.

Llinás RR, Paré D. Of dreaming and wakefulness. Neuroscience (1991) 44(3):521–535.

Llinás R, Ribary U, Contreras D, Pedroarena C. The neuronal basis for consciousness. Philos Trans R Soc Lond B Biol Sci (1998) 353(1377):1841–1849.

Llinás R, Urbano FJ, Leznik E, Ramírez RR, van Marle HJ. Rhythmic and dysrhythmic thalamocortical dynamics: GABA systems and the edge effect. Trends Neurosci (2005) 28(6):325–333.

Maren, S Baudry M. Properties and mechanisms of long-term synaptic plasticity in the mammalian brain: relationships to learning and memory. (1995) 63(1):1-18.

Martin SJ, Grimwood PD, Morris RG. Synaptic plasticity and memory: an evaluation of the hypothesis. Annu Rev Neurosci (2000) 23:649–711.

Montgomery SM, Buzsáki G. Gamma oscillations dynamically couple CA3 and CA1 regions during memory task performance. Proc Natl Acad Sci USA (2007) 104(36):14495–144500.

Miltner WH, Braun C, Arnold M, Witte H, Taub E. Coherence of gamma-band EEG activity as basis for associative learning. Nature (1999) 397:434–436.

Nunez P. Neocortical dynamics and human EEG rhythms. (1995) Cambridge: Oxford University Press. 708.

Olufsen MS, Whittington MA, Camperi M, Kopell N. New roles for the gamma rhythm: population tuning and preprocessing for the beta rhythm. J Comput Neurosci (2003) 14(1):33–54.

Picton TW, Alain C, Otten L, Ritter W, Achim A. Mismatch negativity: different water in the same river. Audiol Neurootol (2000) 5(3-4):111–139.

Palva S, Palva JM. New vistas for alpha-frequency band oscillations. Trends Neurosci (2007) 30(4):150–158.

Rodriguez E, George N, Lachaux JP, Martinerie J, et al. Perception's shadow: long distance synchronization of human brain activity. Nature (1999) 4(397):430–433.

Roelfsema PR, Engel AK, König P, Singer W. Visuomotor integration is associated with zero time-lag synchronization among cotical areas. Nature (1997) 385(6612):157–161.

Salenius S, Hari, R. Synchronous cortical oscillatory activity during motor action. Cur Opin Neurobiol (2003) 13(6):678–684.

Sarnthein J, Petsche H, Rappelsberger P, Shaw GL, von Stein A. Synchronization between prefrontal and posterior association cortex during human working memory. Proc Natl Acad Sci USA (1998) 9(12):7092–7096.

Schnitzler A, Timmerman L, Gross J. Physiological and pathological oscillatory networks in the human motor system. J Physiol Paris (2006) 99(1):3–7.

Seth AK, Baars BJ, Edelman DB. Criteria for consciousness in humans and other mammals. Conscious Cogn (2005) 14(1):119–39.

Srinivasan R, Russell DP, Edelman GM, Tononi G. Increased synchronization of neuromagnetic responses during conscious perception. J Neurosci (1999) 19:5435–5448.

Supp GG, Schlögl A, Trujillo-Barreto N, Müller MM, Gruber T. Directed cortical information flow during human object recognition: analyzing induced EEG gamma-band responses in brain's source space. PLoS ONE (2007) 2(1):e684.

Tallon-Baudry C, Bertrand O. Oscillatory gamma activity in human and its role in object representation. Trends Cogn Sci (1999) 3(4):151–162

Tallon-Baudry C, Bertrand O, Hénaff MA, Isnard J, Fischer C. Attention modulates gamma-band oscillations differently in human lateral occipital cortex and fusiform gyrus Cereb Cortex (2005) 15(5):654–662.

Thompson RF. The search for the engram. Am Psychol (1976) 31(3):209–227.

Tononi G. Consciousness, information integration, and the brain. Prog Brain Research (2005) 52(1):155–168.

Uhlhaas PJ, Singer W. Neural synchrony in brain disorders: relevance for cognitive dysfunctions and pathophysiology. Neuron (2006) 52(1):155–168.

Varela F, Lachaux JP, Rodriguez E, Martinerie J. The brainweb: phase synchronization and large-scale integration. Nat Rev Neurosci (2001) 2(4):229–239.

von Stein A, Sarnthein J. Different frequencies for different scales of cortical integration: from local gamma to long range alpha/theta synchronization. Int J Psychophysiol (2000) 38:301–313.

CHAPTER 2: LARGE-SCALE GAMMA-BAND PHASE SYNCHRONIZATION AND SELECTIVE ATTENTION[1]

2.1 Abstract

Explaining the emergence of a coherent conscious percept and an intentional agent from the activity of distributed neurons is key to understanding how the brain produces higher cognitive processes. Gamma-band synchronization has been proposed to be a mechanism for the functional integration of neural populations that together form a transitory, large-scale, task- and/or percept-specific network. The operation of this mechanism in the context of attention orienting entails that cortical regions representing attended locations should show more gamma-band synchronization with other cortical areas than would those representing unattended locations. This increased synchronization should be apparent in the same time frame as that of the *deployment* of attention to a particular location. In order to observe this effect, we made electroencephalogram recordings while subjects attended to one side or the other of the visual field (which we confirmed by event-related potential analysis) and calculated phase-locking statistics between the signals recorded at relevant electrode pairs. We observed increased gamma-band phase synchronization between visual cortex contralateral to the attended location and other, widespread, cortical areas approximately 240–380 ms after the directional cue was presented, confirming the prediction of a large-scale gamma synchronous network oriented to the cued location.

[1] A version of this chapter has been published. Doesburg SM, Roggeveen AB, Kitajo K, Ward LM. Large-scale gamma-band phase synchronization and selective attention. Cerebral Cortex (2008) 18(2): 386-396. Differences between this chapter and the published version are in formatting only.

2.2 Introduction

Performance of the myriad perceptual and cognitive processes of which the brain is capable requires transient functional coupling, and subsequent decoupling, of specific, task-relevant, neural populations. Gamma-band synchronization is a plausible mechanism for the selection and integration of such neuronal groups (e.g., Varela et al. 2001). Direct brain recordings show that increased gamma-band synchronization *within* a cortical area occurs most strongly between columns representing information that is being integrated, for example, between columns representing features of a common object (Gray and Singer 1989; Gray et al. 1989; Engel, Kreiter et al. 1991). Stimulus-specific gamma synchronization has been observed between monkey V1 and V2, between V1 and extrastriate motion areas, and between left and right hemisphere V1s of cats (Engel, König, and Singer 1991; Engel, König et al. 1991; Frein et al. 1994). The summation of such gamma synchronous activation yields increased gamma-band power in the electroencephalogram (EEG) and has been experimentally linked to a wide range of cognitive processes including attention, learning, and memory and visual and auditory perception (Ward 2003; Kaiser and Lutzenberger 2005).

Human EEG recordings also reveal increased long-range gamma-band synchrony *between* task-relevant brain areas during associative learning, mental rotation, conscious recollection, visual working memory, and coherent perception (Tallon-Baudry et al. 1998; Miltner et al. 1999; Rodriguez et al. 1999; Bhattacharya et al. 2001; Burgess and Ali 2002; Gruber et al. 2002). Such results support the hypothesis that gamma-band synchronization enables the selective activation of a functionally coupled ensemble of

neuronal groups relevant for the performance of a particular task and for binding the features of an object into a unified percept (Engel and Singer 2001; Varela et al. 2001).

Of more specific relevance to the present experimental paradigm, the deployment of covert attention in humans has been linked to changes in local oscillatory synchronization in the alpha band. Covert deployment of visuospatial attention entails that attended areas in the visual field receive enhanced processing, whereas ignored areas are suppressed (e.g., Posner et al. 1980). Whereas EEG studies have traditionally focused on the enhanced processing of attended targets relative to unattended distractors (for a review, see Gazzaniga et al. 2002), recent research has focused on the anticipatory biasing of the cortex after attention has been deployed to a location but before the appearance of the target. Attending to one visual hemifield yields a sustained increase of alpha-band EEG activation over the ipsilateral visual cortex, a process thought to accomplish the suppression of distractors (Worden et al. 2000; Sauseng et al. 2005; Kelly et al. 2006). Moreover, these lateralized changes in local oscillatory activity have been shown to determine the speed of detection for subsequently appearing targets (Thut et al. 2006).

Cortical gamma-band activity, conversely, appears to be relevant for the enhanced processing of attended information, as studies using implanted electrodes and human EEG have shown that local gamma synchrony is increased by selective attention (Tiitinen et al. 1993; Fries et al. 2001; Gobbele et al. 2002). Such evidence, taken together with the data cited above implicating gamma-band synchronization in feature binding and transient functional connectivity between brain areas and the assumption that many of the effects of attention would seem to require transient functional coupling between select

populations of cortical neurons, leads to the hypothesis that large-scale gamma-band synchrony might play an important role in selective attention.

As mentioned earlier, the allocation of attention to one location results in certain advantages being given to stimuli appearing at that location, relative to those at unattended locations. Specifically, attended stimuli are promoted for processing in cortical regions responsible for higher cognition and are biased for inclusion in consciousness, a highly integrated yet, apparently, anatomically distributed state (Treisman 1996; Tononi 2004). Attention also produces more effective feature binding both within and across sensory modalities. For example, attended stimuli avoid illusory conjunctions and receive feature binding that can be absent for unattended stimuli (for reviews, see Treisman 1996; Wright and Ward 1998). Accordingly, cortical areas representing attended loci must be biased for inclusion in a large-scale functional network to support the enhanced feature binding, higher processing, and propensity for conscious experience that stimuli appearing at such a locus of attention are known to receive. We hypothesized that long-range gamma-band synchronization mediates this transient functional network, enabling the increased communication between cortical areas representing attended loci and other diverse cortical regions and creating a preparatory network for the enhanced processing of attended stimuli.

To test this hypothesis, we recorded EEG while subjects were engaged in a covert attention-orienting task. Our specific *a priori* hypothesis was that when attention was deployed endogenously to one side of visual space, electrodes over the contralateral visual cortex would show increased gamma-band phase synchronization with other,

widespread cortical areas, indexing the establishment of the predicted long-range gamma synchronous attentional network. We also predicted that this would occur in the same time frame as that uncovered in behavioral studies of endogenous orienting that is beginning around 250–300 ms after cue onset (see Wright and Ward 1998). Moreover, we expected that the establishment of this long-range network would occur in coordination with reciprocal changes in local alpha-band and gamma-band activation (see Ward 2003).

2.3 Methods

2.3.1 Subjects and Task

Thirteen healthy adults (8 males) with normal or corrected-to-normal vision participated in the experiment after giving written informed consent (approved by University of British Columbia Behavioral Research Ethics Board; mean age, 19.4 years; standard deviation, 1.2 years). Subjects were seated with eyes approximately 35 cm from a computer monitor and were instructed to maintain fixation on a plus sign in the center of the screen. An arrow cue appeared at the center of the screen, replacing the fixation plus, to instruct subjects to covertly attend to a box either to the left or to the right (18.5° visual angle laterally) of fixation on a given trial (see Figure 2.1). Arrow cues (1.64° by 1.64° visual angle) were presented for 100 ms, after which the fixation point (1.31° by 1.31° visual angle) reappeared. Targets were presented in boxes (1.97° by 1.97° visual angle), which were positioned 6.2° below the plane of fixation (Figure 2.1). Either a "+" or an "x" (50/50 probability) would appear in one of the 2 boxes (50/50 probability) 1000–1200 ms after the cue onset (rectangular distribution to produce random jitter, both to reduce the overlap of event-related potentials (ERPs) from the cue on those to the

target and to reduce the effects of evoked neural sources on phase synchrony measures). Target stimuli were presented for 100 ms and subtended a visual angle of 1.64° by 1.64°. Subjects were instructed to make a button-press response if they detected a "+" but *not* if they detected an "x" in the cued location and to make no response if either stimulus appeared at the uncued location. This paradigm was adapted from that of an earlier study (Worden et al. 2000) and was chosen because it successfully produced lateralized changes in ongoing local power following the deployment of spatial selective attention.

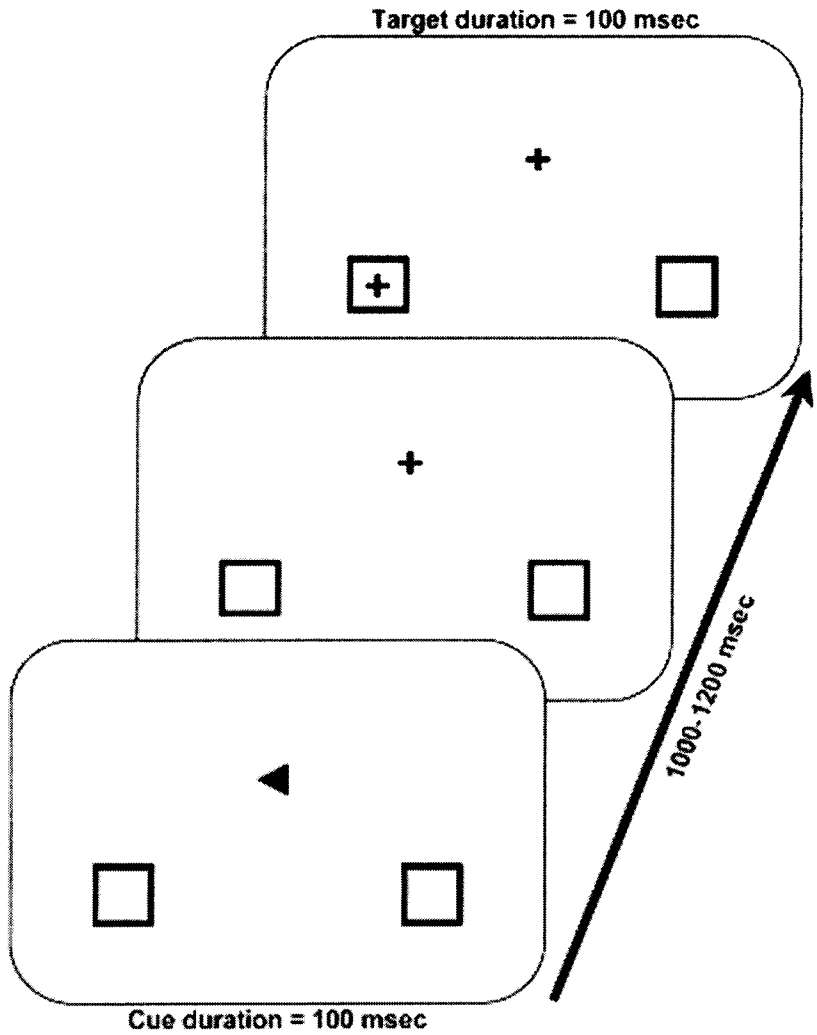

Figure 2.1

Stimulus display and its time course (not drawn to scale for clarity). See text for measurement intervals for synchrony and ERP analyses.

The EEG was recorded from 59 electrodes positioned at standard 10-10 locations plus 3 electrodes at nonstandard sites near the inion. The electro-oculogram (EOG) was recorded bipolarly with electrodes positioned 1 cm from the outer canthi of both eyes and above and below the right eye. Electrode impedances were kept below 15 kΩ (sufficient because of amplifier input impedance >2 GΩ). EEG and EOG were amplified with a gain of 20 000, band-pass filtered between 0.1 and 100 Hz, digitized at 500 Hz, and stored on disk for analysis. Scalp voltages were referenced to the right mastoid.

2.3.2 Synchrony Analysis

Four subjects were excluded for the synchrony analysis due to particularly noisy data in the postcue period and/or in the high frequency domain (both of which are irrelevant for the ERP analysis; mean age of the 9 analyzed subjects, 19.6 years; SD, 1.3 years; 6 males). Epochs for the synchrony analysis were extracted from 400 ms before the cue until 1200 ms after its onset. After deleting any epochs containing ocular or nonocular artifacts (identified by the automatic rejection algorithm in EEGLAB; Delorme and Makeig 2004), 3530 epochs for the left cue and 3584 epochs for the right cue remained for all 9 subjects combined ranging from 130 to 598 epochs per subject per cue condition. The data in the retained epochs were band-pass filtered digitally at 1 Hz intervals between 6 and 60 Hz [passband = $f \pm 0.05f$, where f represents the filter frequency; e.g., at 40 Hz the passband was from 40 – (0.05 x 40) = 38 to 40 + (0.05 x 40) = 42 Hz]. Then, using algorithms in the MATLAB Signal Processing Toolbox, we calculated the analytic signal

$$\varsigma(t) = f(t) + i\tilde{f}(t) = A(t)e^{i\phi(t)}$$

of the filtered waveform for each epoch, $f(t)$, to obtain the instantaneous phase, $\phi(t)$, and amplitude, $A(t)$, at each sample point (800 points per epoch), where $\tilde{f}(t)$ is the Hilbert transform of $f(t)$ and $i = \sqrt{-1}$ (Pikovski et al. 2001). Instantaneous amplitudes from this analysis represent the envelope of the filtered waveform and are roughly equivalent to Fourier amplitudes except that they are estimated for each instant in time rather than as an average over a sliding window. We interpreted these amplitudes as reflecting variations in local neural synchrony in the various frequency bands, much as do power spectral densities (Fourier amplitude squared) from a Fourier analysis.

We measured long-range neural phase synchrony by calculating phase-locking values (PLVs) both for individual data and for the combined data. PLVs were obtained by comparing the instantaneous phases of the signals recorded by various pairs of electrodes, for example, electrodes j and k, at each point in time, t, across the N epochs available (Lachaux et al. 1999):

$$PLV_{j,k,t} = N^{-1}\left|\sum_{N} e^{i\left[\phi_j(t)-\phi_k(t)\right]}\right|$$

PLV is a real value between 0 (random phase difference, no phase locking) and 1 (constant phase difference, maximum phase locking). Because of distortions involved in calculating the Hilbert transform at the edges of the analyzed epochs (e.g., Freeman 2004), we do not display the first or the last 200 ms (100 sample points) of the synchrony analyses of our epochs (note that the last 200 ms also would be contaminated by the target presentation at a random time within that interval). Thus, we report amplitude and phase-

locking measures only for reduced epochs from 200 ms before until 1000 ms after cue onset.

To remove the record of ongoing synchrony unrelated to the task, we standardized PLVs and amplitudes relative to the precue interval from 200 ms before cue onset until cue onset (0 ms). This was done by subtracting the mean PLV for the baseline interval at a given frequency from the PLV for every data point at that frequency and dividing the difference by the SD of PLV for the baseline interval at that frequency. The resulting index, PLV_z, indicates standardized changes from the average baseline PLV at a given frequency in the direction of increased synchronization (positive values) or decreased synchronization (negative values). The same standardization was applied to the amplitude values. To reduce the effects of volume conduction (see Appendix for a more detailed discussion of the problem of volume conduction in the analysis of phase locking using these techniques) and to remove spurious synchronization arising from using a right mastoid reference electrode, the same calculations were performed for the scalp current density (SCD) or more properly the scalp divergence of the current density, a reference-free measure that sharpens the borders of synchronous regions and reduces spurious synchronies (Lachaux et al. 1999).

Classically, SCD = -1 x scalp conductivity x Laplacian of scalp potential, where the Laplacian is the local second spatial derivative. Perrin et al. (1987) showed that SCD, in a spherical coordinate system, could be approximated for any point on the scalp surface using a 3-concentric sphere head model, Legendre polynomials, and spline interpolation. To compute SCD, we used a MATLAB script supplied by Carsten Allefeld

(http://www.agnld.uni-potsdam.de/~allefeld/index.html) that implements the algorithm of Perrin et al. (1987) (see their eqs 3 and 5). Allefeld's script computes a spherical Laplacian operator using Legendre polynomials, the supplied spherical coordinates of a set of electrodes, and splines of order 4. In a separate script, we then applied the Laplacian operator to the potentials recorded at our electrodes to compute SCD. This procedure has been shown to be superior to other methods used previously to approximate SCD from recorded potentials and to give a close approximation to the "true" SCD (Perrin et al. 1987, 1989).

All reported results pertain to the PLV_z values based on SCD unless otherwise specified, although analyses of scalp potentials and SCDs gave highly similar results. For this reason and because the SCD derived from the scalp potential at a given electrode should reflect primarily neural sources in cortical regions close to that electrode (see Appendix), we often refer to synchrony changes between the cortical regions underlying the relevant electrodes interchangeably with the recording electrodes themselves. In addition, we measured long-range synchrony only for a sparse array of 19 electrodes distributed uniformly across the scalp; the distance between the closest electrode pairs was approximately 4 cm. At this distance, the effect of volume conduction on phase synchrony is much reduced, both for intracranial electrodes (Lachaux et al. 1999) and for scalp electrodes (Nunez et al. 1999; see Appendix). This array was chosen before any analyses were conducted and was used in previous studies as well (e.g., Doesburg et al. 2005).

Finally, to characterize the statistical reliability of changes in synchronization and desynchronization in the time courses of recorded potentials and inferred SCD between pairs of electrodes, relevant sets of epochs were shuffled 200 times for each frequency and data point combination, measuring PLV_z in the same way for each shuffled data set, to create surrogate distributions of PLV_z values (Lachaux et al. 1999). This procedure produces distributions of PLV_z that very closely approximate a normal distribution. We considered a measured PLV_z above the 97.5th percentile of the relevant surrogate distribution to be a significant increase in synchronization and one below the 2.5th percentile to be a significant decrease in synchronization. Only changes in synchronization that met or exceeded this criterion are discussed. This still results in a large number of possible tests, and the surrogate method by itself does not protect against the accumulation of experimentwise Type I error from making many such tests. To deal with this problem, we rely upon demonstrations that 1) the changes we observed were predicted *a priori* in the regions of interest (ROIs) in which they were found and 2) the patterns of changes we observed persist across several nearby frequencies and time points, the surrogate distributions of which are derived from independent shufflings, rendering it highly unlikely that the observed patterns resulted from a random set of false positives.

2.3.3 ERP Analysis

Epochs for analysis of ERPs were extracted from 100 ms before until 600 ms after *target* onset. After deleting any of these epochs contaminated by ocular or non-ocular artifacts (in this case using the automatic rejection algorithm of ERPSS from the

University of California San Diego ERPLAB), ERPs to *targets* were computed by averaging the EEG signal across artifact-free epochs for each subject. For these ERP analyses, the EEG records were digitally rereferenced to averaged mastoids and, after averaging, digitally low-pass filtered using a half-amplitude Gaussian filter to view ERPs <13 Hz. Three of the 13 subjects were excluded from the ERP analysis because their EEG signals contained too many artifacts, in particular eye movements or blinks after the presentation of the target, resulting in a large number of trials being rejected from their data. Thus, the subject groups used in the ERP analysis differed slightly from that used in the synchronization analysis. Although the subgroup used for ERP analysis is the optimum one for that analysis, ERPs were also analyzed using data only from the 9 subjects included in the PLV analysis in order to ensure that any observed ERP effects were also present in that data set.

Multiway analyses of variance (ANOVAs) were performed on averaged ERPs. ERPs at electrodes P7 and P8, the electrodes of interest in the phase synchronization analysis, were analyzed, as were electrodes PO7, POz, and PO8, which are electrodes typically of interest when examining ERPs in visual attention tasks. These particular electrodes are known to reflect attentional modulation of activity over parietal and occipital cortices reflected by shifts of attention at the electrode contralateral to visual field presentation (see Results for a more extensive rationale). Because our interest in the ERP analyses was solely to confirm that attention had been directed to the cued location by the arrow cue and maintained there until target onset, our analyses focused on the P1 component, the first positive component, within a window of 75–150 ms after target onset

and the N1 component, or first negative component, within a window of 100–200 ms after target onset.

2.4 Results

2.4.1 Phase Synchronization

Our main *a priori* prediction was confirmed, as increased gamma-band (36–43 Hz) phase synchronization was observed between posterior visual cortical areas contralateral to the cued location and other, widespread, cortical areas occurring from about 240 ms until about 380 ms after the cue appeared (Figure 2.2). The most prominent increases were observed between electrode P7 and electrodes over widespread cortical areas, and electrode P8 and electrodes over widespread cortical areas, following right and left cues, respectively (Figure 2.2A,B). Although present following the onset of either directional cue, the effect is more pronounced and more prolonged following the left cue. We interpret this burst of increased, lateralized, phase synchronization as an indicator of the establishment of the hypothesized gamma synchronous attentional network. This effect was maximal around 39 Hz (because the data were filtered using a bandwidth of $0.1f$, this signal contains energy from nearby frequencies) but was also visible at other frequencies in the gamma band (see Supplementary Material A). A second burst of lateralized large-scale gamma-band phase synchronization, again maximal at 39 Hz, was also observed approximately 520–580 ms postcue onset (Figure 2.2C,D). As was the case for the first burst of increased gamma-band synchronization, this lateralization was anchored at electrodes P7 and P8 following the right and left cues, respectively, and was more pronounced and more prolonged following the left cue. No such bursts of long-

range synchronization lateralized as a function of cue direction were present in other frequency bands; they occurred only in the gamma frequency band, although nonlateralized increases and decreases in synchronization did occur in other frequency bands around the time of the first gamma burst (see Supplementary Material A). No reliable patterns of coordinated synchronization or desynchronization in other frequency bands were observed in conjunction with the second gamma burst. Analysis of individual subject data revealed similar, although less striking, patterns of lateralized gamma-band synchronization (because of poorer signal-to-noise ratio, which is a function of the number of epochs analyzed). For some subjects, reliable effects closely resembled those in the group data, whereas for some others, the pattern took the form of *decreases* in synchronization between visual cortical areas *ipsilateral* to the cued hemifield and widespread electrodes as well as, or in place of, the increases contralateral to the cued hemifield observed in the main effect for our group data (see Supplementary Material B).

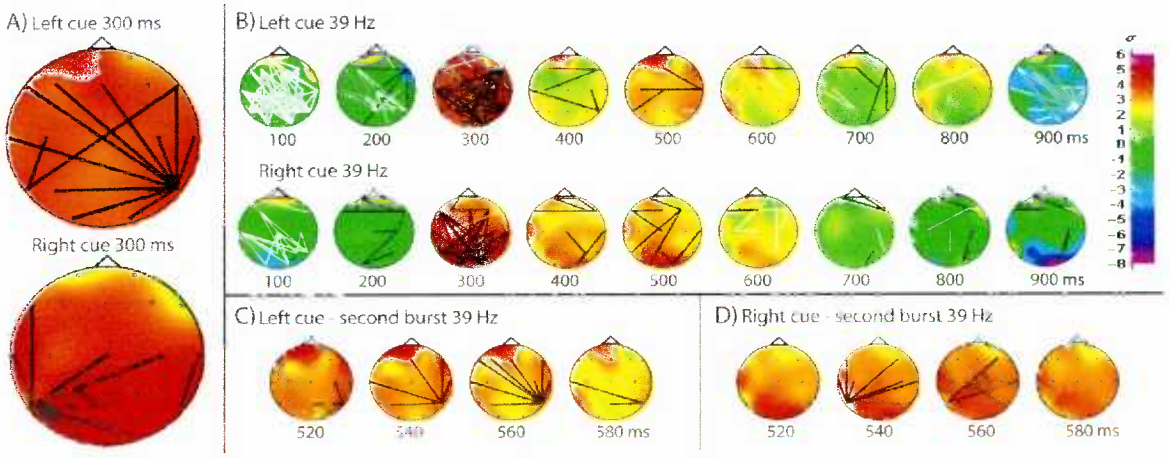

Figure 2.2

Lateralization of large-scale gamma-band phase synchronization at 39 Hz in source current density (SCD). Black lines indicate reliable increases in synchronization, and white lines indicate reliable decreases in synchronization; colors represent interpolated instantaneous amplitude (SCD). (***A***) Long-range 39-Hz synchronization 300 ms after cue onset for all electrode pairs that include either P7 or P8. (***B***) Time course of synchronization/desynchronization for all electrode pairs throughout the analyzed epoch after presentation of the left and right cues, respectively. (***C***) Time course of the second lateralized gamma burst following the left cue for all pairs that include P7 or P8. (***D***) Time course of the second gamma burst following the right cue for all pairs that include P7 or P8.

In addition to the changes in long-range gamma-band synchrony just described, we observed a reduction in the local (standardized) amplitude of the signal in the alpha frequency band (8–12 Hz) occurring from about 200 to 650 ms after cue onset over the left visual cortex and from cue onset until about 500 ms after it over the right visual cortex (Figure 2.3). This reduction of alpha-band amplitude coincided with an increase in gamma-band amplitude (Figure 2.3) and with the lateralized gamma-band synchronization patterns described earlier. The decrement in alpha amplitude was, surprisingly, larger at visual electrodes *ipsilateral* to the cued location than at contralateral electrodes. A subsequent reversal was then observed as *greater* alpha-band amplitude was seen at electrodes ipsilateral to the cued location relative to that at contralateral electrodes. This latter effect endured from about 650 ms until about 1000 ms after cue onset over the left visual cortex and from about 500 ms after cue onset until beyond the end of the displayed epoch over the right visual cortex (Figure 2.3) and replicates the pattern reported by Worden et al. (2000). Although also visible in the SCD, plotted data for this result are taken from the scalp potentials because they pertain only to local EEG amplitude (comparable SCD amplitude data can be seen in Supplementary Material A).

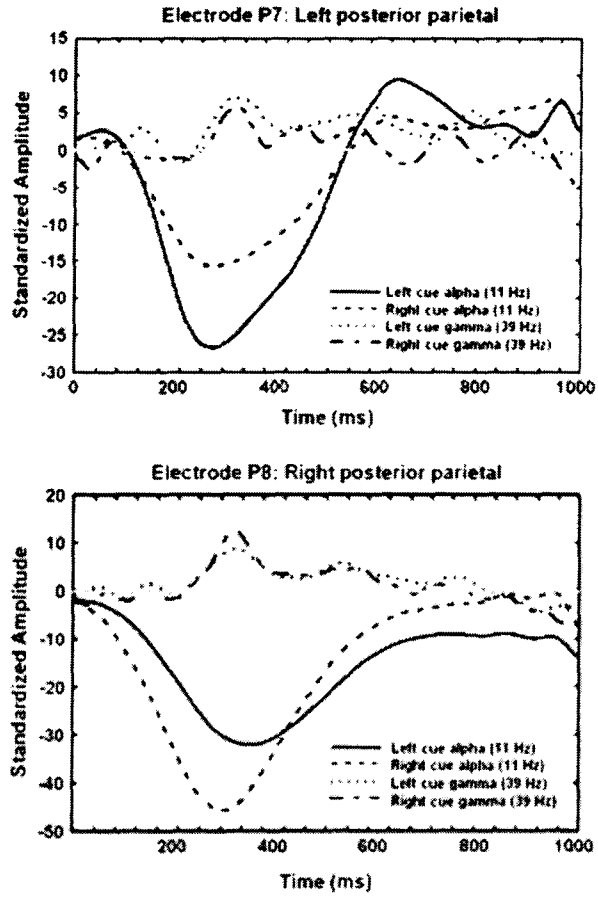

Figure 2.3

Standardized amplitude from filtered (alpha, 11 Hz and gamma, 39 Hz) electrode (P7 and P8) potentials (vertical axes) as a function of time after cue onset (at 0 ms) for the various cue conditions.

The possibility should be considered whether the bursts of lateralized gamma-band synchrony we observed could have arisen from a single oscillating source whose activity could have been volume conducted to several electrodes, for example, a strong local gamma-band activation located in visual cortex contralateral to the cued location. Such a scenario, however, would entail a much greater gamma amplitude increase over contralateral visual cortex than over ipsilateral visual cortex. This was not observed; in fact, gamma amplitude increased more over *ipsilateral* visual cortex than over contralateral visual cortex (see Figures 2.2 and 2.3 and Appendix). For these reasons, we can confidently reject the notion that our lateralized long-range phase synchrony results arose from this kind of volume conduction scenario. Other possibilities are discussed in the Appendix.

An increase in beta-band (15-29 Hz) phase synchronization also was observed from about 220 ms until about 400 ms after the cue onset (see Supplementary Material A). This increased synchronization was strongly anchored at the right occipitoparietal and left frontal electrodes, with strong connectivity linking these 2 regions and increased phase synchrony between these electrodes and other cortical areas. Corresponding local amplitude changes were also evident, with prominent increases in left frontal, right occipitoparietal electrodes, and those over the right frontal areas. The topology of this beta oscillatory network emerged following both the left and the right cue but did not appear to be affected by the direction of attentional deployment.

2.4.2 Event-Related Potentials

The current paradigm was chosen due to its success in a previous study in illuminating changes in local EEG power during selective visual attention (Worden et al. 2000). In that study, electrophysiological measures were used to confirm that attention had been effectively deployed, as no behavioral measures are available in this paradigm, and it is important to any arguments about the mechanism of attention deployment to confirm that attention was indeed deployed as specified to subjects. Worden et al. (2000) did confirm appropriate attention deployment in their study although they based their conclusion only on attentional modulation of the N1 amplitude. They failed to find P1 modulations although some other studies with similar endogenous orienting paradigms have found modulations of both components (e.g., Mangun and Hillyard 1991; Sauseng et al. 2005).

We also confirmed that attention indeed was shifted to the cued location by analyzing ERPs to the targets. Figure 2.4 presents the results of our analyses (see Supplementary Material C). For trials where the stimulus presented was a target, we performed 2 sets of 3-way ANOVAs on the P1 and N1 amplitudes separately: Electrode (P7, P8) x Stimulus side (Left, Right) x Validity (Valid, Invalid) and Electrode (PO7, POz, PO8) x Stimulus side (Left, Right) x Validity (Valid, Invalid).

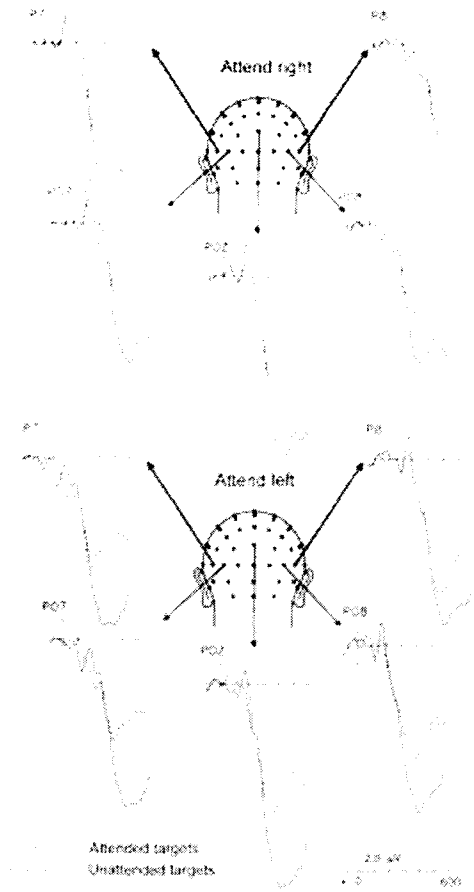

Figure 2.4

ERP waveforms to targets at electrodes P7, P8, PO7, POz, and PO8. Waveforms to targets presented in the right visual field are at the top of the figure; waveforms to targets presented in the left visual field are presented at the bottom of the figure. Note that N1 amplitude to validly cued targets is largest contralateral to target presentation.

Analysis of the N1 component revealed a significant attention modulation, replicating the results of Worden et al. (2000). At electrodes P7 and P8, a significant main effect of validity was found ($F_{1,9} = 5.47$, $P < 0.05$), showing that N1 amplitude was larger on trials where the stimulus appeared in a validly cued location. The interaction of Electrode x Side was also significant ($F_{1,9} = 19.89$, $P < 0.01$), revealing that N1 amplitude was greatest when the stimulus was presented contralateral to the recording electrode. The 3-way interaction between Electrode, Side, and Validity was also significant ($F_{1,9} = 7.49$, $P < 0.05$), indicating that the effect of attention on the N1 was larger on the side contralateral to the cued location.

Analysis of N1 amplitude at electrodes PO7, POz, and PO8 showed the same pattern with a significant main effect of Validity ($F_{1,9} = 6.51$, $P < 0.05$). Also as for electrodes P7 and P8, an interaction between Electrode and Side was found ($F_{2,9} = 24.37$, $P < 0.01$), with larger amplitude to targets presented contralateral to electrodes PO7 and PO8 and larger amplitude at electrode POz to targets presented to the left of fixation. Finally, there was also a significant 3-way interaction between Electrode, Side, and Validity ($F_{2,9} = 5.28$, $P < 0.05$). Analysis of ERPs using only data from the 9 subjects included in the synchrony analysis showed the same patterns of results, confirming that results from the main ERP analysis generalize to the subject group for whom the synchrony results are presented (see Supplementary Material C).

The same analyses showed no attentional modulation of P1 amplitudes, again, as found by Worden et al. (2000). For electrodes P7 and P8, there was no main effect of, nor significant interactions involving, Validity. There was an interaction between Side and

Electrode, with larger P1 amplitude for targets presented contralateral to the electrode ($F_{1,9} = 6.93$, $P < 0.05$). For electrodes PO7, POz, and PO8, as for P7 and P8, the analysis revealed no main effect, nor any interactions involving, Validity. There was, however, an interaction between Side and Electrode ($F_{2,9} = 7.65$, $P < 0.01$), with larger amplitude contralateral to target presentation for electrodes PO7 and PO8 and larger amplitude to targets to the left of fixation at electrode POz.

Although they reveal nothing new about attention orienting in this paradigm, these ERP results do provide convincing evidence that attention was indeed directed to the cued location by the arrow cue and maintained there until target onset. First, as mentioned earlier, previous experiments with similar endogenous attention-orienting paradigms have found that the N1 ERP component is larger when targets are presented in an attended (cued) location than when presented in an unattended location and in particular that the ERP modulation is closely tied to faster responding to the target at the cued location, a more traditional behavioral measure of attention orienting (e.g., Mangun and Hillyard 1991). Our finding of a significantly larger N1 component to targets presented at the cued location is a strong indicator that subjects were reliably shifting their attention to that location when directed to do so by the arrow cue. The fact that we, and Worden et al. (2000), found no significant cue effect on the P1 component in this paradigm does not contradict this interpretation. Modulations of P1 and N1 components are known to be dissociable from one another depending upon the task (e.g., Luck et al. 1990). In endogenous cueing tasks involving stimulus discrimination like the one used in this experiment, Luck et al. (1990) found that whereas the N1 was significantly larger on validly cued trials, this effect was not found for the P1 component. Further, Vogel and

Luck (2000) found evidence that the N1 component is a reflection of the discrimination of visual stimuli; as our task was a visual discrimination task, it is reasonable to understand the modulation of the N1 component to be a reliable indicator of the subjects' successful shift of attention to the cued location.

2.5 Discussion

2.5.1 General Discussion

Cue-directed deployment of attention to one side of the visual field, confirmed by the modulation of the N1 component of the ERP to the subsequent target, coincides with an increase in gamma-band phase synchronization between the contralateral visual cortex and other, widespread cortical areas. Our results support the view that gamma-band synchronization is the mechanism that implements 1) the selective properties of attention (certain neuronal groups are biased for inclusion into the network and others are not), 2) its integrative properties (when neurons corresponding to attended objects' features are included in a long-range network they are more integrated with other perceptual and cognitive representations), and 3) the special relationship between attention and conscious executive processes (inclusion in the network is equivalent to inclusion in a global conscious workspace allowing cognitive and behavioral operations on this information that are informed by other considerations such as goal and context; e.g., Dehaene and Naccache 2001). Synchronously oscillating neurons can perform such integration because they communicate more effectively than do nonsynchronous neurons. Bursts of action potentials from a sending neuron must be consistently received during the depolarized phase of a target neuron's membrane potential fluctuation in order for those action

potentials to be efficacious, and this happens when the sending and receiving neurons are phase locked (Fries 2005). What is still mysterious is how and why synchronization in the various frequency bands plays the role it does. Our results on the relationship between local and long-range synchronization in alpha, beta, and gamma bands begin to address this question.

2.5.2 Gamma-Band Phase Synchronization

The selection and integration of information into a large-scale complex that extends across brain areas has been posited to *be* consciousness (Tononi 2004). We propose that the selection of certain neuronal groups for integration into a large-scale gamma synchronous network accounts for how selective attention enables the increased integration of attended information, relative to unattended information, within and across sensory modalities and biases attended information for higher processing and entry into consciousness (cf., Lamme 2003; Koch and Tsuchiya 2006). In this view, the emergence of a dynamic executive consciousness within the brain may result from a large-scale gamma-synchronous network of task-relevant neural populations. This implements functional integration and serves to activate a specific network from a large repertoire of possible networks. The representational contents of neural groups included in this coherently oscillating network define the content of consciousness and are dynamically assigned according to task demands, perceptual input, and motor output (Varela et al. 2001).

Local brain recordings have demonstrated that synchronously gamma oscillatory cortical columns code figure-ground segregation and the binding of features for the

encoding of global stimulus properties, leading to the proposal that gamma-band synchrony underlies sensory awareness (Gray et al. 1989; Engel, König and Singer 1991; Engel and Singer 2001). Long-range complexes of gamma synchronous brain regions correspond to the emergence of a coherent conscious percept and the binding of local features into a global visual percept (Rodriguez et al. 1999; Doesburg et al. 2005; Rose et al. 2006). Such results show frequency specificity similar to the results reported here, suggesting a common neural mechanism of large-scale integration. Conscious recollection, moreover, is associated with greater gamma-band EEG connectivity than is familiarity (Burgess and Ali 2002). Gamma oscillations are generally restricted to brain states associated with consciousness (waking and rapid eye movement sleep) and are more spatially segregated than low-frequency oscillations present during nonconscious central nervous system states, thereby allowing the increased specificity of information selection required for consciousness (Nunez 1995).

A variety of previous findings support the notion that gamma-band synchrony is relevant for attention and that it is a mechanism for functional integration across brain areas. These include: lateralization of induced gamma-band responses to somatosensory stimulation and visual stimuli can be modulated by selective attention (Gruber et al. 1999; Gobbele et al. 2002); the auditory 40-Hz transient response is larger for attended stimuli than it is for those that are ignored (Tiitinen et al. 1993); intracranial recordings of area V4 in monkeys show greater gamma-band synchronization between neurons activated by an attended stimulus relative to those activated by an unattended stimulus (Fries et al. 2001); intracranial EEG recordings in humans have shown that successful memory formation is associated with greater gamma-band synchronization between the rhinal

cortex and the hippocampus (Fell et al. 2001); increased EEG gamma-band coherence between somatosensory and primary visual areas occurs when subjects learn an association between a finger shock and a visual stimulus (Miltner et al. 1999); gamma-band phase synchronization across posterior electrodes is greater when a stimulus is identified in a fragmented pattern, relative to when a stimulus is not identified (Gruber et al. 2002); EEG phase synchronization between posterior and frontal cortical regions is increased during mental rotation (Bhattacharya et al. 2001); gamma-band activity is increased at frontal and occipitotemporal electrodes during the delay phase of a short-term memory task (Tallon-Baudry et al. 1998); and perceptual grouping is associated with increased gamma-band oscillations in the high gamma band (70–120 Hz) at central occipital locations, whereas the requirement to focus attention on the perceptual groups activates additional low gamma-band (44–66 Hz) oscillations in parietal locations (Vidal et al. 2006).

The prominence of increased long-range gamma-band synchronization at right parietal electrodes in our data strengthens the attentional interpretation of the effect, as the right parietal lobe is particularly relevant for visual attention (Egly et al. 1994), and this area shows increased gamma activity when attentional focusing is required (Vidal et al. 2006). This introduces a theoretical bridge between gamma-band phase synchronization and current knowledge about the functional neuroanatomy of attention. Moreover, coordinated changes in gamma and alpha synchronization are maximal ~280 ms after the onset of the cue, at the time where previous work has shown that behavioral enhancement as a function of attention reaches its zenith (Wright and Ward 1998). Prior to the increase in gamma-band phase synchronization, a period of desynchronization is

also observed in our data beginning when the cue is presented and lasting until about 175 ms after cue onset (Figure 2.2B; see Supplementary Material A for detailed time course). This may reflect phase scattering, a process thought to disrupt existing gamma synchronous neural assemblies in order to enable the emergence of new transient assemblies. Similar patterns have been found preceding transient bursts of increased gamma-band synchronization in coherent perception (Rodriguez et al. 1999; Doesburg et al. 2005). Moreover, stimulus processing can produce either local synchronization or desynchronization in the gamma band depending on task relevance (Mazeheri and Picton 2005). Our analysis of individual subjects' data revealed some instances of global gamma-band desynchronization between visual cortex ipsilateral to the cued hemifield and widespread electrodes (Supplementary Material A). We interpret this as a functional decoupling between cortical regions representing the to-be-ignored location, thus indicating a suppression of unattended information.

Our results indicate that bursts of lateralized gamma-band phase synchronization are transient, occurring about 240–380 ms after cue. Although this is within the predicted time frame for the initiation of endogenous orienting (e.g., Wright and Ward 1998), our subjects were required to maintain their attention at the cued location far beyond the termination of this gamma burst. This suggests that the observed synchronization is related to the deployment of attention to a location but is not required for the maintenance of attention at that location. Bursts of gamma-band phase synchronization related to the onset of a coherent percept have also been found to be short lived relative to the duration of the percept itself (Rodriguez et al. 1999; Doesburg et al. 2005). Large-scale gamma-

band synchronization must therefore be regarded as a mechanism for integrating a functional network rather than one that is responsible for maintaining that integration.

Our analysis revealed a second burst of lateralized long-range gamma synchrony at 520–580 ms after cue onset. This finding echoes earlier findings from coherent perception where a second burst of long-distance gamma-phase synchrony has also been recorded (Rodriguez et al. 1999; Doesburg et al. 2005). The temporal relationship between the first and second burst of gamma synchrony in this, as well as in previous studies, is consistent with a theta frequency (4–7 Hz) cycle. Phase coupling between theta and gamma activity has been observed across brain regions during cognitive processing in studies employing scalp or intracranial EEG and has been interpreted as a mechanism mediating neural communication across long distances (Schack et al. 2002; Canolty et al. 2006). In light of this, it seems likely that the second burst of lateralized long-range gamma synchrony reported here may be related to the maintenance or refinement of the attentional network established by the first burst.

2.5.3 Alpha-Band Amplitude Reduction

Previously it has been shown that shifts of visuospatial attention to locations in one hemifield yield a sustained increase in alpha activation over ipsilateral visual cortical areas beginning around 500 ms after cue onset (Worden et al. 2000; Thut et al. 2006). Our study replicated this result. We also replicated an earlier reduction of alpha activity over both contralateral and ipsilateral visual areas reported by Worden et al. (2000). Our results, however, also indicated that this early reduction was much more pronounced over visual cortex ipsilateral to the attended location. One possible explanation for this

discrepancy between our results and those of Worden et al. (2000) is the several differences in the analysis techniques used. Here we report local activity changes in instantaneous amplitude that are standardized relative to the mean of a precue baseline, whereas studies using temporal spectral evolution, which report lateralization only for the later-occurring alpha-band evolution, plotted the nonstandardized amplitude of the filtered, rectified, and smoothed signal as a function of time (Worden et al. 2000; Thut et al. 2006).

A striking temporal correspondence is evident between the early, bilateral but unequal, decrease of local alpha amplitude, the similar bilateral but unequal increase of local gamma amplitude, and the first burst of lateralized long-distance gamma-band phase synchronization: all these effects were maximal ~300 ms after cue onset. This suggests that the activities of oscillatory mechanisms in multiple frequency bands interact across local and long-distance scales to enable selective visuospatial attention. Specifically, we propose that local alpha-band activity reflects suppression of a cortical area, local gamma-band activity reflects active processing in a cortical area, and long-range gamma synchronization serves to establish a transient network promoting the transfer of information appearing at attended locations from the relevant modality-specific cortical areas (in this case contralateral occipital and posterior temporal cortices) to other cortical regions (cf., Ward 2003). The lateralization effects in local amplitude discussed earlier, however, suggest that the relationship between neural oscillations and attentional processing is more complex, given that gamma-band amplitude is slightly lower in the hemisphere contralateral to the attended location during this period. A possible explanation for this is that when cortical tissue is engaged in a long-range gamma-band

synchronous assembly, increased columnar selection and segregation occur locally, leading to relatively lower gamma-band and relatively higher alpha-band amplitude as a comparatively restricted set of columns are engaged in active processing. In support of this notion, it has been found that cortical stimulation at 40 Hz produces increasingly focal responses (intercolumnar inhibition), whereas 10 Hz stimulation propagates to other cortical areas (Llinás et al. 1998).

If long-distance synchronization between neural groups underlies transient functional integration, as we and others have proposed, then increased long-distance synchronization should be exhibited throughout the period during which the neural populations in question are coupled. In the case of selective attention, this entails synchrony between cortical areas representing attended information and other brain regions throughout the period of attention maintenance. In support of this notion, 2 studies have found evidence for long-duration, long-range coupling of attention-related brain regions in an attention-orienting paradigm. First, in a cued target-discrimination paradigm, increased high–alpha-band phase coupling in the EEG between frontomedial electrodes and parietal electrodes contralateral to the attended hemifield was found to occur during the 200 ms just preceding target onset (Sauseng et al. 2005). Second, our own magnetoencephalographic results using a paradigm identical to the experiment reported here showed increased long-distance high–alpha-band phase synchronization between sensors over occipital cortex contralateral to the cued location and sensors over other, widespread cortical regions beginning ~500 ms after cue onset and lasting throughout the period of attentional maintenance (Doesburg and Ward 2007). Moreover, we also observed an initial, bilateral, long-range desynchronization in the alpha-band

peaking around 280 ms after cue onset. The tight correspondence of these effects with the amplitude changes in the alpha band described here suggests that an alpha oscillatory mechanism involving local desynchronization and long-range synchronization is responsible for the maintenance of selective attention.

2.5.4 Beta-Band Attention Network

Previous magnetoencephalographic results from an attention blink paradigm have shown that when subjects were able to successfully report perceiving the second of 2 successive targets in a rapid-serial-visual-presentation stream, compared with trials on which perception of the second target was not reported, synchronization of a beta-band oscillatory network was observed between the right cingulum, right posterior parietal lobe, and left frontal areas shortly after the second target was presented (Gross et al. 2004). A long-range beta oscillatory network bearing a similar topography and time course was also present in our data (see Supplementary Material A). This effect was maximal at about 18 Hz, did not vary according to the direction of attentional deployment, and reached its maximum during the peak of the lateralized gamma-band synchronization. This suggests that this beta synchronous network is of general relevance for attentional deployment and that this mechanism operates in tandem with gamma-band oscillations. The pattern of interactions between the gamma-band and beta-band networks is still to be explored. On the basis of these results, however, we postulate that the beta-band network is a general mechanism that implements attentional preparation, or readiness, whereas the gamma-band network selects task-relevant neural populations and integrates them into a transient functional network.

2.6 Appendix: Volume Conduction

In the context of EEG and MEG recordings of brain activity, volume conduction refers to the propensity for electric or magnetic fields to be transmitted from an electrical source through the tissues of the brain, skull, and scalp to sensors distributed over a wide area on or near the scalp. The problem has been considered extensively in the context of source analysis in EEG and MEG. Here the well-characterized inverse problem is to reconstruct the primary current distribution within the brain from the electric or magnetic fields measured on or near the scalp. Extensive modeling and sophisticated algorithms have made this problem less of an issue in recent times. In the context of the analysis of neural phase synchrony, however, much less work has been done and the possibility of volume conduction creating spurious synchronies remains a serious consideration.

The most extensive research relevant to this problem was done by Lachaux et al. (1999). They defined and investigated, in the context of intracranial EEG recordings, the measure of PLV used here. They also specifically addressed the possibility of spurious synchrony indicated by this measure arising from volume conduction and concluded that long-range synchronies were unlikely to arise because of this effect. This conclusion was based on both direct measurements of PLV at intracranial electrodes spaced at 1 cm intervals, over which volume-conduction–induced spurious synchrony did not extend further than 2 cm in normal tissue, and on simulations using local field potential recordings from a subject as dipole sources and forward calculating the resulting scalp potential using a 3-layer spherical head model. In the simulation, they calculated PLV for scalp potential, SCD (the local second spatial derivative of the scalp potential), and

electrocorticogram (ECoG, obtained from a deblurring technique introduced by Le and Gevins 1993) for scalp electrodes at various positions relative to the 2 radial dipole sources, which were located in separate hemispheres around the midline. Both the SCD and the deblurred ECoG sharpened synchronous regions in the simulations and reduced spurious synchronies relative to those calculated for the scalp potential. They had this effect because both reduce the overlap of the volumes recorded by different scalp electrodes, in particular eliminating the contributions of deep sources and shrinking the surface areas of the scalp affected by shallow sources. In addition, another study by Nunez et al. (1997) also found that SCD or ECoG reduced the effects of volume conduction on coherence between scalp electrodes at various distances (which includes but is not the same as phase synchrony because coherence is also influenced by amplitude correlation), with spurious coherence dropping to near zero when scalp electrodes were separated by 4 cm or more.

The studies of Lachaux et al. (1999) were based on instantaneous phase and instantaneous amplitude obtained from convolving a Morlet wavelet of appropriate frequency interval with the EEG signals. An alternative approach, and the one we use here, is to obtain these quantities from the analytic signal, based on the Hilbert transform, for the filtered EEG signals (Tass et al. 1998). Le Van Quyen et al. (2001) directly compared the 2 methods for analysis of neural synchrony for data from neuronal models, intracranial EEG, and scalp EEG and found that they were essentially equivalent. We have also analyzed some of our other data using both methods, but we found the areas of synchrony to be more sharply delineated with the Hilbert transform–based technique, so we used that technique here.

To set the problem of volume conduction effects on neural synchrony measured by sensors more sharply, consider the simple case simulated by Lachaux et al. (1999). We have two radial dipoles oscillating at some frequency, call them x_1 and x_2, located at some distance from one another, recorded by two electrodes, each near to one of the sources. The dipoles generate signals

$$x_1 = a_1 \exp i(\omega t + \phi_1)$$

$$x_2 = a_2 \exp i(\omega t + \phi_2) \qquad \text{(A1)}$$

where $i = \sqrt{-1}$, a_1 and a_2 are the amplitudes of the signals, ϕ_1 and ϕ_2 are the respective phase angles, and ω is the common frequency (for clarity, we are assuming noiseless signals with constant phase offset; however, the results apply to the averages of noisy signals). The signals actually recorded by the electrodes are affected by the conductivity of the brain, skull, and scalp (here assumed to be one constant, average value, c) and the distance of electrode j from source k (d_{jk}), so that the recordings can be written as

$$e_1 = \frac{c}{d_{11}^2} x_1 + \frac{c}{d_{12}^2} x_2$$

$$e_2 = \frac{c}{d_{21}^2} x_1 + \frac{c}{d_{22}^2} x_2 \qquad \text{(A2)}$$

Because the conductivity and distance are constants and substituting for x_1 and x_2 from equations A1, we can write

$$e_1 = a_{11}' \exp i(\omega t + \phi_1) + a_{12}' \exp i(\omega t + \phi_2)$$

$$e_2 = a_{21}' \exp i(\omega t + \phi_1) + a_{22}' \exp i(\omega t + \phi_2) \qquad \text{(A3)}$$

and summing the signals for each electrode using the rules of vector addition, we obtain

$$e_1 = a'_{1\bullet} \exp i(\omega t + \phi_{1\bullet})$$

$$e_2 = a'_{2\bullet} \exp i(\omega t + \phi_{2\bullet}) \qquad \text{(A4)}$$

where the dots (e.g., $a'_{1\bullet}$) indicate the sums across sources and where

$$a'_{1\bullet} = \left[(a'_{11}\cos\phi_1 + a'_{12}\cos\phi_2)^2 + (a'_{11}\sin\phi_1 + a'_{12}\sin\phi_2)^2\right]^{1/2}$$

$$a'_{2\bullet} = \left[(a'_{21}\cos\phi_1 + a'_{22}\cos\phi_2)^2 + (a'_{21}\sin\phi_1 + a'_{22}\sin\phi_2)^2\right]^{1/2} \qquad \text{(A5)}$$

and

$$\phi_{1\bullet} = \arctan\left[\frac{a'_{11}\sin\phi_1 + a'_{12}\sin\phi_2}{a'_{11}\cos\phi_1 + a'_{12}\cos\phi_2}\right]$$

$$\phi_{2\bullet} = \arctan\left[\frac{a'_{21}\sin\phi_1 + a'_{22}\sin\phi_2}{a'_{21}\cos\phi_1 + a'_{22}\cos\phi_2}\right] \qquad \text{(A6)}$$

These expressions (A1–A6) readily generalize to any number of sources. When we add these electrode recordings to i times their Hilbert transforms to obtain the analytic signal (see Methods), we obtain

$$\varsigma_1 = e_1 + i\tilde{e}_1 = A_1 \exp i\phi_{1\bullet}$$

$$\varsigma_2 = e_2 + i\tilde{e}_2 = A_2 \exp i\phi_{2\bullet} \qquad \text{(A7)}$$

where $A_1 = a'_{1\bullet}$ and $A_2 = a'_{2\bullet}$. Recall that

$$PLV_{j,k,t} = N^{-1}\left|\sum_{N} e^{i[\phi_j(t)-\phi_k(t)]}\right|$$

so that given the above development (i.e., especially eq. A6), and $\phi_j(t) = \phi_{1\bullet}$ and $\phi_k(t) = \phi_{2\bullet}$ for any specific time t,

$$PLV_{1,2,t,} = f(a_1, a_2, \phi_1, \phi_2)$$

This means that raw PLV depends on the relative amplitudes of the 2 sources as well as the constancy of their relative phases across trials. For this reason, we use the standardized PLV_z to eliminate the volume conduction effects of sources whose amplitudes do not change from those in the baseline period (see Methods). For PLV_z to be different from zero, one (or possibly both) of 2 things must happen: 1) $\phi_1 - \phi_2$ must become more (or less) constant across trials, making $\phi_{1\bullet} - \phi_{2\bullet}$ also more (or less) constant across trials (true synchronization or desynchronization) or 2) the amplitude of one source must increase (or decrease) reliably across trials and by enough that both $\phi_{1\bullet}$ and $\phi_{2\bullet}$ now contain significantly more (or less) contribution from that particular source, thus making $\phi_{1\bullet} - \phi_{2\bullet}$ more (or less) constant across trials (spurious synchrony caused by volume conduction). The latter could happen either because a source that is already active becomes more (or less) active reliably across trials or because a source that is inactive during the baseline is reliably activated by the task during part of the analyzed epoch. This means that spurious, volume-conducted synchrony does not appear in the absence of changes in local amplitude. For this reason, we emphasize inspection of both PLV_z and local amplitude in our interpretation of synchrony changes. In particular, the lateralized

changes we found in 39 Hz PLV_z anchored at P7 and P8 occurring at approximately 300 ms after cue onset were not accompanied by corresponding changes in local amplitude, so we can be confident that these changes are not spurious (Figs 2 and 4).

2.7 Supplementary Material A: Synchronization at Other Frequencies

2.7.1 Introduction

The current project's data analysis method produces a large data space. Our primary protection against type 1 error is the specificity of our *a priori* hypotheses about our main effect: Lateralized long-distance gamma-band phase synchronization would be found following the directional cue between the visual cortex contralateral to the cued location and other, widespread, cortical areas

The purpose of these supplementary materials is to impress upon the reader that our data set indicates:

a) This effect is robust. It can be seen in frequency bands adjacent to those shown at 39 Hz. Since data were bandpass filtered at 1 Hz intervals and then subjected to PLV analysis results in adjacent frequency bands represent independent calculations, yet capture overlapping neural energies (bandwidth = ± 0.05 of the filtered frequency). That this effect is evidenced across multiple adjacent frequencies confirms that it did not occur by chance, but rather reflects the predicted neural response.

b) This lateralization of long-distance phase synchronization is specific to the frequency band reported and does not exist in other frequency bands.

c) The pattern of long-range 39 Hz desynchronization discussed in the text is shown (as a detailed time course cannot be seen in the figure 2).

d) Normalized SCD at frequencies discussed in the text are presented without indexes of long-distance synchronization/desynchronization for ease of interpretation.

A common legend for the SCD is found at the end of the document. As in the figures provided in the article, black lines indicate statistically significant synchronization while white lines indicate statistically significant desynchronization.

2.7.2 Part a) Lateralized Gamma Synchronization at Frequencies Near 39 Hz

38 Hz SCD PLV: all pairs

Left cue

Right cue

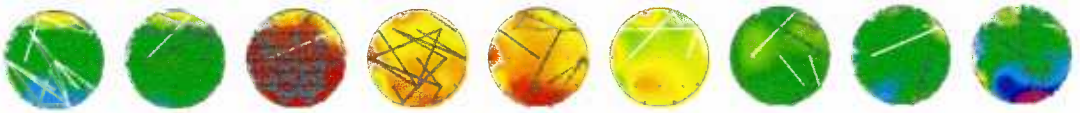

38 Hz SCD PLV: anchor electrode - first gamma burst

Left cue

Right cue

38 Hz SCD PLV: anchor electrode - second gamma burst

Left cue

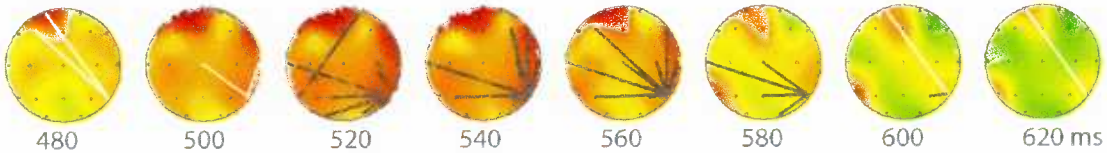

Right cue

40 Hz SCD PLV: all pairs

Left cue

100 200 300 400 500 600 700 800 900 ms

Right cue

100 200 300 400 500 600 700 800 900 ms

40 Hz SCD PLV: anchor electrode - first gamma burst

Left cue

240 260 280 300 320 340 360 380 ms

Right cue

240 260 280 300 320 340 360 380 ms

40 Hz SCD PLV: anchor electrode - second gamma burst

Left cue

480 500 520 540 560 580 600 620 ms

Right cue

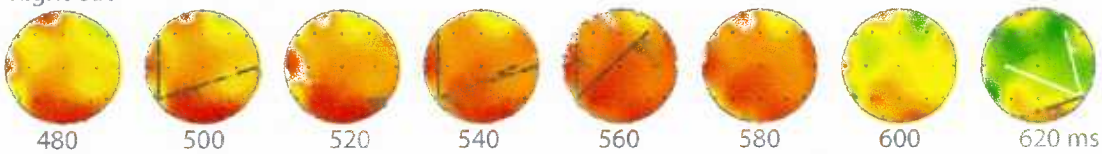

480 500 520 540 560 580 600 620 ms

2.7.3 Part b) Synchronization in Other Frequency Ranges

Long-distance synchronization in other frequency bands demonstrates that our main effect is specific to the gamma band. Plotted frequencies are chosen as they are representative of spectral peaks in the waking human EEG and/or because they represent other bandwidths that have been related to cognitive processing. For the beta-band we also show the pattern long-range synchronization reported in the results section of the article.

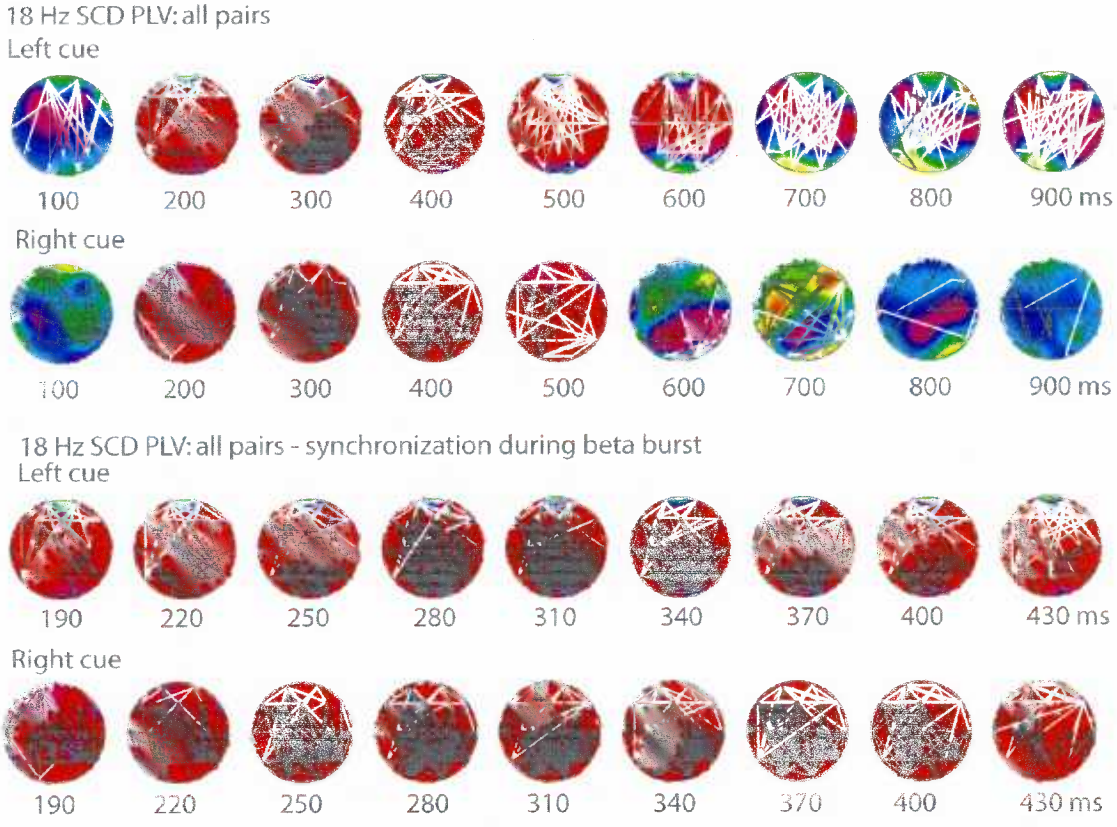

13 Hz SCD PLV: all pairs - high alpha band synchronization

Left cue

100 200 300 400 500 600 700 800 900 ms

Right cue

100 200 300 400 500 600 700 800 900 ms

9 Hz SCD PLV: all pairs - low alpha band synchronization

Left cue

100 200 300 400 500 600 700 800 900 ms

Right cue

100 200 300 400 500 600 700 800 900 ms

6 Hz SCD PLV: all pairs - theta band synchronization

Left cue

100 200 300 400 500 600 700 800 900 ms

Right cue

100 200 300 400 500 600 700 800 900 ms

2.7.4 Part c) Long-range Desynchronization Occurring After Cue Onset

2.7.5 Part d) SCD Topography

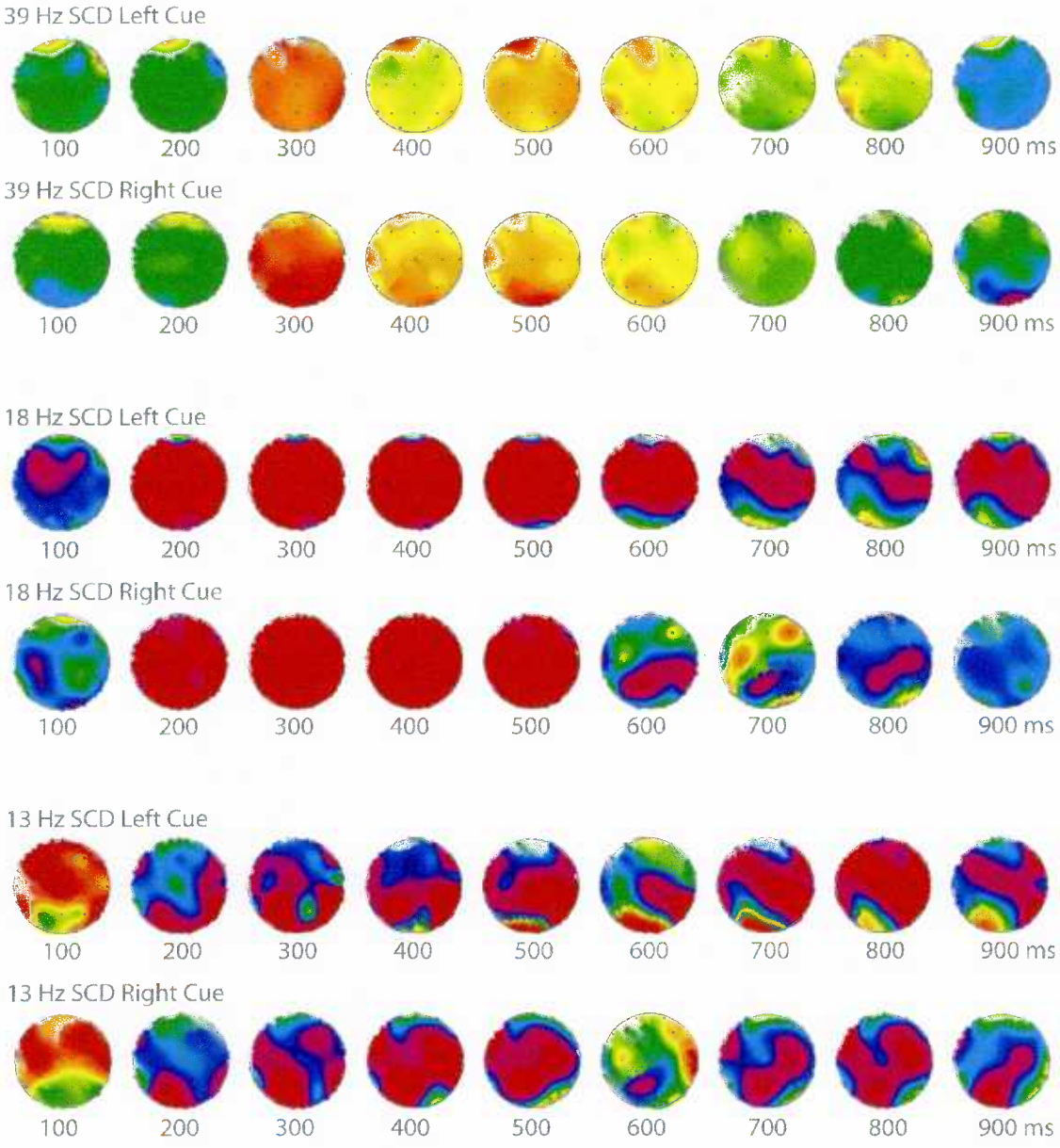

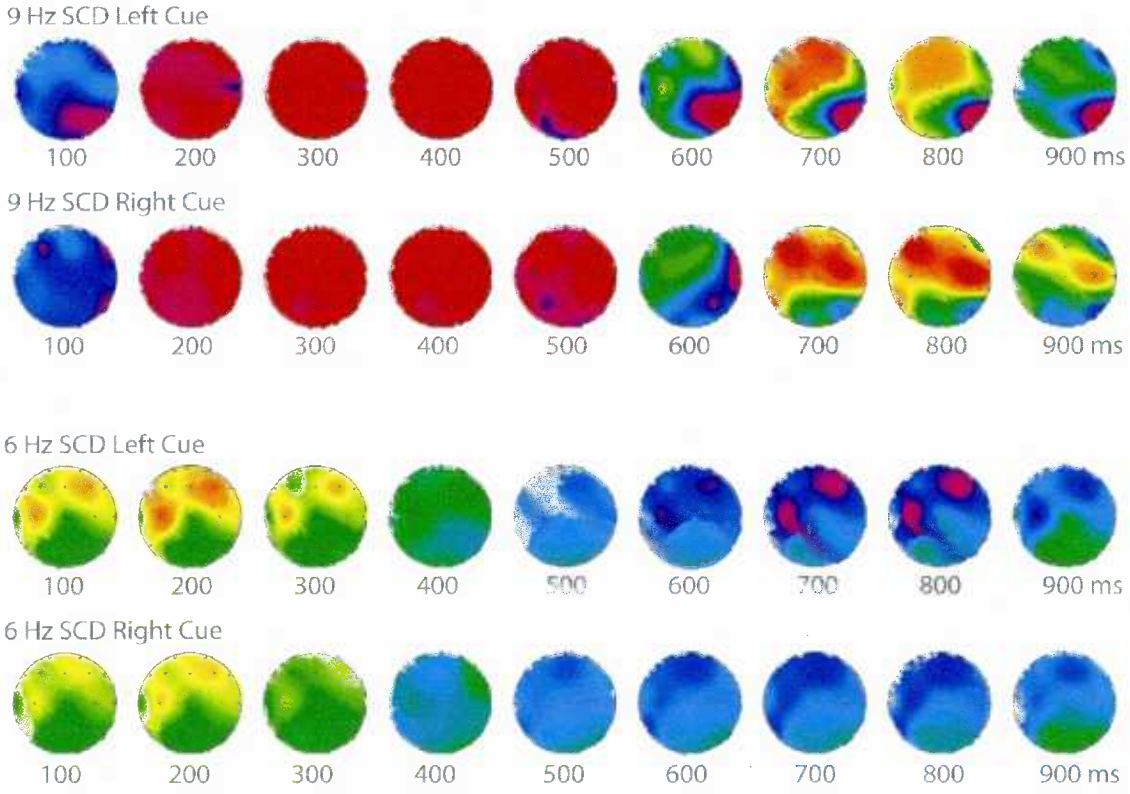
9 Hz SCD Left Cue
100
200
300
400
500
600
700
800
900 ms
9 Hz SCD Right Cue
100
200
300
400
500
600
700
800
900 ms
6 Hz SCD Left Cue
100
200
300
400
500
600
700
800
900 ms
6 Hz SCD Right Cue
100
200
300
400
500
600
700
800
900 ms

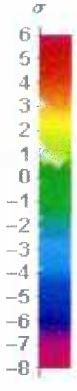
σ
6
5
4
3
2
1
0
−1
−2
−3
−4
−5
−6
−7
−8

2.8 Supplementary Material B: Individual PLV Data

Since data were grouped together and epochs were shuffled across subjects, we analyzed data from individual subjects to assure that our reported main effect was not driven by only one or two subject's data. Subjects from the main analysis who had more than 600 epochs uncontaminated by artifacts surrounding the left and right cues combined were selected for individual analysis. The PLV analysis detailed in the methods section was repeated using individual subject's data using the same statistical criteria reported in the methods section. Synchronization and desynchronization is shown for all pairs including either electrode P7 or P8. The SCD data shown are filtered around 39 Hz and are plotted during the period of where the first burst of lateralized gamma-band synchronization is seen in the group data. Colors represent changes in SCD amplitude. For ease of interpretation, figure 1 displays the lateralization of long-range gamma-band phase synchronization during the first gamma burst for the group data, as well as by data from individual subjects that show characteristic patterns. Individual subject data is subsequently shown for all subjects that were not presented in figure SMB1 (SCD legend is included at the end of this document). These data show that greater gamma-band phase synchronization between the visual cortex contralateral to the attend hemifield is also observed in individual subjects as well as in the group data. Interestingly, for some subjects this lateralization takes the form of desynchronization between the visual cortex ipsilateral to the cued hemifield is seen as well/in place of the main effect. We interpret this as a decoupling between cortical areas representing to-be-ignored information and other brain areas. This could index suppression of the ignored

hemifield, rather than enhancement of information in the attended hemifield, relative to baseline. Data from some subjects show patterns that are less distinct and less organized, as should be expected given that individual subject data suffers from a much lower signal-to-noise ratio.

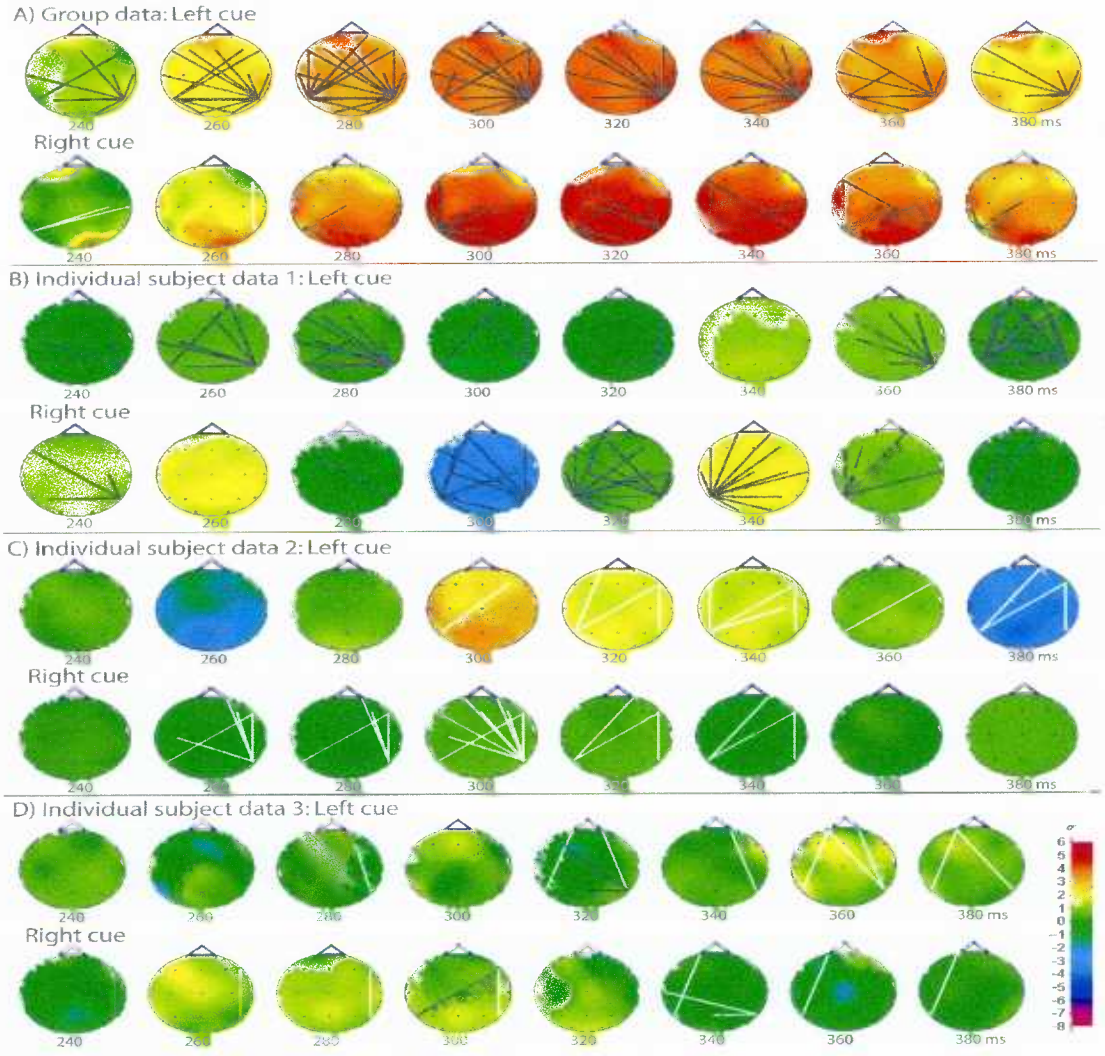

Figure SMB1

Time course of lateralized long-range gamma-band phase synchronization during the first burst for group data and for individual subjects showing representative patterns. (**A**) Lateralization for group data. (**B**) Lateralization from an individual subject showing results similar to the group data (385 left cue epochs; 385 right cue epochs). (**C**) Lateralization from a subject showing desynchronization between visual cortex ipsilateral to the attended location and other, widespread, cortical areas (598 left cue epochs; 386 right cue epochs). (**D**) Data for a subject displaying lateralization patterns that are less organized, and less prominent, than those seen in group data and for some individual subjects (296 left cue epochs; 326 right cue epochs).

Subject 1: 296 left cue epochs; 326 right cue epochs

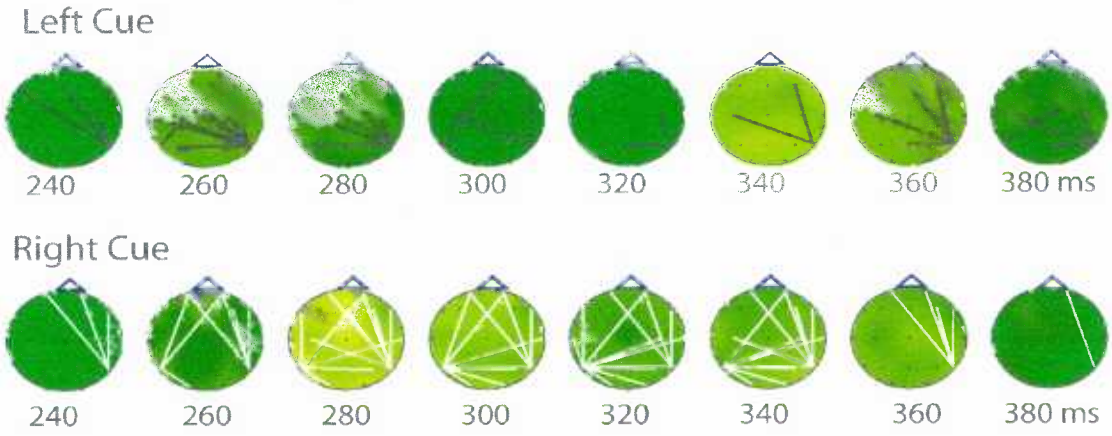

Subject 2: 344 left cue epochs; 494 right cue epochs

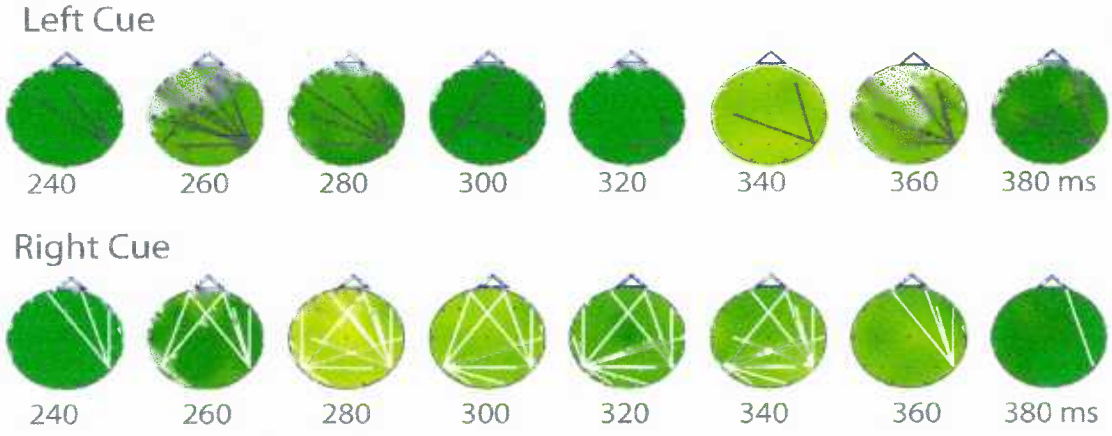

Subject 3: 460 left cue epochs; 494 right cue epochs

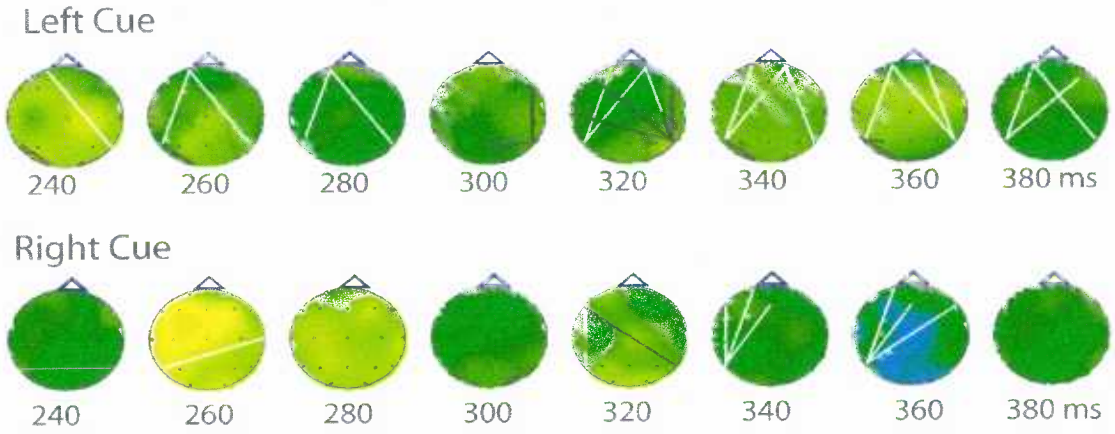

Subject 4: 459 left cue epochs; 448 right cue epochs

Subject 5: 515 left cue epochs; 511 right cue epochs

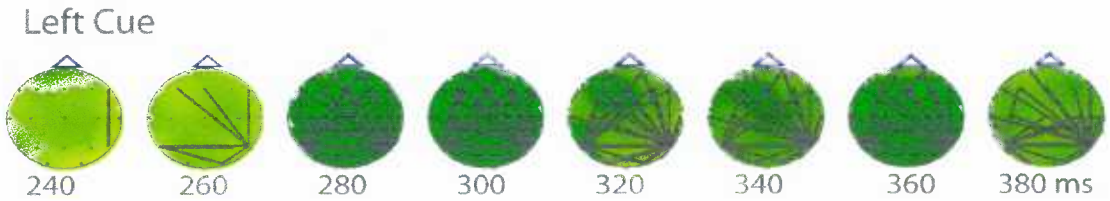

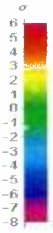

2.9 Supplementary Material C: ERP Results for Subjects used in PLV Analysis

In order to ensure that no spurious ERP effects were found using a subject group that differed slightly from the same group used in the PLV analysis, we also conducted additional analyses using the same subjects as the PLV analysis. The subjects who were excluded from the ERP analysis in the paper were done so for reasons of large number of artifacts in the epoch relevant to ERP analysis. Therefore, those subjects included here who were not in the main ERP group have a smaller number of trials per condition available for ERP analysis, and contribute a greater degree of noise to the signal. This is evident in the poor baseline.

As in the main Results section of the paper, analyses of variance (ANOVAs) were performed separately on the P1 and N1 values for electrodes P7 and P8, and PO7, POz, and PO8. For the P1 component, at electrodes P7 and P8 (Electrode (P7, P8) x Stimulus side (Left, Right) x Validity (Valid, Invalid)), there was a significant three-way interaction between Electrode, Stimulus side, and Validity ($F(1,8) = 5.6$, $p < 0.05$), which showed that P1 amplitude was greater for validly cued targets at electrodes ipsilateral to target presentation. There were no other significant interactions or main effects with Validity for electrodes P7 and P8, nor PO7, POz, and PO8.

While there are clear modulations of the N1 component with attention, with larger N1 amplitude for validly sued targets at electrodes contralateral to target presentation, the ANOVAs for electrode P7 and P8 and PO7, POz, and PO8 revealed only marginally significant three-way interactions of Electrode, Stimulus side, and Validity (P7/P8: $F(1,8) = 2.85$, $p < 0.14$; PO7/POz/PO8: $F(1,8) = 2.24$, $p < 0.14$). This is likely because of the

smaller number of subjects in this group, as well as the poorer signal-to-noise ratio for the ERPs of several of those subjects, than in the group discussed in the main Results section.

Overall, the pattern of findings in the ERPs for the same subjects used in the PLV analysis is highly similar to those of the ERPs in the main Results section, indicating that these subjects were shifting their attention, as indexed by the P1 and N1 modulation, to the cued location (see also Table SMC1).

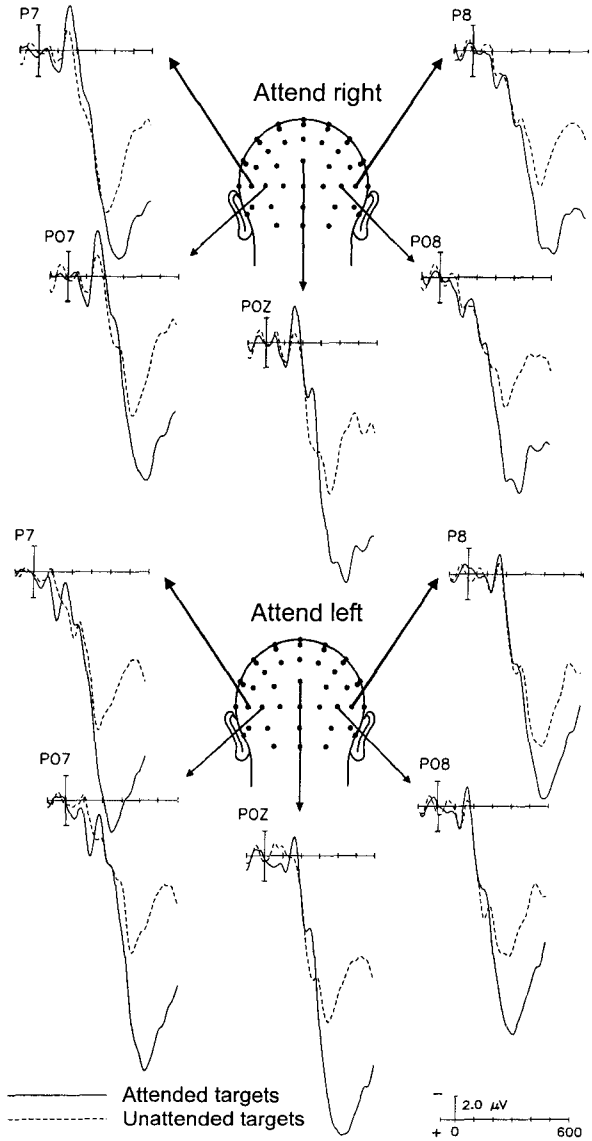

Figure SMC1

ERP waveforms to targets at electrodes P7, P8, PO7, POz, and PO8 for subjects used in PLV analysis. Waveforms to targets presented in the right visual field are at the top of the figure; waveforms to targets presented in the left visual field are presented at the bottom of the figure. Though not statistically significant, note that N1 amplitude to validly cued targets is clearly larger contralateral to target presentation. The lack of statistical significance is primarily due to a lack of power because of the smaller number of subjects in this group.

	P1 amplitude (75 ms – 150 ms)				N1 amplitude (100 – 200 ms)			
	Left Side		Right Side		Left Side		Right Side	
Electrode	Valid	Invalid	Valid	Invalid	Valid	Invalid	Valid	Invalid
P7	4.8 μV	2.7 μV	2.3 μV	2.2 μV	-0.7 μV	-0.5 μV	-4.9 μV	-2.8 μV
P8	2.6 μV	2.2 μV	3.5 μV	2.4 μV	-2.6 μV	-1.3 μV	-0.2 μV	-0.2 μV
PO7	5.4 μV	3.3 μV	3.1 μV	3.0 μV	-0.5 μV	-0.7 μV	-5.4 μV	-3.2 μV
POz	2.9 μV	1.5 μV	2.6 μV	2.3 μV	-2.7 μV	-1.8 μV	-4.2 μV	-1.8 μV
PO8	2.7 μV	2.9 μV	3.7 μV	2.9 μV	-2.7 μV	-1.6 μV	-0.2 μV	0.6 μV

Table SMC1

Means for ERPs analyzed for the subjects included in the main PLV analysis.

2.10 References

Bhattacharya J, Petsche H, Feldmann U, Rescher B. EEG gamma-band phase synchronization between posterior and frontal cortex during mental rotation in humans. Neurosci Lett (2001) 311:29–32.

Burgess AP, Ali L. Functional connectivity of gamma EEG activity is modulated at low frequency during conscious recollection. Int J Psychophysiol (2002) 46(2):91–100.

Canolty RT, Edwards E, Dalal SS, Soltani M, Nagarajan SS, Kirsch HE, Berger MS,

Barbaro NM, Knight RT. High gamma power is phase-locked to theta oscillations in human neocortex. Science (2006) 313:1626–1628.

Dehaene S, Naccache L. Towards a cognitive neuroscience of consciousness: basic evidence and a workspace framework. Cognition (2001) 79:1–37.

Delorme A, Makeig S. EEGLAB: an open source toolbox for analysis of single-trial EEG dynamics. J Neurosci Methods (2004) 134:9–21.

Doesburg SM, Ward LM. Long-distance alpha-band MEG synchronization maintains selective visual attention. International Congress Series 1300 (2007) 551-544.

Doesburg SM, Kitajo K, Ward LM. Increased gamma-band synchrony precedes switching of conscious perceptual objects in binocular rivalry. Neuroreport (2005) 16(11):1139–1142.

Egly R, Diver J, Rafal RD. Shifting visual attention between objects and locations: evidence from normal and parietal lesion subjects. J Exp Psychol Gen (1994) 123:161–177.

Engel AK, König P, Kreiter AK, Singer W. Interhemispheric synchronization of oscillatory neuronal responses in cat visual cortex. Science (1991) 252:1177–1179.

Engel AK, König P, Singer W. Direct physiological evidence for scene segmentation by temporal coding. Proc Natl Acad Sci USA (1991) 88:9136–9140.

Engel AK, Kreiter AK, König P, Singer W. Synchronization of oscillatory neuronal responses between oscillatory neural responses between striate and extrastriate visual cortical areas of the cat. Proc Natl Acad Sci USA (1991) 88:6048–6052.

Engel AK, Singer W. Temporal binging and the neural correlates of sensory awareness. Trends Cogn Sci (2001) 5:16–25.

Fell J, Klaver P, Lehnertz K, Grunwald T, Schaller C, Elger CE, Fernández G. Human memory formation is accompanied by rhinal-hippocampal coupling and decoupling. Nature Neuroscience (2001) 4:1259–1264.

Freeman WJ. Origin, structure, and role of background EEG activity. Part 1. Analytic amplitude. Clin Neurophysiol (2004) 115:2077–2088.

Frein A, Eckhorn R, Bauer R, Woelbern T, Kehr H. Stimulus-specific fast oscillations at zero phase between visual areas V1 and V2 of awake monkey. Neuroreport (1994) 5:2273–2277.

Fries P. A mechanism for cognitive dynamics: neuronal communication through neuronal coherence. Trends Cogn Sci (2005) 9:474–479.

Fries P, Reynolds JH, Rorie AE, Desimone R. Modulation of oscillatory neuronal synchronization by selective visual attention. Science (2001) 291:1506–1507.

Gazzaniga MS, Ivry RB, Mangun GR. Cognitive neuroscience. (2002) 2nd edition. New York: WW Norton.

Gobbele R, Waberski TD, Schmitz S, Strum W, Buchner H. Spatial direction of attention enhances right hemispheric event-related gamma-band synchronization in humans. Neurosci Lett (2002) 327:57–60.

Gray CM, König P, Engel AK, Singer W. Oscillatory responses in cat visual cortex exhibit inter-columnar synchronization which reflects global stimulus properties. Nature (1989) 338:334–337.

Gray CM, Singer W. Stimulus-specific neuronal oscillations in orientation columns of cat visual cortex. Proc Natl Acad Sci USA (1989) 86:1698–1702.

Gross J, Schmitz F, Schnitzler I, Kessler K, Shapiro K, Hommel B, Schnitzler A. Modulation of long-range neural synchrony reflects temporal limitations of visual attention in humans. Proc Natl Acad Sci USA (2004) 101(35):13050–13055.

Gruber T, Müller MM, Keil A. Modulation of induced gamma band responses in a perceptual learning task in the human EEG. J Cogn Neurosci (2002) 14(5):732–744.

Gruber T, Müller MM, Keil A, Elbert T. Selective visual-spatial attention alters induced gamma band responses in the human EEG. Clin Neurophysiol (1999) 110:2074–2085.

Kaiser J, Lutzenberger W. Human gamma-band activity: a window to cognitive processing. Neuroreport (2005) 16(3):207–211.

Kelly SP, Lalor EC, Reilly RB, Foxe JJ. Increases in alpha oscillatory power reflect an active retinotopic mechanism for distracter suppression during sustained visuospatial attention. J Neurophysiol (2006) 95(6):3844–3851.

Koch C, Tsuchiya N. Attention and consciousness: two distinct brain processes. Trends Cogn Sci (2006) 11:16–22.

Lachaux JP, Rodriguez E, Martinerie J, Varela FJ. Measuring phase synchrony in brain signals. Hum Brain Mapp (1999) 8(4):94–208.

Lamme VAF. Why visual attention and awareness are different. Trends Cogn Sci (2003) 7:12–18.

Le J, Gevins A. Method to reduce blur distortion from EEG's using a realistic head model. IEEE Trans Biomed Eng (1993) 40(6):517–528.

Le Van Quyen M, Foucher J, Lachaux J-P, Rodriguez E, Lutz A, Martinerie J, Varela FJ. Comparison of Hilbert transform and wavelet methods for the analysis of neural synchrony. J Neurosci Methods (2001) 111:83–98.

Llinás R, Ribary U, Contreras D, Pedroarena C. The neuronal basis for consciousness. Philos Trans R Soc Lond B Biol Sci (1998) 353(1377):1841–1849.

Luck SJ, Heinze HJ, Mangun GR, Hillyard SA. Visual event-related potentials within bilateral stimulus arrays. Electroencephalogr Clin Neurophysiol (1990) 75:528–542.

Mangun GR, Hillyard SA. Modulation of sensory-evoked brain potentials provide evidence for changes in perceptual processing during visual-spatial priming. J Exp Psychol Hum Percept Perform (1991) 17:1057–1074.

Mazeheri A, Picton TW. EEG spectral dynamics during discrimination of auditory and visual targets. Brain Res Cog Brain Res (2005) 24:81–94.

Miltner WH, Braun C, Arnold M, Witte H, Taub E. Coherence of gamma-band EEG activity as basis for associative learning. Nature (1999) 397:434–436.

Nunez P. Neocortical dynamics and human EEG rhythms. (1995) Cambridge: Oxford University Press. 708.

Nunez PL, Silberstein RB, Shi Z, Carpenter MR, Srinivasan R, Tucker DM, Doran SM, Cadusch PJ, Wijesinghe RS. EEG coherency II: experimental comparisons of multiple measures. Clin Neurophysiol (1999) 110:469–486.

Nunez PL, Srinivasan R, Wetrdorp AF, Wijesinghe RS, Tucker DM, Silberstein RB, Cadusch PJ. EEG coherency I: statistics, reference electrode, volume conduction, Laplacians, cortical imaging and interpretation at multiple scales. EEG Clin Neurophysiol (1997) 103:499–515.

Perrin F, Bertrand O, Pernier J. Scalp current density mapping: value and estimation from potential data. IEEE Trans Biomed Eng (1987) 34:283–288.

Perrin F, Pernier J, Bertrand O, Echalier J. Spherical splines for scalp potential and current density mapping. Electroencephalogr Clin Neurophysiol (1989) 72:184–187.

Pikovski A, Rosenblum M, Kurths J. Synchronization: a universal concept in nonlinear sciences. (2001) Cambridge: Cambridge University Press. 432.

Posner MI, Snyder CRR, Davidson BJ. Attention and the detection of signals. J Exp Psychol (1980) 109:160–174.

Rodriguez E, George N, Lachaux JP, Martinirie J, Renault B, Varela FJ. Perception's shadow: long-distance synchronization of human brain activity. Nature (1999) 397:430–433.

Rose M, Sommer T, Büchel C. Integration of local features to a global percept by neural coupling. Cereb Cortex (2006) 16:1522–1528.

Sauseng P, Klimesch W, Stadler W, Schabus M, Doppelmayr S, Gruber WR, Birbaumer N. A shift of visual spatial attention is selectively associated with human EEG alpha activity. Eur J Neurosci (2005) 22:2917–2926.

Schack B, Vath N, Petsche H, Geissler HG, Moller E. Phase-coupling of theta-gamma EEG rhythms during short term memory processing. Int J Psychophysiol (2002) 44(2):143–163.

Tallon-Baudry C, Bertrand O, Peronet F, Pernier J. Induced γ-band activity during the delay of a visual short-term memory task in humans. J Neurosci (1998) 18:4244–4254.

Tass P, Rosenblum MG, Weule J, Kurths J, Pikovsky A, Volkmann J, Schnitzler, Freund H. Detection of n:m phase locking from noisy data: application to magnetoencephalography. Phys Rev Lett (1998) 81:3291–3294.

Thut G, Nietzel A, Brandt SA, Pascual-Leone A. α-Band electroencephalographic activity over occipital cortex indexes visuospatial attention bias and predicts viosual target detection. J Neurosci (2006) 26:9494–9502.

Tiitinen H, Sinkkonen J, Reinikainen K, Alho K, Lavikainen J, Naatanen R. Selective attention enhances the auditory 40-Hz transient response in humans. Science (1993) 291:1560–1563.

Tononi G. An information integration theory of consciousness. BMC Neurosci (2004) 5(1):42.

Treisman A. The binding problem. Curr Opin Neurobiol (1996) 6:171–178.

Varela F, Lachaux JP, Rodriguez E, Martinerie J. The brainweb: phase synchronization and large-scale integration. Nat Rev Neurosci (2001) 2(4):229–239.

Vidal JR, Chaumon M, O'Regan JK, Tallon-Baudry C. Visual grouping and the focusing of attention induce gamma-band oscillations at different frequencies in human magnetoencephalogram signals. J Cogn Neurosci (2006) 18:1850–1862.

Vogel EK, Luck SJ. The visual N1 component as an index of a discrimination process. Psychophysiol (2000) 37:190–203.

Ward LM. Synchronous neural oscillations and cognitive processes. Trends Cogn Sci (2003) 17:553–559.

Worden MS, Foxe JJ, Wang N, Simpson GV. Anticipatory biasing of visuospatial attention indexed by retinotopically specific α-band electroencephalography increases over occipital cortex. J Neurosci (2000) 20 RC63:1–6.

Wright RD, Ward LM. The control of visual attention. In: Visual attention—Wright RD, ed. (1998) New York: Oxford University Press. 132–186.

CHAPTER 3A: LONG-DISTANCE ALPHA-BAND MEG SYNCHRONIZATION AND SELECTIVE VISUAL ATTENTION[2]

3.1 Abstract

An emerging body of evidence suggests that the brain's ability to produce a transient functional network relies on oscillatory synchronization between task-relevant brain regions. Human attention requires that its object be selected from among others, and that the representation of the attended object be effectively integrated with information in other brain areas mediating higher cognitive processing. MEG data were recorded while subjects were engaged in a task requiring attending to one visual hemifield on any given trial, and phase locking was calculated between sensors over widespread brain regions. Increased phase synchronization in the high-alpha band was found between sensors over visual cortex contralateral to the attended location and other, widespread brain regions. These and other data suggest that neural synchronization mediates the maintenance of a transient network of coupled cortical regions allowing for the enhanced processing of attended information.

3.2 Introduction

Impressive strides have been made toward understanding the functional anatomy of the brain. How the brain is able dynamically to assign functional connectivity between its various regions to support the plethora of cognitive acts that characterize human life, however, remains largely unknown. Understanding the emergence of integrated

[2] A version of chapter 3A has been published. Doesburg SM, Ward LM. Long-distance alpha-band MEG synchronization maintains selective visual attention. International Congress Series 1300 (2007) 551-554. Differences between chapter 3A and the published version are in formatting only.

perception and a unified actor from a distributed population of neurons is critical to explaining how the brain gives rise to higher cognitive processes. Oscillatory synchronization has been proposed as the mechanism underlying transient functional coupling between brain areas and feature binding in sensory awareness (Varela et al. 2001; Engel and Singer 2001). In this view, neurons that oscillate in synchrony consistently exchange bursts of action potentials during the depolarized phase of the target neurons' membrane potential fluctuation, thereby enabling effective communication (Fries 2005).

A prototype for transient functional coupling is the process of selective attention. Attention is integrative because it serves to select certain information for consciousness, for processing in higher cortical areas, and for more effective integration with features represented in other sensory cortical areas. Selective attention must first be deployed to, and then maintained at, an attended spatial location. We propose that these attention mechanisms are implemented via phase synchronization of the brain areas representing attended information with other relevant cortical regions. In an earlier EEG study we found that cue-directed deployment of attention to one side of the visual field induces a transient increase of gamma-band phase synchronization around 300 ms after cue onset between electrodes over the contralateral visual cortex and other, widespread cortical areas (Doesburg et al. 2008). We interpreted this burst of gamma-band synchronization to be the mechanism that implements attention deployment by establishing a cortical network that enables enhanced processing of attended contents. We also observed a bilateral reduction in alpha-band amplitude and an increase in gamma-band amplitude at the same electrodes and in the same time frame as the burst of long-range gamma-band

synchronization, implicating these activities in the establishment of the cortical attention network. If long-range (4+ cm) synchronization of relevant neural groups underlies the brain's ability to selectively attend, however, then both the deployment and maintenance of attention must induce increased long-distance synchrony between areas representing attended information and other, widespread, cortical areas. While a later, sustained, lateralization of alpha amplitude was observed, no such changes were detected in long-range synchronization. Since MEG is more sensitive to certain neural generators, more efficacious for revealing oscillations in lower frequency bands, and less susceptible to volume conduction, we endeavoured to further explore the relationship between brain synchronization and attention using neuromagnetic recordings. MEG data were recorded as subjects were engaged in the same attention orienting task used in the EEG study.

3.3 Methods

On each trial, a 100 ms-duration arrow cue appeared at a central fixation point to direct subjects' covert attention either to a box at the lower left or to one at the lower right of the visual field. Either a target or a nontarget (50/50% probability) appeared in one of the two boxes (50/50% probability) 1000–1200 ms after cue onset. Subjects responded only to targets (e.g. +) occurring in the cued box. Stimuli were presented in the lower visual field as this has previously been demonstrated to be more effective for eliciting attentional modulation of neural oscillations (Worden et al. 2000). Data were digitized at 600 Hz from 151 sensors in a CTF MEG system. Artefact-free epochs were extracted from 19 sensors evenly-distributed about the scalp ($\geq$ 4 cm apart) and matching electrodes analysed in the EEG study from 400 ms before the cue until 1200 ms after it,

resulting in 2556 left cue and 2806 right cue epochs combined from six subjects (4 female; mean age = 25.67, SD ± 5.82). Data were bandpass filtered at 1 Hz intervals from 6–60 Hz (bandwidth = ± 0.05 times the filtered frequency). The analytic signal ($\varsigma(t) = f(t) + i\tilde{f}(t) = A(t)e^{i\phi(t)}$) of each filtered waveform $f(t)$ was calculated to obtain the instantaneous phase $\phi(t)$ and amplitude $A(t)$ at each sample point. PLVs ($PLV_{j,k,t} = N^{-1}\left|\sum_{N} e^{i[\phi_j(t)-\phi_k(t)]}\right|$) were calculated from the instantaneous phases of pairs of sensors and normalized relative to a 200 ms pre-cue baseline. Statistical significance was assessed relative to surrogate distributions of normalized PLV*z* values: a measured PLV*z* above the 97.5th or below the 2.5th percentile of the relevant surrogate distribution was considered to be a significant increase or decrease in synchronization, respectively.

3.4 Results

A sustained increase of long-range phase synchronization in the high-alpha band was observed between sensors over the visual cortex contralateral to the attended location and other, widespread cortical areas from ~ 500 ms after cue onset until the end of the analysed epoch (Figure 3.1). This lateralized increase of long-range high-alpha synchronization was coupled with a decrease in synchronization between sensors over visual cortex ipsilateral to the cued location and many other brain regions (Figure 3.2). This reflects the functional coupling of cortical areas representing attended locations with widespread cortical areas, while cortical areas representing the to-be-ignored hemifield are functionally decoupled from the rest of the cortex. These results do not reflect volume

conduction from local oscillatory activity given the distance between sensors, the analysis techniques used, and the insensitivity of MEG to volume conduction (Nunez et al. 1999).

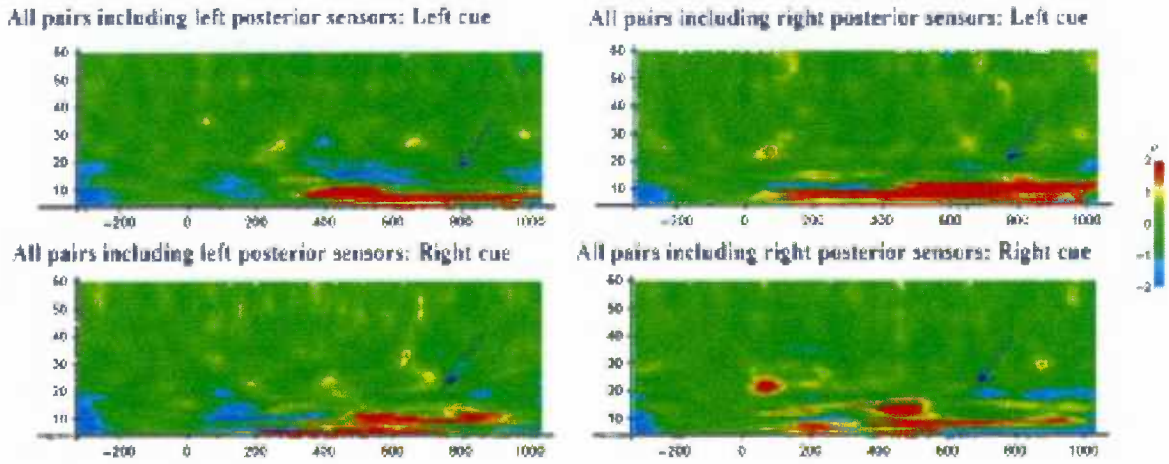

Figure 3.1

Normalized phase locking values as a function of time (horizontal axis) and frequency (vertical axis) for all pairs of sensors including any sensors over the left visual cortex (all pairs including sensors LO41, LO22 & LO43), or right visual cortex (all pairs including sensors RO41, RO22 & RO43), respectively. Arrows indicate the sustained increase in long-range high-alpha band synchronization between sensors over the visual cortex *contralateral* to the attended location and those over the rest of the head, or the lack of high-alpha band synchronization between sensors *ipsilateral* to the attended location and those over the rest of the head.

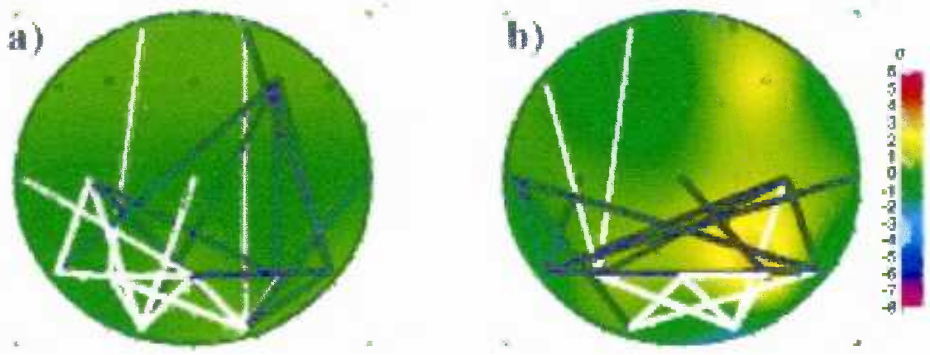

Figure 3.2

Statistically significant 14 Hz synchronization (black lines) and desynchronization (white lines) 800 ms after the onset of a) the left cue, b) the right cue for all pairs including sensors over the left or right visual cortex. Colours represent normalized instantaneous amplitude according to the scale at right. (For interpretation of the references to colour in this figure legend, the reader is referred to the web version of this article.)

3.5 Discussion

We propose that deployment of attention is enabled by transient gamma-band synchrony which establishes functional integration between brain areas, whereas the maintenance of attention involves synchronization of relevant neural populations in the high-alpha band. This early, transient, and lateralized long-distance gamma-band synchrony was visible in our EEG recordings, while the sustained, lateralized long-range synchronization in the high-alpha band was present in our MEG recordings. This is attributable to the differential sensitivity of EEG and MEG to certain generators and to neural activity in particular frequency bands. Lateralization of long-distance neural synchronization can account for both the integrative and selective properties of attention in this paradigm. Integration of attended contents is enabled because neuronal synchrony acts to enhance communication between neurons (Fries 2005). The synchronization of neural populations coding for attended information with other cortical areas, whilst regions representing ignored information are decoupled from the rest of the brain via desynchronization, accounts for how attention selects the contents of a particular spatial location for higher-order processing and suppresses elaborated processing of contents of non-selected locations. A tight temporal correspondence is present between local changes in high-alpha amplitude in the EEG study and long-distance, lateralized, synchronization in this bandwidth in the MEG data. In the EEG study, an initial bilateral reduction in alpha amplitude was observed peaking $\sim$ 280 ms after cue onset during which amplitude was greater over visual cortex contralateral to the cued location, followed by a period beginning $\sim$ 500 ms post-cue where the pattern reversed: alpha amplitude was greater

ipsilateral to the cued location, as has been reported in previous experiments (Doesburg et al. 2008; Worden et al. 2000). This initial dip in alpha amplitude was greatest during the period of lateralized long-range EEG gamma-band synchronization. In the MEG data an early decrease in high-alpha band phase synchrony is observed between sensors over visual cortex contralateral to the cued location, followed by a sustained increase (above baseline) in long-distance phase synchronization between sensors over the visual cortex contralateral to the cued location, and sensors over the rest of the head (Figure 3.1). These effects inform an emerging view of interacting gamma-band and alpha-band mechanisms active across local and long-range scales in implementing selective attention.

CHAPTER 3B: LONG-DISTANCE PHASE SYNCHRONIZATION BETWEEN ALPHA-BAND SOURCES[3]

3.6 Abstract

Previously, we reported that when selective attention is sustained in one visual hemifield, increased long-distance alpha-band synchronization is observed between magnetoencephalographic (MEG) sensors over visual cortex contralateral to the locus of attention and sensors over other, widespread, cortical regions. We interpreted this effect as an indication that synchronization was occurring between early visual cortex representing the attended location and other brain areas, thereby effecting greater functional coupling and thus serving to enhance the processing of stimuli appearing at the attended location. To test this hypothesis we localized sources of alpha activation using the beamformer technique, and calculated phase synchronization between sources. It was found that although local alpha power was greater ipsilateral to attended locations, long-distance alpha-band synchronization was greater between occipital and parietal cortex contralateral to the attended hemifield. This suggests that local alpha synchronization is relevant for inhibition, while long-range alpha synchronization is relevant for integration.

3.7 Introduction

Deployment of attention to one side of the visual field yields increased alpha EEG activity over the ipsilateral visual cortex (Doesburg et al. 2008; Kelly et al. 2006; Sauseng et al. 2005; Thut et al. 2006; Worden et al. 2000). Recent EEG and MEG

[3] These results were previously reported in a poster at the 2007 Meeting of the Cognitive Neuroscience Society in New York City by Doesburg SM, Herdman AT and Ward LM.

findings have indicated that long-range phase synchronization in the alpha and gamma frequency bands are also involved in the deployment and maintenance of visual attention, respectively (Doesburg et al. 2008; Doesburg and Ward 2007). This suggests that oscillatory synchronization may mediate functional connectivity between brain areas relevant for selective attention. A limitation of these earlier studies, however, is that synchronization was calculated between sensors on or near the scalp, rather than between reconstructed sources of electrical or magnetic activity in brain space. This makes it very difficult to draw inferences about the putative involvement of specific brain regions. As a first step toward illuminating what anatomical networks give rise to the aforementioned synchronization effects we used Synthetic Aperture Magnetometry (SAM) beamformer analysis to localize changes in oscillatory neuromagnetic power underlying endogenous attentional deployments, and calculated phase synchronization between these reconstructed sources. The data presented here are taken from the MEG experiment reported earlier in this chapter (3A). The purpose of the present analysis is to determine whether synchronization patterns observed on the scalp are also evident between sources of brain activity. This demonstration aims to buttress the interpretation that long-distance phase synchronization computed between electrodes or MEG sensors is relevant for visual attention control. To this end, we present preliminary data indicating that attending to one visual hemifield increases alpha- and gamma-band synchronization between contralateral occipital and parietal sources.

3.8 Method

3.8.1 Task

Subjects were engaged in the same attention cueing paradigm described in Chapters 2 and 3A. On each trial an arrow cue appeared at a central fixation cross to instruct subjects to attend covertly either to a box to the left or to the right. Either a target or a nontarget (50/50 probability) appeared in one of the two boxes (50/50 probability) 1000-1200 ms after the cue. Subjects responded only to targets appearing at the cued location.

3.8.2 MEG Recording and SAM Source Analysis

MEG was recorded from six subjects using a 151-sensor CTF system. Epochs were extracted surrounding the left and right cues. SAM acts as a spatial filter that determines activation for a particular voxel in a specified time-frequency window by removing correlations with all other voxels. SAM was used to identify sources in individual subjects' data that showed power increases in the 8–15 Hz frequency range 600-1000 ms after cue onset, relative to a 400 ms pre-cue baseline. This time-frequency window was chosen on the basis of previous results linking oscillatory power changes to selective visuospatial attention (Doesburg et al. 2008; Sauseng et al. 2005; Worden et al. 2000). Sources of increased or decreased alpha power (reflective of local synchronization or desynchronization) were identified in individual subjects' data. Sources showing recurrence across subjects were then identified by visual inspection. Bilateral activation in early occipital cortex and bilateral activation of parietal cortex was

found in the majority of the subject's data. Our initial study was comprised of six subjects. While this proved to be an appropriate number for the statistical determination of synchronization between sensors, it falls considerably short of the number of subjects required for a proper statistical test of source recurrence in SAM data (approximately ten subjects are normally required for this). Moreover, not all subjects showed exactly the same pattern of evident sources. Thus, in order to investigate synchronization between sources in this occipital-parietal network for the available data, subjects were selected who showed activation with a pseudo-t value (t-statistic corrected for depth) greater than 2.0 at each of the four recurrent source locations (bilateral occipital and bilateral parietal) for both left-cue and right-cue conditions. SAM data from two subjects showing distinct and representative sources were selected for phase locking value (PLV) analysis.

3.8.3 Synchronization Analysis

Broadband time series data were extracted from peak voxels of SAM sources and were combined across the 2 subjects (994 left cue and 1023 right cue epochs). Data were bandpass filtered at 1 Hz intervals (bandwidth ± 0.05 times the filtered frequency) between 6 Hz and 60 Hz. The analytic signal ($\varsigma(t) = f(t) + i\tilde{f}(t) = A(t)e^{i\phi(t)}$) of each filtered waveform *f(t)* was calculated to obtain the instantaneous phase $\phi(t)$ and amplitude *A(t)* at each sample point *t*. *PLV*s ($PLV_{j,k,t} = N^{-1}\left|\sum_{N} e^{i[\phi_j(t)-\phi_k(t)]}\right|$) were calculated by comparing the instantaneous phases of pairs of SAM sources, *j* and *k*, and standardizing them relative to a 200 ms pre-cue baseline as described in Chapter 2.

3.9 Results

SAM revealed bilateral alpha sources in occipital cortex and parietal cortex 600 – 1000 ms post-cue. Larger occipital alpha power increases were seen ipsilateral to the cued hemifield. Long-range alpha-band phase synchronization, conversely, was found to be *greater* during this period between occipital and parietal sources *contralateral* to the attended location, as was found in our MEG sensor synchronization analysis (Figure 3.3).

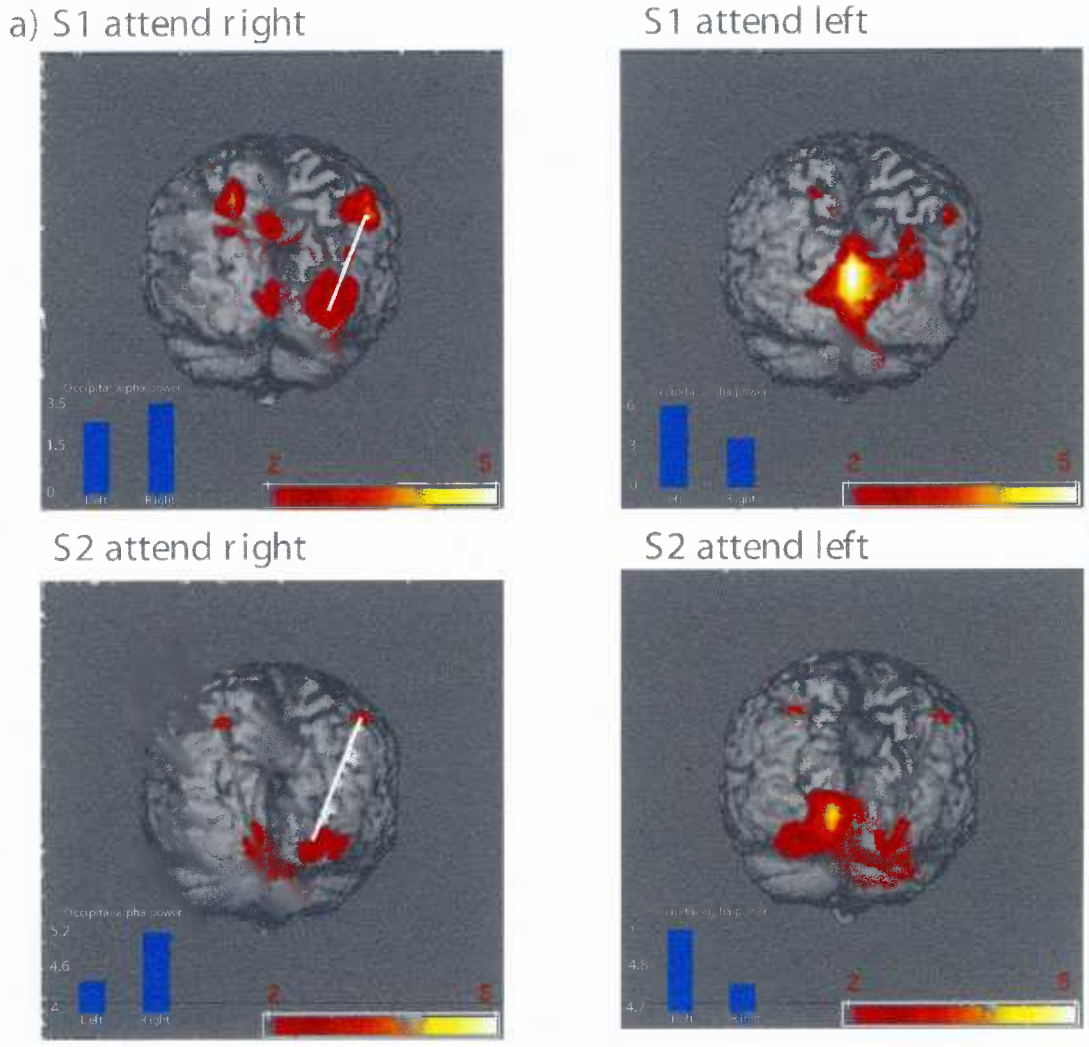

Figure 3.3

Reddish regions represent locations of increased alpha activation for subjects one and two 600-1000 ms after the onset of the right and left cues. Black-red-yellow color scale at bottom right denotes alpha-band power for the four source voxels. Blue bars represent alpha-band power of peak voxels for occipital sources averaged over the 600-1000 ms post cue interval. Power results are reported using a pseudo-T statistic (corrected for depth). Black lines between sources indicate alpha-band synchronization 600 – 1000 ms post-cue while white lines between sources indicated alpha desynchronization during that period (2.5 or more standard deviations above or below baseline). The red stars represent source locations not visible in this surface projection.

Evidence of lateralized long-range synchronization is also seen in the gamma-band with greater synchrony being expressed between occipital and parietal sources contralateral to the cued hemifield (Figure 3.4). Bursts of long-distance gamma-band synchronization and desynchronization, moreover, appear short lived but periodic. This timing of these recurrent gamma-band synchronizations/desynchronizations is consistent with a carrier frequency in the theta band.

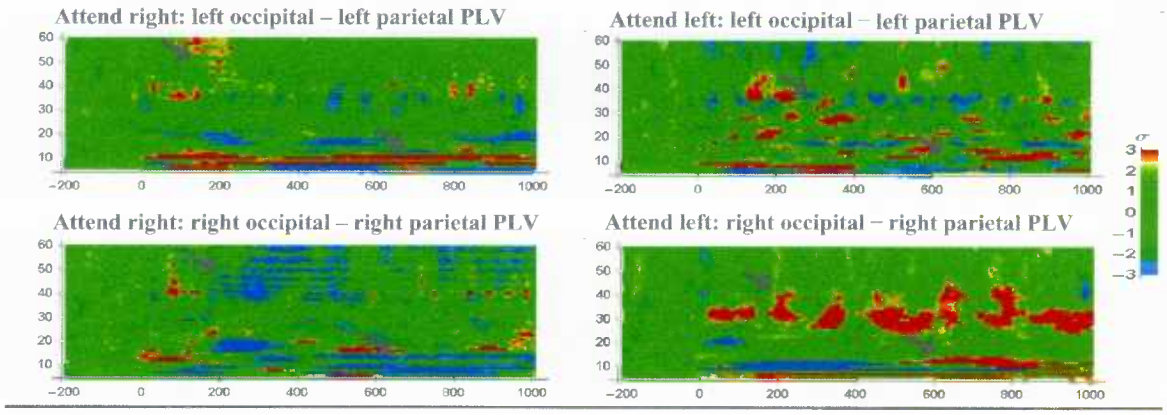

Figure 3.4

Time-frequency plots for lateralized occipital-parietal synchronization following the left and right cues. Arrows indicate lateralized alpha-band synchronization and lateralized gamma-band synchronization. Synchronization and desynchronization are measured in standard deviations of change from the pre-cue baseline, legend at right

3.10 Discussion

We found that alpha power in early occipital cortex (in or near primary visual cortex) was greater ipsilateral to the visual hemifield to which attention was deployed. This lateralization is consistent with previous results obtained from the scalp using EEG (Doesburg et al. 2008; Sauseng et al. 2005; Worden et al. 2000). The localization of this lateralized alpha power is consistent with earlier work that indicates that the sources of these changes are in early visual areas (Yamagishi et al. 2005). Local amplitude measures replicate results from previous research suggesting that increased alpha activity reflects suppression of information in the ignored visual hemifield (Kelly et al. 2006).

Long-distance alpha-band synchronization between occipital and parietal sources, conversely, was found to be greater in the hemisphere contralateral to the cued location. This corroborates our MEG sensor analysis and supports the hypothesis that long distance alpha-band synchrony, like long distance synchrony in higher frequency ranges, is relevant for transient functional integration between brain areas. The dissociation of local and long-range synchronization effects in this paradigm reflects a growing theoretical understanding that while local alpha synchronization appears relevant for inhibition, synchronization of distant brain areas may represent task-dependant coupling (see Klimesch et al. 2007 and Palva and Palva 2007 for reviews).

It was also found that occipital and parietal sources contralateral to the attended location showed increased gamma-band synchronization, relative to ipsilateral sources, consistent with results obtained using scalp EEG (Doesburg et al. 2008). Bursts of long-distance gamma synchronization also appeared to be 'refreshed' at a theta rate, consistent

with the hypothesis that n:m phase locking exists between the theta and gamma cycles, and that this relationship serves to integrate local and long-distance functional integration in the human brain (Canolty et al. 2006; von Stein and Sarnthein 2000). The common interpretation of this relationship is that because conduction delays are greater between more distant neural populations, a slower carrier frequency is required to maintain precise timing relationships needed for neural synchronization to affect functional integration.

These findings support the view that the integrative and selective capacities of attention are accomplished by the synchronization of relevant neural populations. However, a limitation of this preliminary confirmatory analysis is that the number of subjects available was insufficient for complete statistical testing of source recurrence and, as a consequence of that, synchronization effects were tested using data from only two subjects. Confirmation of these effects awaits analysis of synchronization between magnetic or electrical sources using a larger number of subjects.

3.11 References

Canolty RT, Edwards E, Dalal SS, Soltani M, et al. High gamma power is phase-locked to theta oscillations in human neocortex. Science (2006) 313:1626–1628.

Engel AK and Singer W. Temporal binding and the neural correlates of sensory awareness. Trends Cog Sci (2001) 5: 16–25.

Fries P. A mechanism for cognitive dynamics: neuronal communication through neuronal coherence. Trends Cogn. Sci. (2005) 474–479.

Doesburg SM, Roggeveen AB, Kitajo K, Ward LM. Large-scale gamma-band phase synchronization and selective attention. Cer Cortex (2008) 18(2): 386-396.

Doesburg SM, Ward LM. Long-distance alpha-band MEG synchronization maintains selective visual attention. International Congress Series 1300 (2007) 551-544.

Kelly SP, Lalor EC, Reilly RB, Foxe JJ. Increases in alpha oscillatory power reflect an active retinotopic mechanism for distracter suppression during sustained visuospatial attention. J Neurophysiol (2006) 95(6):3844–3851.

Klimesch W, Sauseng P, Hanslmayr S. EEG alpha oscillations: the inhibition timing hypothesis. Brian Res Rev (2007) 53(1):63–88.

Nunez PL, Silberstein RB, Shi Z, Carpenter MR, Srinivasan R et al. EEG coherency II: experimental comparisons of multiple measures. Clin Neurophysiol (1999) 110(3): 469–486.

Palva S, Palva JM. New vistas for alpha-frequency band oscillations. Trends Neurosci (2007) 30(4):150–158.

Sauseng P, Klimesch W, Stadler W, Schabus M, Doppelmayr S, Gruber WR, Birbaumer N. A shift of visual spatial attention is selectively associated with human EEG alpha activity. Eur J Neurosci (2005) 22:2917–2926.

Thut G, Nietzel A, Brandt SA, Pascual-Leone A. α-Band electroencephalographic activity over occipital cortex indexes visuospatial attention bias and predicts viosual target detection. J Neurosci (2006) 26:9494–9502.

Varela F, Lachaux JP, Rodriguez E, Martinerie J. The brainweb: phase synchronization and large-scale integration. Nat Rev Neurosci (2001) 2(4):229–239.

von Stein A, Sarnthein J. Different frequencies for different scales of cortical integration: from local gamma to long range alpha/theta synchronization. Int J Psychophysiol (2000) 38:301–313.

Worden MS, Foxe JJ, Wang N, Simpson GV. Anticipatory biasing of visuospatial attention indexed by retinotopically specific α-band electroencephalography increases over occipital cortex. J Neurosci (2000) 20(6):RC63:1–6.

Yamagishi N, Goda N, Callan DE, Anderson SJ, Kawato M. Attentional shifts towards an expected visual target alter the level of alpha-band oscillatory activity in the calcarine cortex. Cog Brain Res (2005) 25:799-809.

CHAPTER 4: ANTICIPATORY HEMISPHERIC BIASING IN ATTENTION: OCCIPITAL-PARIETAL ALPHA-BAND SYNCHRONIZATION[4]

4.1 Abstract

Neural synchronization has been proposed as a mechanism for the transient functional coupling of cortical regions. Previous work has demonstrated that when selective attention is maintained at a location in one visual hemifield greater alpha-band synchronization is observed between magnetoencephalographic (MEG) sensors over visual cortex contralateral to the locus of attention and other, widespread, sensors (Chapter 3A), and also between neural sources in occipital and parietal cortices (Chapter 3B). To determine whether this synchronization effect could be observed between cortical regions known to be relevant for visuospatial attention, in a larger, and more statistically reliable sample of subjects, and for EEG-recorded neural activity, we applied phase synchronization analysis to an existing data set that had revealed reliable sources of electrical activation in a set of cortical areas known to be relevant for endogenous control of visual attention. We found that alpha-band neural synchronization was greater between primary visual cortex and superior parietal lobule contralateral to the attended visual hemifield. We propose that the observed occipital-parietal synchronization may index the selective aspect of endogenous visuospatial attention orienting, serving to maintain attentional focus on a specific region of visual space.

[4] The results presented here are under preparation for publication in a paper by Doesburg SM, Green JJ, McDonald JJ and Ward LM. These results are based on a reanalysis of data recorded by, and electrical source activations reported in, a separate publication of Green JJ and McDonald JJ (PLoS Biology, in press).

4.2 Introduction

Attending to a location in visual space promotes the processing of stimuli appearing there, relative to stimuli appearing at unattended locations (for example, Luck et al. 1990; Mangun and Hillyard 1991). This effect suggests either that stimuli appearing at attended locations in visual space receive enhanced processing, that the processing of stimuli appearing at ignored locations is inhibited, or both. It has been demonstrated that attending to one side of the visual field produces an anticipatory biasing of the visual cortex, alpha power being greater over visual cortex ipsilateral to the locus of attention (Doesburg et al. 2008; Kelly et al. 2006; Sauseng et al 2005; Thut et al. 2006; Worden et al. 2000). This effect is consistent with a large body of evidence indicating that alpha oscillations within a cortical area reflect inhibitory processing (see Klimesch et al. 2007 for review). More recent research into the role of neural synchronization in cognitive processing has indicated that long-distance synchronization between brain regions could transiently increase communication between those regions (see Varela et al. 2001 for review). In the context of selective attention it has been demonstrated that deployment of attention to one side of visual space increases gamma-band synchronization between electrodes over visual cortex contralateral to the attended location and electrodes over many other brain areas (Doesburg et al. 2008). This transient synchronization is interpreted as indexing the establishment of increased communication within a network of brain areas that will promote the transfer of attended information to higher processing areas. Moreover, it has previously been shown that maintaining visuospatial attention at a location is accompanied by long-distance alpha-band phase synchronization between magnetoencephalographic (MEG) sensors over

visual cortex contralateral to the attended visual hemifield and sensors over other, widespread, cortical areas (Doesburg and Ward 2007). This lateralized long-distance alpha-band synchronization is sustained until target onset and has been posited to be a mechanism for the maintenance of selective attention. To determine the anatomical generators of this observed synchronization, as well as to provide converging evidence that the observed synchronization did not arise from volume conduction, we performed phase locking value (PLV) analysis on previously published data for which the beamformer source analysis technique was used to image cortical regions showing increased theta oscillations during the deployment and maintenance of selective visuospatial attention. A detailed exposition of the task and beamformer source analysis is provided by Green and McDonald (in press). The work presented here is intended as an extension of the source analysis targeted at examining phase locking within an anatomically plausible attention network. Analysis of phase locking between reconstructed theta-band electrical sources revealed that during the period of attention maintenance a greater sustained increase in alpha-band synchronization was observed between primary visual cortex (V1) and superior parietal lobule (SPL) contralateral to the attended visual hemifield, relative to the ipsilateral hemifield. The SPL is a brain area that has been implicated in the endogenous selection of particular regions of visual space by attention (e.g., Corbetta & Shulman, 2002). This result supports the view that the integrative properties of selective attention, as well the propensity for attended information to be promoted for higher processing, arise from increased functional coupling, mediated by neural synchronization, between primary visual cortex

representing attended regions of visual space, and posterior parietal cortex involved with the maintenance of attention selection.

4.3 Method

4.3.1 Data Set

The data presented here are based on an application of PLV analysis to a data set already published elsewhere, and a more detailed description of the experimental paradigm and beamformer source reconstruction is presented in the original publication of these data (Green and McDonald in press). Data recording and source localization analysis were performed at the Human Electrophysiology Laboratory at Simon Fraser University. EEG data were recorded at 500 Hz from 63 scalp electrodes referenced to the right mastoid while 12 neurologically normal subjects performed a covert attention cueing task. This task consisted of a central cue which would, on each trial, instruct subjects to attend to target boxes located above, to the left, or to the right of the cue. Directional cues predicted the location of target with 80% accuracy. Attention was to be maintained at the indicated location for 900 ms until a target appeared in one of the cue boxes. On some trails a neutral cue consisting of a centrally located square would appear directing subjects not to attend to any particular location. Subjects were instructed to discriminate the orientation of a bar which could appear at either cued or uncued locations.

Epochs were extracted time-locked to cue onset and epochs containing the record of ocular and nonocular artifacts were rejected using an automatic rejection algorithm in

the Brain Electrical Source Analysis (BESA) software suite. In order to reconstruct sources of theta activation associated with attention deployment rather than with processing of the cue itself, beamformer analysis was performed using BESA Multiple Source Beamformer analysis software. This method estimates the contribution to scalp activation made by a given voxel, within a specified time-frequency window, while minimizing the contributions of all other voxels. By computing a separate beamformer solution for each point in a three dimensional grid, a spatial filter is implemented to estimate electrical activity at each point in the brain. Beamformer was used to image differences in theta activation between trial conditions (for example, voxels showing more activity in the left cue than the neutral cue trials) in each of 18 consecutive 50 ms intervals between cue and target. In this manner, the anatomical locations of theta activation contributing to voluntary attention control were identified. For a more detailed description of this method see Scherg et al. (2002). More detailed explanation of the behavioural paradigm, as well as the source analyses, are available in the original publication of these data (Green and McDonald in press). The presentation of data here is not intended to fully detail (or receive credit for) this initial work, but rather to use the existing data set to investigate the role of long-distance synchronization between activated sources in selective attention.

4.3.2 Phase Synchronization Analysis

Theta source activations in our data set represent activational differences between trials on which subjects are required to shift their attention and neutral trials on which no shifting of attention is required. As such they represent source electrical activity relevant

for the endogenous control of attention. To investigate synchronization between sources broadband activations were computed for peak voxels for sources identified using the beamformer technique. Epoched data were then band-pass filtered digitally at 1 Hz intervals between 4 and 60 Hz (passband $= f \pm 0.05f$, where f represents the filter frequency). We then calculated the analytic signal

$$\varsigma(t) = f(t) + i\tilde{f}(t) = A(t)e^{i\phi(t)}$$

of the filtered waveform for each epoch, $f(t)$, to obtain the instantaneous phase, $\phi(t)$, and amplitude, $A(t)$, at each sample point, where $\tilde{f}(t)$ is the Hilbert transform of $f(t)$ and $i = \sqrt{-1}$.

We measured long-range neural phase synchrony by calculating phase-locking values (PLVs). PLVs were obtained by comparing the instantaneous phases between pairs of time series from reconstructed theta sources, for example, sources j and k, at each point in time, t, across the N available epochs (Lachaux et al. 1999):

$$PLV_{j,k,t} = N^{-1}\left|\sum_{N} e^{i\left[\phi_j(t)-\phi_k(t)\right]}\right|$$

Our goal was to identify long-distance synchronization effects relevant to visuospatial attention rather than effects relevant to the processing of the cue. To this end, we calculated differences in phase locking between the shift and neutral conditions (i.e. phase locking that was not common to, for example, activity following the right cue and the neutral cue). To accomplish this we calculated phase locking for a given source pair for both an attention shift cue (right directional cue, for example) and also calculated

PLVs between that same pair for the neutral cue condition. The PLVs of both conditions were expressed as a value between 0 (random phase difference, no phase locking) and 1 (constant phase difference, maximum phase locking). PLVs from the neutral cue trials were then subtracted from the PLVs for one of the attention shift conditions. These time series of PLVs indicating differences between conditions were then standardized relative to a 300 ms pre-stimulus baseline. Standardization was performed on the PLV difference time series by subtracting the mean baseline difference PLV from the difference PLV for each data point and dividing by the standard deviation of the baseline difference PLV. The resulting difference PLV_z scores indicate changes from the average baseline difference PLV expressed in units of standard deviation. Large positive or negative values of the difference PLV_z indicate noticeable increases or decreases, respectively, in synchronization between right or left attention shift conditions and the neutral condition where no shift took place.

To assess the statistical reliability of differences in long-range synchronization and desynchronization between conditions we employed the surrogate statistical method (Lachaux et al. 1999). To accomplish this we scrambled the epochs for both of the to-be-compared conditions (e.g., right shift versus neutral). We then computed PLVs for the scrambled data for each frequency and data point combination for each pair of sources. The resulting PLVs were used to create difference PLVs as was done for the unscrambled data. The resulting difference PLVs were then normalized relative to the (scrambled) 300 ms pre-cue baseline. This process was repeated 200 times to create a surrogate distribution for the differences between the conditions being compared. The percentile rankings of real data from the normalized PLV difference values within the surrogate

distributions were used to assess the statistical significance of observed synchronizations and desynchronizations.

4.4 Results

Theta-weighted beamformer analyses revealed several statistically reliable electrical sources in these data. These sources were: bilateral V1, bilateral SPL, bilateral inferior parietal lobule and bilateral medial frontal gyrus. To test our hypothesis that neural synchronization enhances processing of attended information by increasing functional coupling between primary sensory cortex and cortical regions relevant for attention control, we focused on synchronization between V1 and source activations in the SPL, as it has a direct connection to V1 and has been said to exert influence on V1 to select a particular region of the visual field for enhanced processing (e.g., Corbetta & Shulman, 2002). Furthermore, we focused on the left-neutral and right-neutral analyses since lateralization effects should be most evident in this comparison.

Greater alpha-band synchronization was observed between V1 and SPL contralateral to the attended hemifield in the time period preceding target onset (Figure 4.1). Lateralized occipital-parietal synchronization appeared to be centred at two distinct, but nearby, frequency ranges. The strongest lateralized long-range synchronization effects were centred at 9 Hz, while a less pronounced effect was observed centred at 15 Hz. Other instances of synchronization and desynchronization between V1 and SPL are also evident, including those that appear very shortly after the appearance of the cue. It should be noted, however, that such differences do not appear to be systematic and are thus likely not to be interpretable in a theoretically meaningful way. A problem

introduced by analyzing very large data sets with the volume of information typical of those used in EEG synchronization analyses is an increased probability of observing spurious effects. Accordingly, synchronization effects that do not show a reliable, systematic relationship to the task or stimuli are most likely spurious.

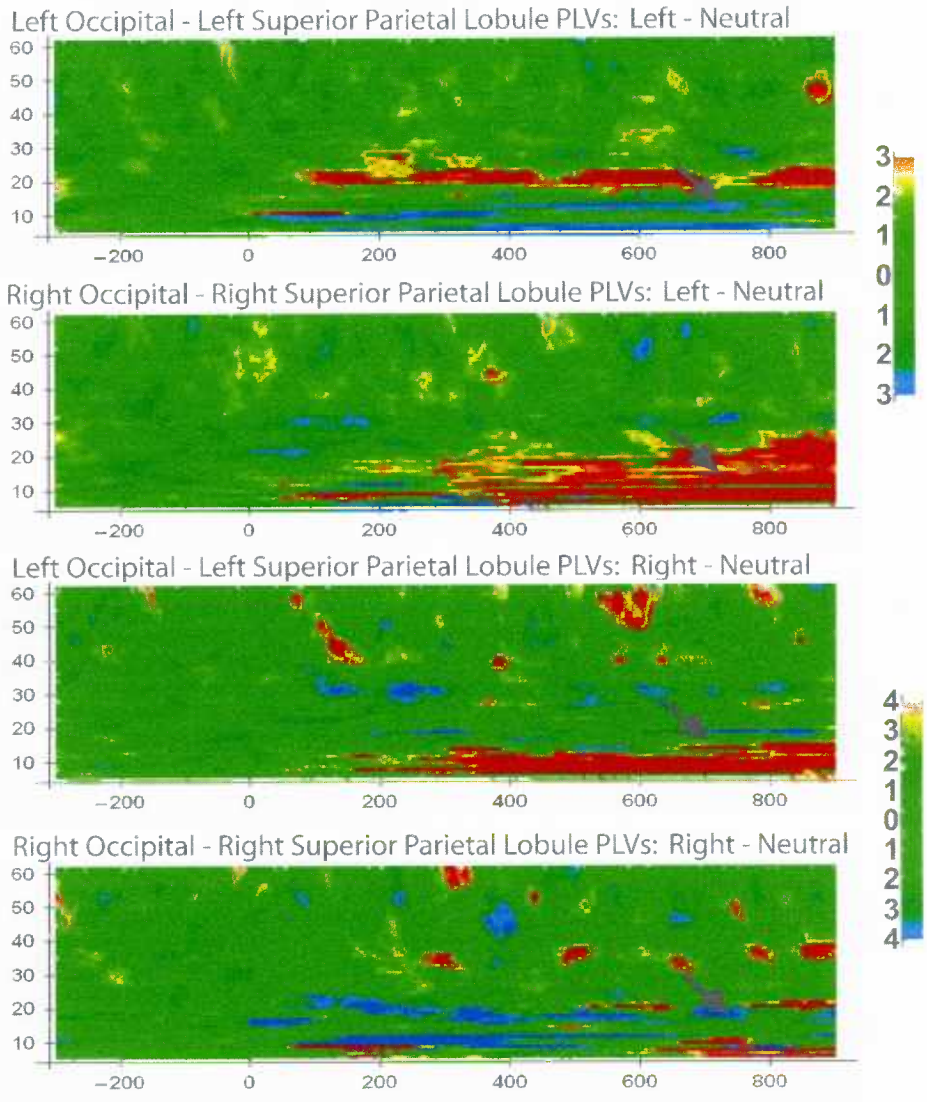

Figure 4.1

Long-distance synchronization between V1 and SPL for left cue minus neutral cue and right cue minus neutral cue analyses. Arrows indicate lateralized cue-locked alpha-band synchronization. Legends at right indicate differences in standard deviations.

Surrogate statistical analysis of synchronization between sources confirmed that alpha-band synchronization between V1 and SPL is greater when attention is paid to the contralateral visual field. This took the form of a wider band of statistically significant synchronizations for the effect centred at 9 Hz, and a more prolonged synchronization and wider bandwidth of synchronization for effect centred at 15 Hz. Synchronization centred at 9 Hz reached statistical significance ($p<0.01$) around 200 ms post cue in both hemispheres following both directional cues. Strong lateralization in the width of the band of synchronized frequencies was, however, seen in the 600-900 ms post cue period: synchronization between left V1 and left SPL for the right-neutral analysis reached significance for frequencies 5-12 Hz while only 6-8 Hz synchronization was observed in the left-neutral analysis; synchronization between right V1 and left SPL reached significance for 5-10 Hz in the left-neutral analysis while only synchronization at 6 Hz is seen in the right-neutral analysis ($p<0.01$). For the lateralized synchronization centred at 15 Hz: left hemisphere V1-SPL synchronization reached significance ~625 ms post cue for the right-neutral analysis and encompassed 13-17 Hz, while for the left-neutral analysis significant synchronization began ~775 ms post-cue and was only seen at 15 Hz. Right hemisphere V1-SPL synchronization, conversely, reached significance ~725 ms post cue and encompasses the 14-16 Hz frequency range for the left-neutral analysis while no statistically significant synchronization was seen for the right-neutral analysis ($p<0.01$).

Lateralization of alpha-band synchronization was also observed between V1 and inferior parietal lobule (IPL). Again, this took the form of greater synchronization contralateral to the attended hemifield. This lateralization, furthermore, preceded the

onset of the target and was sustained (rather then transient or periodic) suggesting this might also be relevant for anticipatory biasing of intracortical communication. The differences were not statistically significant, however, and are not shown for reasons of brevity.

4.5 Discussion

The analysis of phase synchronization between previously identified sources of theta-band activation during endogenous control of visuospatial attention reveals that increased alpha-band synchronization occurs between early visual cortex and superior parietal lobule contralateral to the attended visual hemifield. This confirms that earlier results showing similar patterns of synchronization between MEG sensors near the scalp (Doesburg and Ward 2007) were unlikely to have arisen from a volume conduction scenario wherein activity from a single alpha oscillatory source propagated to multiple sensors. It is also consistent with the results of the analysis in Chapter 3B, where sustained synchronization between occipital and parietal MEG sources was observed in two subjects' data. Moreover, this result demonstrated that lateralized long-distance synchronization during anticipatory attention biasing occurs between brain areas known to be involved in attention control (Corbetta and Shulman 2002). This is consistent with the view that long-distance synchronization may account for the enhanced processing of targets appearing at attended locations as primary sensory cortex representing attended locations benefits from increased functional coupling with cortical regions higher in the visual processing stream mediated by sources in the parietal cortex (Doesburg et al. 2008; Doesburg and Ward 2007). A novel contribution of this study is that lateralization of low

frequency long-distance synchronization occurs in two distinct bands. On the basis of our results, however, it is not possible to determine if these two frequency ranges play distinct roles.

Although the data presented here entail that lateralization of long-range alpha-band synchronization is elicited by attention to one visual hemifield, it should be noted that these sources are reconstructions of theta-band activity. Synchronization analyses reported in earlier chapters, however, were based on broad band signals recorded from scalp electrodes and MEG sensors. For this reason, it is unclear whether all relevant sources of electromagnetic activity were revealed in this analysis. It is therefore impossible to ascertain here whether or not other prominent synchronization effects observed previously might be observed between electrical sources reconstructed according to broad-band activity, or between sources of activation in frequency ranges other than theta. It is interesting, however, that long-distance alpha-synchronization effects were observed between theta weighted sources. This suggest that certain long-range and local synchronization effects might be the result of complex and interrelated mechanisms active within a common brain network.

4.6 References

Corbetta M, Shulman GL. Control of goal-directed and stimulus-driven attention in the brain. Nat Rev Neurosci (2002) 3(3):201-215.

Doesburg SM, Roggeveen AB, Kitajo K, Ward LM. Large-scale gamma-band phase synchronization and selective attention. Cer Cortex (2008) 18(2):386–396.

Doesburg SM, Ward LM. Long-distance alpha-band MEG synchronization maintains selective visual attention. International Congress Series 1300 (2007) 551-544.

Green JJ, McDonald JJ. Electrical Neuroimaging reveals timing of attentional control activity in human brain. PLoS Biology (in press).

Kelly SP, Lalor EC, Reilly RB, Foxe JJ. Increases in alpha oscillatory power reflect an active retinotopic mechanism for distracter suppression during sustained visuospatial attention. J Neurophysiol (2006) 95(6):3844–3851.

Klimesch W, Sauseng P, Hanslmayr S. EEG alpha oscillations: the inhibition timing hypothesis. Brian Res Rev (2007) 53(1):63–88.

Lachaux JP, Rodriguez E, Martinerie J, Varela FJ. Measuring phase synchrony in brain signals. Hum Brain Mapp (1999) 8(4):94–208.

Luck SJ, Heinze HJ, Mangun GR, Hillyard SA. Visual event-related potentials within bilateral stimulus arrays. Electroencephalogr Clin Neurophysiol (1990) 75:528–542.

Mangun GR, Hillyard SA. Modulation of sensory-evoked brain potentials provide evidence for changes in perceptual processing during visual-spatial priming. J Exp Psychol Hum Percept Perform (1991) 17:1057–1074.

Sauseng P, Klimesch W, Stadler W, Schabus M, Doppelmayr S, Gruber WR, Birbaumer N. A shift of visual spatial attention is selectively associated with human EEG alpha activity. Eur J Neurosci (2005) 22:2917–2926.

Scherg M, Ille N, Bornfleth H, Berg P. Advanced tools for digital EEG review: virtual source montages, Whole-head mapping, correlation and phase analysis. J Clin Neurophysiol (2002) 19(2):91–112.

Thut G, Nietzel A, Brandt SA, Pascual-Leone A. α-Band electroencephalographic activity over occipital cortex indexes visuospatial attention bias and predicts visual target detection. J Neurosci (2006) 26:9494–9502.

Varela F, Lachaux JP, Rodriguez E, Martinerie J. The brainweb: phase synchronization and large-scale integration. Nat Rev Neurosci (2001) 2(4):229–239.

Worden MS, Foxe JJ, Wang N, Simpson GV. Anticipatory biasing of visuospatial attention indexed by retinotopically specific α-band electroencephalography increases over occipital cortex. J Neurosci (2000) 20 RC63:1–6.

CHAPTER 5: INCREASED GAMMA-BAND SYNCHRONY PRECEDES SWITCHING OF CONSCIOUS PERCEPTUAL OBJECTS IN BINOCULAR RIVALRY[5]

5.1 Abstract

Gamma-band neural synchrony has been proposed as a correlate of consciousness and as a solution for the binding problem. Research on visual working memory and the perception of coherent images in ambiguous figures supports this view. To test the relationship between perceptual consciousness and gamma synchrony, we recorded electroencephalogram activity while participants were presented with rivalling visual images to each eye. Participants pressed buttons to indicate which image they were perceiving, and response-locked phase-locking values (6–60 Hz) were calculated from the electroencephalogram time series. Results revealed transient bursts of increased global phase synchrony in the gamma-band peaking ~425 and ~260 ms preresponse. This suggests that global gamma synchrony is associated with the emergence of a coherent conscious percept.

5.2 Introduction

Synchronous neural oscillations in specific frequency ranges show reliable covariation with cognitive processes such as memory, attention, perception and consciousness (Ward 2003). Neural synchronization in the gamma band (30–50 Hz) has been proposed as a neural correlate of consciousness and as a mechanism for perceptual

[5] A version of this chapter has been published. Doesburg SM, Kitajo K, Ward LM. Increased gamma-band synchrony precedes switching of conscious perceptual objects in binocular rivalry. Neuroreport 16: 1139-1142. Differences between the chapter and the published version are in formatting only.

binding and for the transient functional integration of neural assemblies across brain areas (Crick 1994; Varela et al. 2001). Several results support these hypotheses. First, electroencephalogram (EEG) recorded gamma activity increases at prefrontal and ventral visual electrodes during the delay phase of visual short-term memory tasks, suggesting that working memory is supported by a transient synchronized cortical network between these areas (Tallon-Baudry et al. 1998). Second, conscious recollection is associated with stronger gamma activity than is familiarity and results in greater functional connectivity in the gamma frequency range between frontal and posterior cortical regions (Burgess and Ali 2002). Third, perception of a face in an ambiguous stimulus generates increased global gamma synchronization relative to seeing a meaningless pattern in the same stimulus (Rodriguez et al. 1999).

To provide a more direct test of the relationship between gamma-band synchrony and conscious perception, we measured phase synchronization in the EEG during binocular rivalry. Binocular rivalry occurs when incongruent visual stimuli are presented to corresponding areas of the two retinas. Rather than a blending of the two images, binocular rivalry results in one image being perceptually dominant, and thus present in conscious awareness, while the other is suppressed. Perceptual dominance, and thus the content of consciousness, alternates unpredictably every few seconds. Neural activity generated during conscious perception of a visual stimulus can be compared with neural activity generated by the identical stimulus when it is suppressed from consciousness. For example, when two rivalling visual stimuli are flickered at different frequencies, perceptual dominance is correlated with increased EEG amplitude at the flicker frequency of the currently perceived stimulus (Brown and Norcia 1997). Moreover,

magnetoencephalogram (MEG) investigations of frequency-tagged stimuli during rivalry have revealed that frequency-specific representations of a given stimulus across diverse brain regions are more coherent when the stimulus is in consciousness (Srinivasan 1999). Similarly, MEG-measured global phase synchrony at the flicker frequency is greater when a rivalling stimulus is in consciousness than when it is suppressed (Cosmelli et al. 2004). In the latter studies, however, neural synchrony was measured only at the stimulus flicker frequencies, around 5–10 Hz. Although highly suggestive as to the role neural synchrony might play in conscious perception, these studies did not answer the question of what functional endogenous changes in EEG/MEG phase synchrony occur when conscious perception changes during binocular rivalry.

To address this question we studied the relationship between phase synchrony and perceptual dominance during binocular rivalry. High-density EEG recordings were taken while participants viewed rivalling stimuli and pressed one of two mouse buttons indicating which of the rivalling stimuli was presently in their consciousness. If long-range gamma synchronization is a neural correlate of perceptual awareness, then increased phase synchrony in this frequency range should be observed across EEG electrodes either throughout periods of perceptual dominance or when dominance changes and the participant becomes aware of a new visual percept.

5.3 Methods

Thirteen healthy adults with normal or corrected-to-normal vision participated in the experiment after giving written, informed consent (mean age, 19.8 years; SD, 1.2 years). Participants viewed rivalling visual stimuli presented on a computer monitor

through a mirror stereoscope. A chin rest maintained participants' head position throughout the experiment. For six participants, the stimuli were vertical red bars flickered at 8 Hz and horizontal blue bars flickered at 10 Hz, both presented on a black background. A white fixation point and border were provided on both images to help participants fuse the stimuli in the stereoscope. Participants were told to hold down the left mouse button when the red bars dominated, to hold down the right button when the blue bars dominated, and to make no response when a mixture of both stimuli was seen. To establish that results apply to binocular rivalry in general and not to flickering stimuli only, an additional seven participants were tested using a variant of the paradigm in which the stimuli did not flicker (mean age, 21.0 years; SD, 1.5 years).

The EEG was recorded from 59 electrodes positioned at standard 10–10 locations and three at nonstandard sites near the inion. The electrooculogram (EOG) was recorded bipolarly with electrodes beside and below the right eye. Electrode impedances were kept below 15 kΩ (sufficient because of amplifier input impedance >2 gigaohms). EEG and EOG were amplified with a gain of 20 000, band-pass filtered between 0.1 and 100 Hz, digitized at 500 Hz, and stored on disk for offline analysis. Scalp voltages were referenced to the right mastoid.

EEG epochs were extracted in which perception of one of the rivalling stimuli persisted for 2 s or longer. Epochs from 10 participants for perception of both stimuli were combined for our main analysis (244 epochs). Data from four participants who viewed nonflickering stimuli (72 epochs) were also separately analysed to ensure that observed effects were not caused by stimulus flickering. Data from three participants in

the nonflickering group were not analysed as they had no epochs meeting the criterion. Epochs were analysed from 1000 ms before the participant pressed the button to indicate a particular stimulus was dominant until 1000 ms after the button press. Data were band-pass filtered at 1 Hz intervals (bandwidth ±0.05 times the filtered frequency) between 6 and 60 Hz. We constructed the analytic signal of each filtered waveform to obtain the instantaneous phase and amplitude at each sample point (Pikovski et al. 2001). Phase-locking values (PLVs) were calculated by comparing the instantaneous phases of two electrodes (Lachaux et al. 1999). PLV is a real value between 0 (random phase difference, no phase locking) and 1 (constant phase difference, maximum phase locking). To minimize the influence of volume conduction on PLVs, we standardized them relative to a baseline 900–700 ms preresponse interval. This was done by subtracting the mean baseline PLV from the PLV for every data point and dividing the difference by the standard deviation of baseline PLV. The resulting index, PLV_z, indicates standardized changes from the average baseline PLV in the direction of increased synchronization (positive values) or decreased synchronization (negative values). To test the statistical significance of synchronization and desynchronization between electrodes, epochs were shuffled to create surrogate distributions of PLV_z values in which a measured PLV_z above the 97.5 percentile was considered to be a significant increase in synchronization, and one below the 2.5 percentile a significant decrease in synchronization. Only significant effects are discussed.

Nineteen, roughly equally spaced, electrodes were selected from the 62 available (necessitated by computational limitations) and phase synchrony was calculated for each electrode pair. PLV_z time series were averaged across all 171 electrode pairs to image the

global pattern of phase synchrony. Because normalized PLV_z scores reflect changes from baseline PLV, they are insensitive to synchrony arising via volume conduction from sources that did not vary in amplitude during the periresponse interval. To control for volume-conducted synchrony induced by sources that did vary within the analysed epochs, we also calculated the scalp current density (SCD) (Lachaux et al. 1999). To further ensure that any observed synchronization was not spurious, we also extracted epochs during which perceptions were stable for 1 s or longer. Computational limitations prevented a group analysis of these data; therefore, data from each participant with more than 30 epochs of perception of each stimulus were analysed separately (eight participants, 1885 epochs). The resulting PLV_zs were averaged across left and right stimuli and across participants.

5.4 Results

Behavioural results show a similar number of perceptions and a similar distribution of perception lengths for left and right-eye stimuli. The average length of a perceptually stable epoch (button press to button release) was ~450 ms. The distribution of epochs was unimodal and positively skewed for the flickering group, but flatter for the nonflickering group (Figure 5.1).

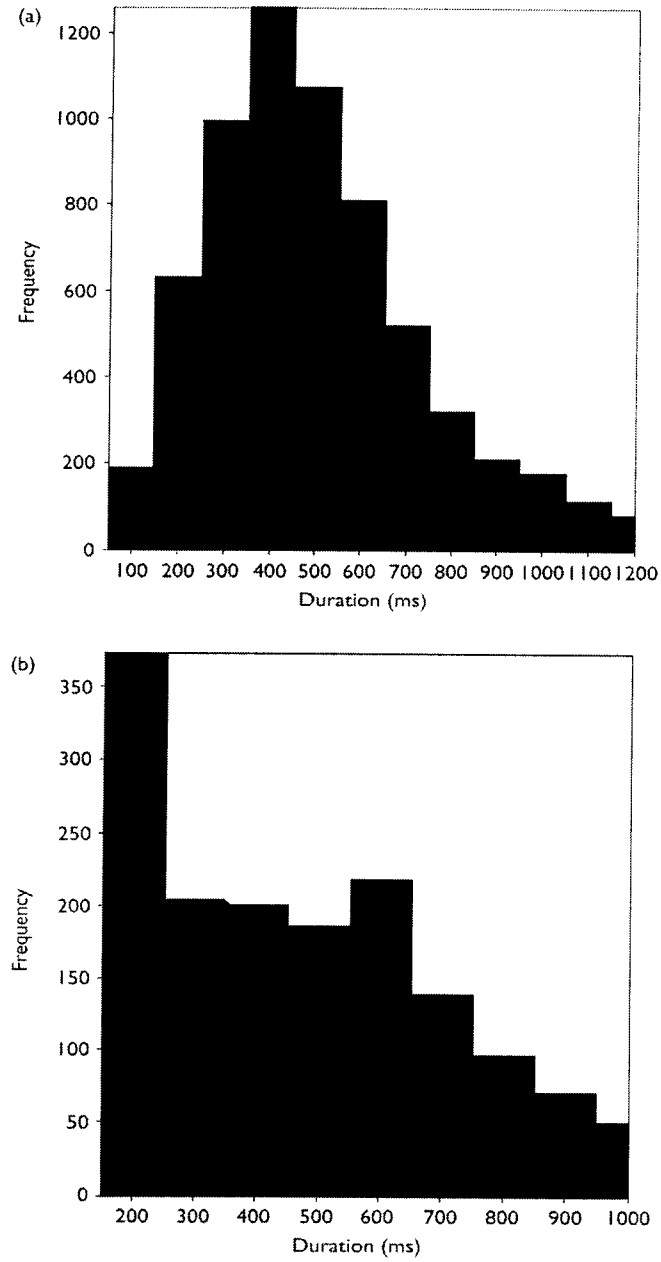

Figure 5.1

(**A**) Distribution of epoch lengths for both left-eye and right-eye stimuli for participants who viewed flickering stimuli. (**B**) Distributions of epoch lengths for both left-eye and right-eye stimuli for participants who viewed nonflickering stimuli.

Significantly increased PLV_z values, indicating increased phase synchrony, were found within the gamma range approximately 440–390 ms (40–48 Hz) and 280–220 ms (36–46 Hz) prior to button pressing in our main analysis (2 s+) (Figure 5.2a). These bursts of increased gamma-phase synchrony show a global topology involving strong synchrony between frontal electrodes and those over visual cortical areas (Figure 5.3a). A periodic pattern was revealed in which bursts of phase synchrony were divided by epochs of decreased or baseline-level gamma synchronization (Figure 5.3a).

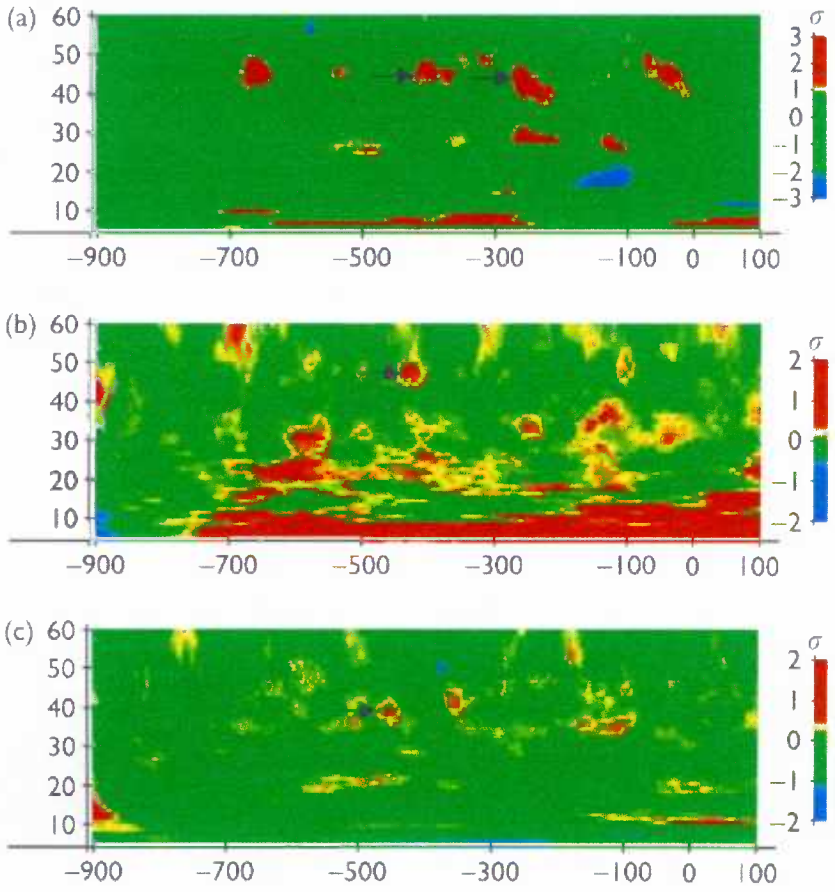

Figure 5.2

(**a**) Response-locked phase synchrony for the main analysis (2-s+ epochs) averaged across all 171 electrode pairs. (**b**) Scalp current density (2-s+ epochs) averaged across all pairs. (**c**) Averaged phase-locking values (PLVs) for 1-s+ epochs (all pairs). Arrows indicate gamma bursts.

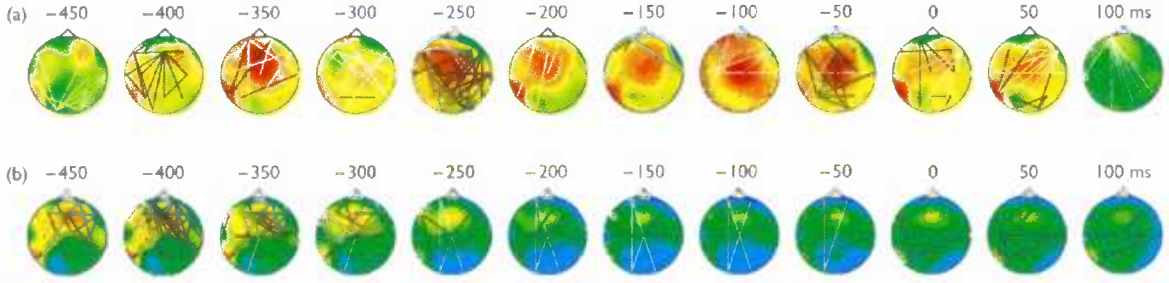

Figure 5.3

(a) Topography of phase synchronization/desynchronization at 45 Hz for selected times in the main analysis (2 s+). **(b)** Topography of synchronization/desynchronization at 7 Hz (main analysis). Black lines show synchronization increases whereas white lines show synchronization decreases.

The increase in gamma-phase synchrony at ~440–390 ms was also found in the SCD analysis for 2-s+ epochs, indicating that the synchrony increase was unlikely to result from a single oscillating cortical source. This possibility is also remote because (1) the increase in synchrony is evident at many distant electrode pairs whereas studies have shown that voltage correlations due to volume conduction are insubstantial at distances over 4 cm (Nunez et al. 1999), (2) volume-conducted synchrony is accompanied by corresponding changes in amplitude, which were not observed. Moreover, this gamma burst was also present in the 1-s+ analysis.

The burst of increased gamma synchrony at ~280–220 ms was also found in both SCD and 1-s+ analyses, although it occurred in a lower frequency range for the SCD (Figure 5.2b) and earlier in the 1-s+ analysis (Figure 5.2c).

The SCD analysis should be taken as secondary to the main analysis because the SCD (1) can both induce and remove spurious synchrony whereas its effect on real synchrony remains unknown (Lachaux et al. 1999), (2) is inferred from the voltage but not directly measured, (3) is insensitive to sources that are tangentially oriented or deep, and (4) has not previously been applied to PLV calculations from real EEG data. Moreover, analysis of 1-s+ epochs did not include between-participant PLV calculations because of computational limitations; the result is a simple unweighted average of individual results. Accordingly, although results with these measures confirm our major findings, they may not represent all features of the main PLV analysis because of these shortcomings.

Increased phase synchrony was also found in the theta frequency range (6–8 Hz) approximately 610–280 ms preresponse (Figure 5.2a) in the main analysis (limited to 6–60 Hz). At its peak (~400 ms) this effect shows a distinct pattern of synchrony between prefrontal electrodes and temporal and posterior visual areas (Figure 5.3b). Increased theta synchrony was also present in the SCD analysis, although analysis of the 1-s+ epochs yielded some decreases in theta synchronization in the same time range.

Right-eye stimulus perception and left-eye stimulus perception epochs were also analysed separately, as were epochs from the flickering and nonflickering groups. All analyses revealed a similar pattern of results. Previous studies investigating event-related potentials to flickering and nonflickering stimuli in binocular rivalry have found no differences in the electrophysiological response (Roeber and Schröger 2004).

5.5 Discussion

The onset of perceptual dominance of either of the rivalling visual stimuli was correlated with short bursts of increased gamma-band phase synchrony. The exact temporal relationship between this gamma burst and the emergence of a coherent conscious percept cannot be known because we have no precise marker for this subjective event. The timing of these gamma bursts at ~440–390 and ~220–280 ms preresponse strongly suggests they coincide with or precede the onset of the perceptual event. This result strengthens the view that gamma-band phase synchrony is a neural correlate of coherent visual awareness.

The increased gamma synchrony was not sustained throughout epochs of perceptual dominance but lasted only about ~50 ms on each occurrence. This suggests that this gamma burst is not associated with being conscious of a stimulus but with becoming aware of it. This interpretation is similar to the idea that the P300 wave indexes the entry of information into consciousness but does not persist as long as that information remains in consciousness (Picton et al. 1992). This result is consistent with other findings, including those of Rodriguez et al. (1999) who reported that the perception of a meaningful figure in an ambiguous stimulus generated increased gamma synchrony lasting only ~60 ms. Visual short-term memory studies, however, have found gamma activity to be sustained for longer periods of time, such as throughout the delay phase of a delayed-matching-to-sample test (Tallon-Baudry et al. 1998). These studies have measured power or coherence within a time window and thus may have been blind to whether these increases were periodic or sustained (Tallon-Baudry et al. 1998). Information could be sustained in consciousness by periodic 'refreshing' of 50–60 ms bursts of increased gamma synchronization. Our data reveal that such bursts of increased synchrony occur at roughly periodic intervals consistent with a theta rate (Figure 5.2a).

The main analysis also revealed a dramatic pattern of theta synchrony between prefrontal and visual electrodes peaking ~400 ms preresponse (Figure 5.3b). Oscillatory models of working memory propose that the contents of working memory are maintained in consciousness by networks synchronized in the gamma range that are refreshed at a slower rate (e.g. Schack et al. 2002; Burle and Bonnet 2000). Long-range synchrony at low frequencies has also been proposed as a mechanism for the implementation of top-down executive processes (von Stein et al. 2000). The increases in theta synchrony

between prefrontal and visual electrodes reported here (Figure 5.3b) may reflect such top-down influences on visual areas responsible for the emergence and/or maintenance of a coherent conscious percept. This view is supported by electrophysiological recordings in humans showing phase coupling of theta and gamma rhythms during the performance of a Sternberg short-term memory task (Schack et al. 2002). EEG recordings during conscious recollection have also shown that functional gamma connectivity was modulated at 3 Hz (Burgess and Ali, 2002).

5.6 Conclusion

Transient bursts of increased gamma phase synchrony accompany the onset of a coherent percept in binocular rivalry, suggesting that gamma synchrony is a mechanism for information integration across brain areas and a neural correlate of consciousness. The periodic resynchronization of gamma oscillations could represent a refreshing of the neural assembly required for consciousness through long-range theta synchrony driven by top-down executive processes in the prefrontal cortex.

5.7 Acknowledgements

Supported by grants from the Natural Sciences and Engineering Research Council of Canada. The authors thank Dr Kentaro Yamanaka, Educational Physiology Laboratory, University of Tokyo.

5.8 References

Brown RJ, Norcia AM. A method for investigating binocular rivalry in real-time with the steady state VEP. Vision Res (1997) 37:2401–2408.

Burgess AP, Ali L. Functional connectivity of gamma EEG activity is modulated at low frequency during conscious recollection. Int J Psychophysiol (2002) 46:91–100.

Burle B, Bonnet M. High-speed memory scanning: a behavioural argument for a serial oscillatory model. Cogn Brain Res (2000) 9:327–337.

Cosmeli D, David O, Lachaux JP, Martinerie J, Garnero L, Renault B et al. Waves of consciousness: ongoing cortical patterns during binocular rivalry. Neuroimage (2004) 23:128–140.

Crick F. The Astonishing Hypothesis. New York: Simon and Schuster (1994).

Lachaux JP, Rodriguez E, Martinerie J, Varela FJ. Measuring phase synchrony in brain signals. Hum Brain Mapp (1999) 8:194–208.

Nunez PL, Silberstein RB, Shi Z, Carpenter MR, Srinivasan R, Tucker DM et al. EEG coherency II: experimental comparisons of multiple measures. Clin Neurophysiol (1999) 110:469–486.

Picton TW, Lins OG, Scherg M. The P300 wave of the human event-related potential. J Clin Neurophysiol (1992) 9:456–479.

Pikovski A, Rosenblum M, Kurths J. Synchronization: A Universal Concept in Nonlinear Sciences. Cambridge: Cambridge University Press (2001).

Rodriguez E, George N, Lachaux JP, Martinerie J, Renault B, Varela FJ. Perception's shadow: long distance synchronization of human brain activity. Nature (1999) 397:430–433.

Roeber U, Schröger E. Binocular rivalry is partly resolved at early processing stages with steady and with flickering presentation: a human event-related brain potential study. Neurosci Lett (2004) 371:51–55.

Schack B, Vath N, Petsche H, Geissler H-G, Möller E. Phase-coupling of theta-gamma EEG rhythms during short-term memory processing. Int J Psychophysiol (2002) 44:143–163.

Srinivasan R, Russell DP, Edelman GM, Tononi G. Increased synchronization of neuromagnetic responses during conscious perception. J Neurosci (1999) 19:5435–5448.

Tallon-Baudry C, Bertrand O, Peronnet F, Pernier J. Induced gamma-band activity during the delay of a visual short-term memory task in humans. J Neurosci (1998) 18:4244–4254.

Varela F, Lachaux JP, Rodriguez E, Martinerie J. The brainweb: phase synchronization and large-scale integration. Nat Rev Neurosci (2001) 2(4):229–239.

von Stein A, Sarnthein J. Different frequencies for different scales of cortical integration: from local gamma to long range alpha/theta synchronization. Int J Psychophysiol (2000) 38:301–313.

Ward LM. Synchronous neural oscillations and cognitive processes. Trends Cogn Sci (2003) 7:553–559.

CHAPTER 6: ASYNCHRONY FROM SYNCHRONY: LONG-RANGE GAMMA-BAND NEURAL SYNCHRONY ACCOMPANIES PERCEPTION OF AUDIOVISUAL SPEECH ASYNCHRONY[6]

6.1 Abstract

Real-world speech perception relies on both auditory and visual information that fall within the tolerated range of temporal coherence. Subjects were presented with audiovisual recordings of speech that were offset by either 30 or 300 ms, leading to perceptually coherent or incoherent audiovisual speech, respectively. We provide electroencephalographic evidence of a phase-synchronous gamma-oscillatory network that is transiently activated by the perception of audiovisual speech asynchrony, showing both topological and time–course correspondence to networks reported in previous neuroimaging research. This finding addresses a major theoretical hurdle regarding the mechanism by which distributed networks serving a common function achieve transient functional integration. Moreover, this evidence illustrates an important dissociation between phase-synchronization and stimulus coherence, highlighting the functional nature of network-based synchronization.

6.2 Introduction

Our conscious window on the world is a multisensory one, but the neural bases for multisensory integration have remained elusive. Mechanisms by which brain activity

[6] A version of this chapter has been published. Doesburg SM, Emberson LL, Rahi A, Cameron D, Ward LM. Asynchrony from synchrony: long-range gamma-band neural synchrony accompanies perception of audiovisual speech asynchrony. Exp Brain Res (2008) 185(1): 11-20. Differences between this chapter and the published version are in formatting only.

can match sensory features from different modalities to a single perceptual object and bind these features together to form a unified percept are necessary to support multisensory perception. Our robust perceptual system tolerates a moderate degree of temporal incoherence between sensory features from different modalities, but when the temporal incoherence goes beyond this range multisensory integration fails to occur (Dixon and Spitz 1980; Lewkowicz 1996). A related problem is that of the perception of simultaneity or repeated simultaneity, also referred to as perceptual synchrony (King 2005).

Audiovisual integration in speech is a promising arena for the investigation of multisensory integration as it provides complex, continuous stimuli for whose perception we typically rely on both auditory and visual information. The classic example of the profound effect of audiovisual integration on speech perception is the McGurk effect, where the presence of coordinated visual information alters the categorical perception of a phoneme from what the auditory information alone would produce (McGurk and MacDonald 1975).

In a comprehensive review of the neuroimaging literature examining audiovisual temporal integration, Calvert (2001) concluded that crossmodal processing involves the activation of multiple brain regions likely working in concert to match and integrate multimodal inputs. A distributed network of brain regions, composed of the superior temporal sulcus (STS), intraparietal sulcus, Heschl's gyrus and the inferior frontal gyrus, has been associated with perception of fused bimodal speech stimuli (Miller and D'Esposito 2005). However, other localization studies have related audiovisual speech

fusion to restricted areas of association cortex located in the superior temporal sulcus (STS) and/or superior temporal gyrus, rather than to the activity of a distributed network (Calvert 2001; Wright et al. 2003). Complementary to the neural mechanisms for audiovisual speech fusion are those that identify mismatches between auditory and visual speech streams. This system functions to ascertain when an auditory speech stream is incongruent with a visual speech stream, and should accordingly belong to a different perceptual object. A robust group of imaging studies has identified a brain network composed of posterior parietal, insular, prefrontal and cerebellar areas that is associated with the perception of asynchronous bimodal speech stimuli (Jones and Callan 2003; Kaiser et al. 2005; Miller and D'Esposito 2005).

It remains a general problem in cognitive neuroscience how these, or any, distributed networks of neural groups achieve functional coupling for the performance of a particular task. Long-range phase synchronization, particularly within the gamma band, has been proposed to be a mechanism that enacts transient functional integration of task-relevant, neural populations and enables perceptual binding (Engel and Singer 2001; Varela et al. 2001). In this view, neural populations participating in an active task-relevant network or representing features belonging to the same perceptual object oscillate synchronously in the gamma-band (Tallon-Baudry and Bertrand 1999).

Previous research supports the hypothesis that long-range gamma synchrony mediates networks associated with the perception of audiovisual stimuli. First, gamma-band activation (GBA), reflective of *local* neural synchrony, has been associated with audiovisual perception in both EEG and magnetoencephalographic (MEG) recordings.

Attention increases GBA more for bimodal versus unimodal audiovisual stimuli, underscoring that GBA is affiliated with integrative brain processes (Senkowski et al. 2005). Perceptual fusion of bimodal speech stimuli has also been related to enhanced GBA (Callan et al. 2001). Furthermore, information integration across modalities, based on semantic congruity between auditory and visual speech streams, is associated with enhanced GBA (Yuval-Greenberg and Deouell 2007). Second, transient *long-range* synchronization in the gamma band has been correlated with coherent perception in both unimodal visual and unimodal auditory perception (Doesburg et al. 2005; Eggermont 2000; Rodriguez et al. 1999). Perceptual integration across modalities, for example between tactile and visual stimuli, has also been linked to long-distance gamma-band synchronization (Kanayama et al. 2007). Of more specific relevance to speech perception, long-range synchronization between brain areas has been found to relate to the matching of auditory speech stimuli to expectations about the speaker's own voice. Gamma-band coherence between frontal and temporal electrodes is greater when subjects hear their own undistorted speech, relative to when they hear their speech frequency-shifted down by one semi-tone (Ford et al. 2005). This finding indicates that long-range interactions may also be involved in the matching of auditory speech streams to their appropriate object, in this case to the speaker.

Given the evidence relating GBA to perceptual binding within and across modalities, together with evidence that long-range gamma-band phase synchrony correlates with coherent perception, our hypothesis was that greater local and long-range gamma synchrony would be observed during coherent audiovisual speech percepts relative to incoherent percepts. Perception of speech asynchrony, however, does not

simply reflect a failure of the neural systems responsible for binding speech stimuli. Rather the activity of a distributed network of brain areas has been linked to the detection of speech asynchrony. We accordingly hypothesized that increased long-range gamma-band synchronization would also be observed during the perception of incoherent audiovisual speech, relative to a prestimulus baseline, as these brain areas were activated and functionally integrated. This latter pattern of synchronization was predicted to be less pronounced than synchronization observed during perception of coherent audiovisual speech as it does not involve crossmodal binding. This pattern of synchrony should show a different topography, reflective of the distinct underlying network involved in detection of speech asynchrony, as opposed to that responsible for perceptual binding of audiovisual speech stimuli. To test these hypotheses we recorded 64 channel EEG while subjects viewed audiovisual speech stimuli in which the auditory and visual streams were offset by either a small or a large amount, leading to integrated or nonintegrated multimodal perception, respectively. Phase locking values were calculated between signals recorded at selected electrodes in order to measure long-distance synchronization in various frequency bands.

6.3 Methods

Audiovisual stimuli were recorded from four human speakers (two female). For each speaker, two segments were identified that contained a complete phrase uttered in approximately 2 s. The visual stream of each of these eight recordings was shifted forward by 30 ms relative to the auditory stream (Figure 6.1) and then the 2-s video segments that contained the complete auditory phrases were extracted. Thus, there was no

stimulus onset asynchrony (SOA) between visual and auditory stimulus streams but there was a temporal incongruence between the streams as the visual events were shifted in time relative to the corresponding audio events. This process was repeated with an offset of 300 ms, producing an additional eight 2-s stimuli for a total of 16 videos for experimental presentation. The offsets were chosen to be well within (30 ms) or outside (300 ms) the range of temporal integration for audiovisual speech stimuli producing perceptually congruent (synchronous) and incongruent (asynchronous) audiovisual streams, respectively (Dixon and Spitz 1980; Miller and D'Esposito 2005). For all stimuli, the audio and visual streams began and ended simultaneously, as the visual stream was shifted relative to the auditory stream before the 2-s stimulus segments were extracted.

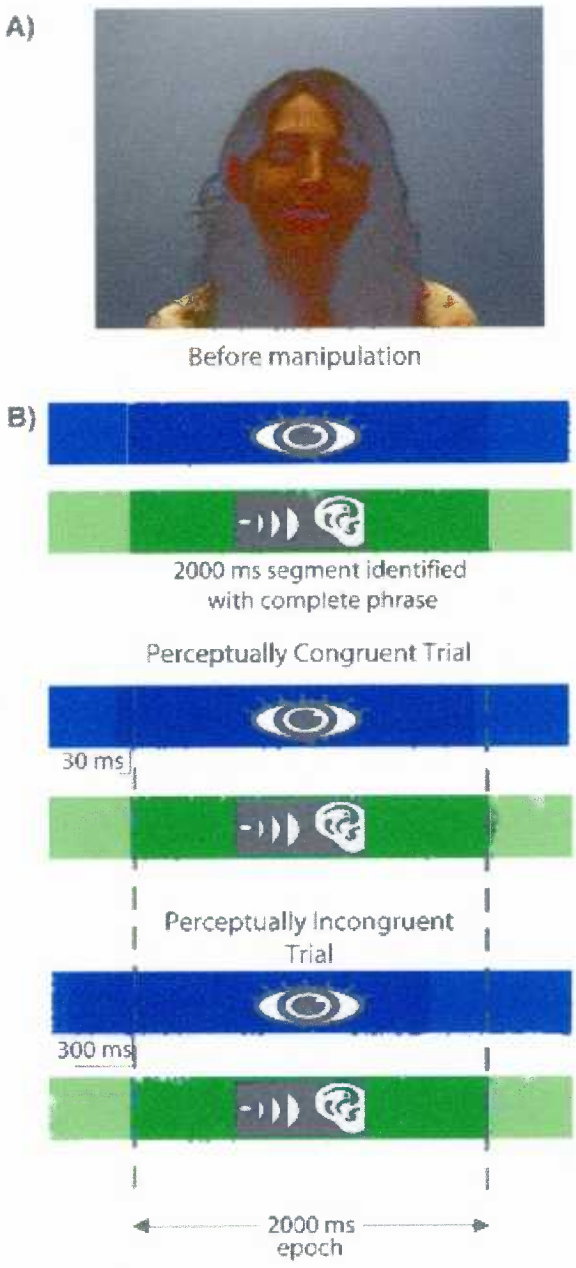

Figure 6.1: (**a**) The stimulus display. (**b**) Construction of congruent and incongruent audiovisual speech stimuli. Two-second epochs of speech containing a complete phrase were identified. The visual stream was shifted forward relative to the auditory stream (30 ms for congruent trials, 300 ms for incongruent trials) and then 2,000 ms stimuli were extracted. There was no SOA between the visual and auditory and visual stimulus streams, as they both began and ended simultaneously

Eleven subjects (average age 20.09; SD 1.76, five male) participated in the study after giving informed consent. Subjects were seated 35 cm in front of a computer monitor and received the auditory speech stimuli through headphones. Visual speech stimuli were presented centrally and subtended a visual angle of 31.92° horizontally and 20.14° vertically (the average size of the speakers' heads within this display was 11.87 × 11.05°). Between trials subjects viewed a grey screen with a centrally-located fixation point (0.82 × 0.82°) for 2 s. Six blocks of 100 stimuli, in which randomly selected congruent and incongruent stimuli occurred in equal numbers, were presented to each subject. Subjects were told that half of the stimuli they would see were congruent and to press the X button on a computer keyboard when they perceived a congruent speech stimulus and the Y button when they perceived an incongruent speech stimulus. Subjects were told to respond only after the end of the 2-s-duration speech stimulus so as to minimize contamination of the EEG recordings by motor artifacts.

EEG data were recorded continuously from 59 electrodes positioned at standard 10–10 locations as well as three at non-standard sites below the inion using an SA isolated bioelectric amplifier, and were referenced to the right mastoid electrode. The electro-oculogram (EOG) was recorded bipolarly using electrodes beside and below the right eye. Electrode impedances were kept below 15 kΩ (sufficient since amplifier input impedance was >2 GΩ). EEG and EOG were amplified using a gain of 20,000, bandpass filtered from 0.1 to 100 Hz, digitally sampled at 500 Hz, and recorded for offline analysis. The protocol used in this research was approved by the Behavioural Research Ethics Board of the University of British Columbia and was conducted in accordance with the principles of the Helsinki Declaration.

Epochs were extracted for trials in which the subjects reported congruent perception when presented with video segments offset by 30 ms, and when subjects reported incongruent perception when presented with video segments offset by 300 ms. Only trials in which subjects responded after the offset of the stimulus were included in the analysis. Epochs containing ocular and nonocular artifacts were removed. Epochs containing artifacts were defined as those in which the EOG contained values outide of the ±75 μV range, or on which the voltage difference between the beginning and the end of the epoch exceeded 70 μV for any electrode other than the EOG (as identified by the automatic rejection algorithm in EEGLAB; Delorme and Makeig 2004). Each subject's data were manually inspected to ensure that the artifact rejection algorithm was working as intended. For some subjects the criteria were slightly adjusted to more accurately identify artifacts. As the surrogate method for PLV analysis used here requires data to be combined across subjects (Lachaux et al. 1999), only the first 200 acceptable epochs from each condition were taken from each subject. This was done to prevent any observed effects in the group data being driven by responses present only in a small number of subjects. This procedure resulted in seven subjects who had more than, or nearly, 200 artifact-free epochs for each condition being included in the main analysis (average age 21.43; SD 1.99, four male, see Table 6.1 for numbers of epochs for each subject/condition). This yielded a total of 1,374 epochs for congruent percepts and 1,354 epochs for incongruent percepts.

Subject #	No. of congruent epochs	No. of incongruent epochs
1	200	200
2	180	199
3	200	198
4	200	200
5	200	200
6	200	157
7	194	200
Total	1,374	1,354

Table 6.1: Total number of epochs for each subject for the congruent and incongruent conditions

Epochs were extracted from 400 ms before stimulus onset until 1200 ms after stimulus onset, but we report analyses only from −200 ms until 1,000 ms to avoid distorting edge effects from the phase locking value (PLV) analysis (see Freeman 2004). To attenuate volume conduction and to remove spurious synchronization resulting from the use of a right mastoid reference electrode, source current density (SCD) was derived from scalp potentials recorded at 62 electrode locations (excluding the EOG and reference channels). This was performed prior to the calculation of PLVs. To compute SCD we used a MATLAB script supplied by Carsten Allefeld (http://www.agnld.unipotsdam.de/~allefeld/index.html) that implements the algorithm of Perrin et al. (1987, see their Eqs. 3 and 5). The SCD is a reference-free measure and largely reflects the activity of superficial neural generators near the recording electrodes (Lachaux et al. 1999). For this reason we refer to electrodes and cortical regions beneath those electrodes interchangeably, as all reported results pertain to the PLV_z values based on SCD. SCD data were analyzed for a 19-electrode montage, selected from the full 62-electrode set, positioned evenly about the scalp (minimum distance between electrodes ≈4 cm). Data were bandpass filtered digitally at 1-Hz intervals (passband = $f \pm 0.05f$, where f represents the filter frequency) between 6 and 60 Hz. The analytic signal

$$\varsigma(t) = f(t) + i\tilde{f}(t) = A(t)e^{i\phi(t)}$$

of each filtered waveform, where $\tilde{f}(t)$ is the Hilbert transform of the EEG recording, $f(t)$, and $i = \sqrt{-1}$ was calculated to determine the instantaneous amplitude, $A(t)$, and the instantaneous phase, $\phi(t)$, for each sample point (Pikovski et al. 2001). Instantaneous

phases between various pairs of electrodes were compared to calculate PLVs between electrodes j and k for each time point t across epochs N (Lachaux et al. 1999):

$$PLV_{j,k,t} = N^{-1}\left|\sum_{N} e^{i\left[\phi_j(t)-\phi_k(t)\right]}\right|$$

PLV is a real value between 0 (random phase difference) and 1 (constant phase difference). To reduce the influence of volume conduction from constant sources on PLVs by removing the record of ongoing synchrony, we standardized them relative to a 200 ms pre-stimulus baseline. Standardization was accomplished by subtracting the mean baseline PLV from the PLV for each data point and dividing the difference by the standard deviation of the baseline PLV. The resulting PLV_z scores indicate changes from the average baseline PLV expressed in units of standard deviation; PLV_z scores usually range from −3 to +3, although they can be more negative or more positive. PLV between each electrode pair was standardized relative to the 200 ms baseline period for that electrode pair for trials within a particular condition. The baselines for the two conditions are essentially equivalent, however, as trials in each condition occurred randomly and with equal probability in each block.

To test the statistical significance of phase synchronization and desynchronization between pairs of electrodes, epochs were shuffled to create surrogate distributions of PLV_z values. Our surrogate distributions contained 200 random shufflings for each electrode pair at each data point. We considered a measured PLV_z above the 97.5th percentile of the surrogate distribution to be a significant increase in synchronization, and one below the 2.5th percentile a significant decrease in synchronization. Only long-range

synchronization/desynchronization effects that reached statistical significance by this measure are discussed.

6.4 Results

Since the degree of temporal offset was chosen according to known windows for perceptual integration of audiovisual speech, subjects responded with high accuracy. However, trials with a 30 ms offset were successfully identified as congruent (3.9% errors) more accurately than the 300 ms offset trials were identified as incongruent (10.2% errors).

Long-range gamma-band phase synchronization was observed 170–250 ms after the onset of incongruent speech stimuli in a band of frequencies ranging from 37 to 44 Hz (Figure 6.2a). A pattern of global phase synchronization in a somewhat lower frequency band, from 23 to 28 Hz, was observed 40–70 ms after the onset of congruent speech stimuli (Figure 6.2b). These effects are also clearly visible in a direct comparison of the PLVs from the two stimulus conditions (Figure 6.2c). No other reliable differences in long-distance synchrony were present during the analyzed epoch. A sustained increase in synchronization from 6 to 9 Hz beginning at the onset of the audiovisual speech stimuli, and a sustained decrease in synchronization from 10 to 19 Hz beginning at 170 ms, however, occurred for both congruent and incongruent speech trials (Figure 6.2a&b). Long-range synchrony during the perception of audio-visually incongruent speech was anchored primarily at electrodes over frontal areas and left posterior cortex, accompanied by substantial synchronization between left temporal cortex and other electrodes (Figure 6.3a). Although far less long-range gamma-band synchronization was seen 170–

250 ms after the onset of audio-visually congruent speech, the topology of observed long-distance synchronization was similar to that seen during incongruent speech perception (Figure 6.3a). These patterns of synchronization were robust as they were also observed at neighboring frequencies (see supplementary material D).

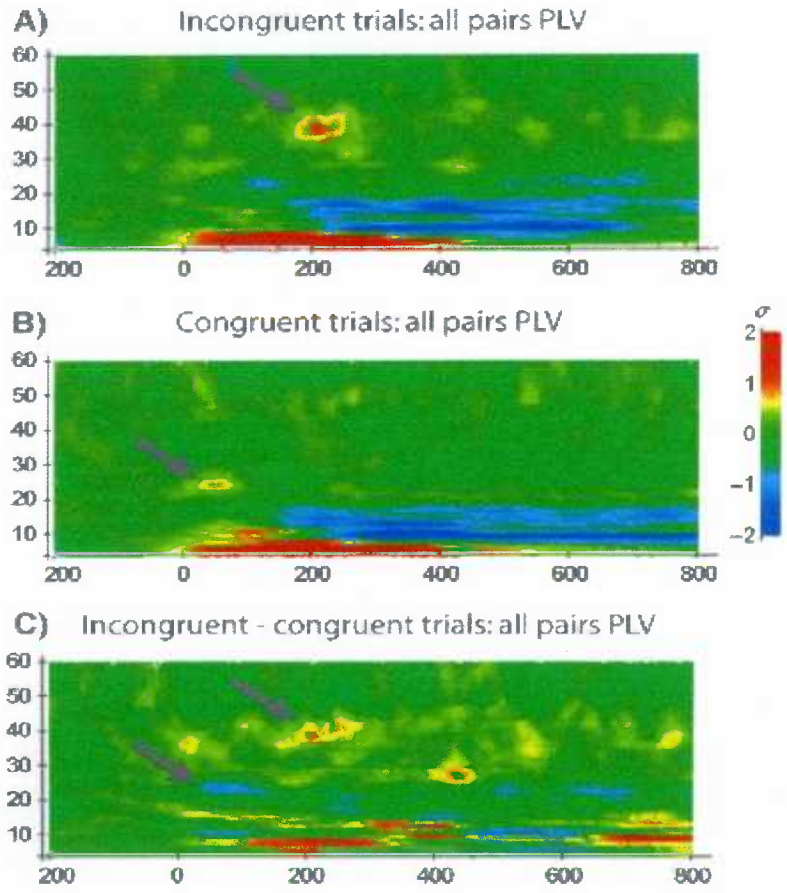

Figure 6.2

(**a**) Global long-range synchrony increase accompanying incongruent perception, time-locked to the onset of audiovisual stimuli. Shown is PLV_z averaged across all analyzed electrode pairs (19 electrodes; 171 pairs). *Arrow* indicates the 37 to 44 Hz burst of increased phase-locking occurring 170 to 250 ms after the onset of incongruent speech stimuli. Changes from the pre-stimulus baseline, both positive (synchronization increase) and negative (synchronization decrease), are measured in standard deviation units (σ in *legend on right*). (**b**) Global long-range phase synchrony increase following the onset of congruent stimuli. Note the burst of increased phase-locking from 23 to 28 Hz occurring from 40 to 70 ms after stimulus onset. (**c**) Difference map displaying a direct comparison of the two stimulus conditions (incongruent–congruent). This demonstrates that effects shown in Figure 6.2a&b are also visible in a direct comparison, as denoted by the *arrows*. The difference map was calculated by subtracting PLV_z, averaged across all 171 electrode pairs, for each data point for the congruent dataset from the corresponding data points in the incongruent dataset. Since the baseline mean and standard deviations are roughly the same for all points, this procedure reveals approximate average differences in PLV in units of standard deviation of the baseline PLV

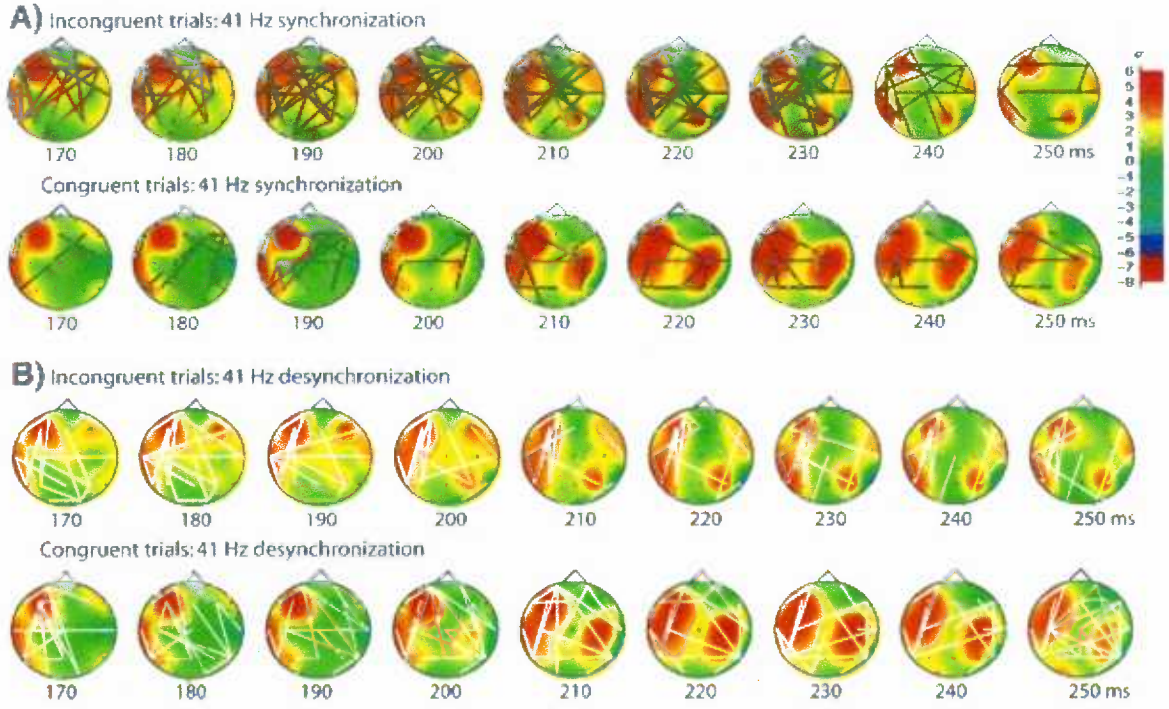

Figure 6.3

(**a**) Topography of long-range gamma-band phase synchronization accompanying incongruent perception. *Black lines* indicate statistically significant increases in phase-locking between electrode pairs. Note the anchoring of the network at frontal and left posterior sites. *Colours* represent spline-interpolated instantaneous SCD amplitudes, expressed in standard deviations from the pre-stimulus baseline (*legend at right*). (**b**) Topography of long-range *desynchonization* during the burst of long-range gamma-band *synchronization*. This effect is anchored at left frontal and left posterior electrodes, and is more medial than the long-range synchronization. As this effect occurs during a time–frequency window in which synchronization is dominant (see Fig. 6.2a), it should be considered to be subsidiary to the synchronization shown in Fig. 6.3a.

It should also be noted that throughout the period of increased long-range synchronization increase there was also a distinct pattern of decrease in long-range gamma-band synchronization (long-range *desynchronization*) that also was considerably more pronounced during incongruent percepts, relative to congruent percepts (Figure 6.3b). This long-range desynchronization appears between left frontal and posterior locations, and has a more medial topography than does the aforementioned long-range synchronization. Perception of coherent speech, conversely, was associated with long-range desynchronization in the gamma-band between right temporal and parietal electrodes and other, widespread locations (Figure 6.3b). Since this long-range desynchronization occurred within a time–frequency window that was dominated by long-range *synchronization*, as indicated by the appearance of only synchronization increases in that time–frequency window in Figure 6.2, they should be considered of secondary importance to the increased phase synchrony displayed in Figure 6.3a.

Gamma-band amplitude, reflective of local gamma synchrony as opposed to synchronization between distant brain regions, showed a pattern of results different from that observed for long-range synchronization. An initial burst of gamma-band activation centred at ~40 Hz and peaking around 200 ms after the onset of audiovisual speech stimuli was present in both conditions (Figure 6.4a). Similar GBAs appear at regular intervals throughout the analyzed epoch, possibly indicating that gamma activity was periodically "refreshed" at a lower frequency, consistent with previous studies indicating a low carrier frequency mediating coordination of gamma rhythms across distant cortical areas during cognitive processing (Canolty et al. 2006; Doesburg et al. 2005; von Stein

and Sarnthein 2000; Ward 2003). Congruent perception culminated in a period of enhanced GBA, relative to incongruent, from about 700 to 900 ms after stimulus onset (Figure 6.4a). The scalp topography of gamma-band activity during the zenith of the long-range synchronization (and early GBA enhancement) was roughly similar across congruent and incongruent percepts, showing widespread activations over left frontal and temporal–parietal locations and more restricted activations over similar areas in the right cortex (Figure 6.4b). Some differences, however, are evident between these topographies for congruent and incongruent percepts including a stronger left frontal activation during congruent percepts. Also, the topography of the right-hemispheric GBA appears to be somewhat more distributed for incongruent percepts, with distinct frontal and parietal components, whereas during congruent perception there is a single parietocentral component.

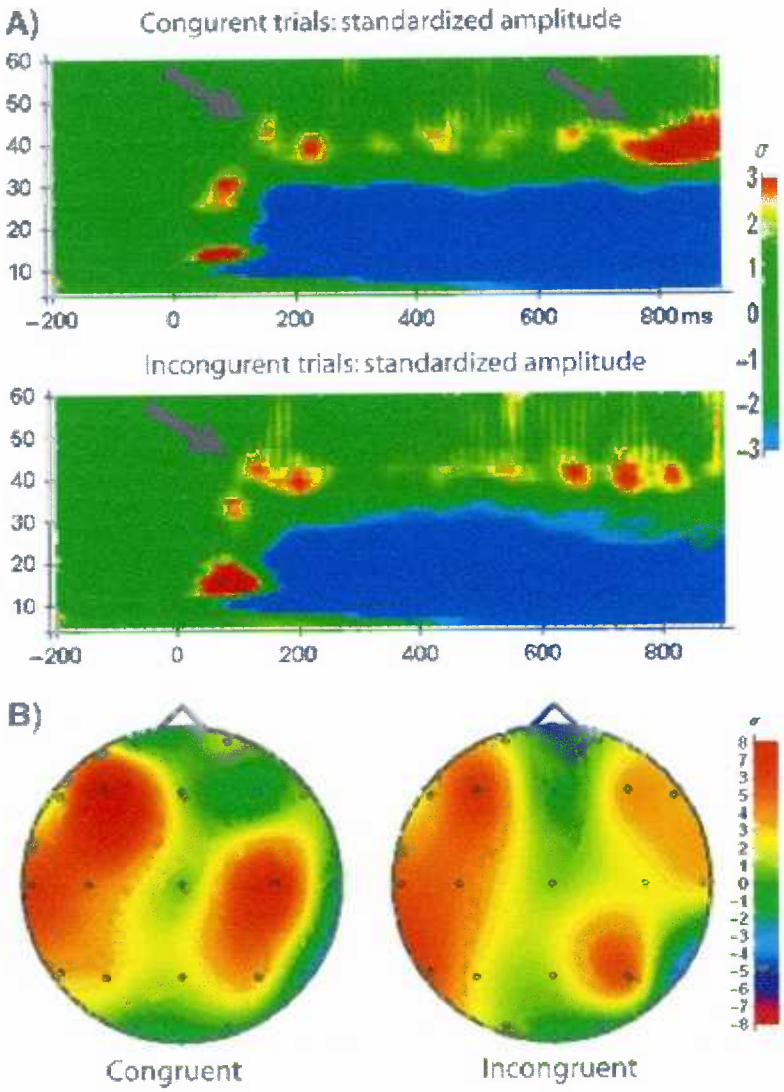

Figure 6.4

(**a**) Global instantaneous amplitude of SCD time-locked to stimulus onset for both incongruent and congruent trials, calculated by averaging the instantaneous amplitude across all electrodes (expressed as number of standard deviations, σ, above or below the pre-stimulus baseline, *legend at right*). *Arrows* indicate the increase in gamma-band activity, apparent for both congruent and incongruent percepts, during the period where increased *long-range* synchrony was seen for incongruent perception. Also denoted by an *arrow* is a late increase in gamma-band activity that was more pronounced during congruent perception. (**b**) Topography of 41 Hz instantaneous amplitude at the zenith of long-range gamma-band synchronization for incongruent perception (210 ms after stimulus onset).

Several other notable amplitude changes were observed during the course of audiovisual speech perception, although these effects did not appear to vary with audiovisual congruence (Figure 6.4a). Most notably, a broadband amplitude decrease occurred from about 8 to 30 Hz beginning about 150 ms after stimulus onset and continuing until the end of the analyzed epoch. The frequency of this effect expanded into lower frequencies at around 500 ms after stimulus onset. This amplitude decrease accompanied the decrease in synchronization in this frequency range that was noted earlier (Figure 6.2a&b). Increases in instantaneous amplitude, centred at 14 and 30 Hz, also occurred from about 70 to 140 ms post stimulus onset. The increased 30 Hz activity occurred in the same time range as the long-range synchronization increase that occurred on the congruent trials, but the 14 Hz activation did not appear to co-occur with any long-distance synchronization changes.

6.5 Discussion

Our results demonstrate increased long-range gamma-band phase synchrony during the perception of temporally incongruent audiovisual speech signals 170–250 ms after stimulus onset. This pattern of synchronization is also visible during the perception of congruent audiovisual speech stimuli, but it is markedly less pronounced there than it is during incongruent perception. Decreased long-distance synchronization was also observed during the same time–frequency window. This desynchronization, however, showed a different topography, involved fewer electrode pairs, and was much less pronounced than the observed synchronization. Previous neuroimaging research has identified a distributed network of brain regions displaying increased activation during

the perception of audiovisual speech asynchrony, comprised principally of insular, prefrontal and posterior parietal regions, with a left hemisphere bias (Jones and Callan 2003; Kaiser et al. 2005; Miller and D'Esposito 2005). These regions are also activated during the detection of audiovisual asynchrony in nonspeech stimuli, indicating that they play a more general role in perceptual segregation (Bushara et al. 2001). When the network is activated by nonspeech stimuli, however, the lateralization tendencies observed during the detection of audiovisual speech asynchrony are not present. This suggests that although neural generators associated audiovisual speech segregation are an outgrowth of more general mechanisms, it is still a distinct process. The topographical pattern of increased gamma-band synchronization observed in the present study displays both a left hemisphere bias and a prefrontal-parietal orientation (Figure 6.2). This implies an anatomical similarity between the imaging activations and the increased long-range gamma-band synchrony beginning at 170 ms after onset of a perceptually incongruent stimulus. We interpret the observed increase of large-scale gamma-synchronization during incongruent percepts as indicative of the functional integration of this network of cortical areas associated with the detection of audiovisual speech synchrony. Recent evidence also gives credence to the notion that the operation of this network is associated with GBA. MEG recordings during perception of audiovisual speech incongruence have revealed significant increase of GBA beginning at about 160 ms (Kaiser et al. 2005), which is strikingly similar to the onset of gamma-synchronization reported here at 170 ms. Moreover, induced ~42 Hz activity is positively correlated with the veridical detection of auditory deviations from visual speech stimuli (Kaiser et al. 2006). Our results, together with those from the more anatomically precise measures of fMRI and

PET, give a convergent account of a functionally integrated yet distributed network of brain regions that is associated with the detection of asynchronous audiovisual speech, and that achieves transient functional integration through gamma-band phase synchronization.

It is not clear what functional role is played by the long-range desynchronization also observed for incoherent percepts during the same 170–250 ms time period. Previous research has attributed such phase scattering to the functional decoupling of neural populations (Rodriguez et al. 1999). In the context of perceptual binding by synchronization (see Engel and Singer 2001), this effect could reflect neural signals indicating that (or effecting that) the two stimulus streams are not integrated into a coherent percept.

Long-range phase synchronization between neural groups provides a mechanism for increased information transfer and provides an account of how distributed networks of brain regions are able to exhibit transient enhancement of functional connectivity (Fries 2005). One criticism of this hypothesis is that synchronous activity between brain regions could, among other causes, merely reflect the temporally cohesive nature of the stimuli themselves (see Shadlen and Movshon 1999, for a review of such criticisms). The present paper uniquely reports an increase in long-range gamma-band synchrony indicating function global synchrony associated with a functionally identified network of brain regions in the absence of both temporal synchrony in the stimulus and temporal coherence of the resulting percept.

It is not clear why no induced increases in long-range gamma-band synchrony were seen during the perception of congruent speech. A distributed network of brain areas has also been identified for the perceptual fusion of audiovisual stimuli, and transient functional integration must be achieved within this network in order to perceptually fuse congruent speech stimuli (Miller and D'Esposito 2005). Previous research has linked operational synchrony in lower frequency bands, indicative of temporal coherence between processing onsets across different cortical regions, to a large-scale network underlying perceptual fusion of audiovisual speech stimuli (Fingelkurts et al. 2003). Our results show an early increase in long-distance synchronization centered at 27 Hz was seen from 40 to 70 ms after the onset of congruent stimuli. This synchronization, however, occurs much too early to account for the perceptual fusion of complex stimuli such as speech. It is consistent, however, with evoked synchronization related to multisensory perception (Callan et al. 2001; Senkowski et al. 2007). This finding, moreover, is consistent with a burgeoning body of evidence indicating that early multimodal processing is mediated by fast interactions between primary sensory regions, although the anatomical origin of this effect cannot be confirmed in our data (Schroeder and Foxe 2005).

One possible explanation for why our study produced no evidence for a distributed network responsible for the fusion of audiovisual speech is that no such network exists. Although some fMRI studies have identified multiple locations associated with bimodal speech integration (see Miller and D'Esposito 2005), others have not. Wright and colleagues (2003), for example, conducted an fMRI study to localize bimodal speech integration areas, and failed to identify any of the brain regions implicated for

speech fusion by Miller and D'Esposito (2005) except for the STS/STG. Calvert et al. (2000) conducted a localization study using stricter criteria for a brain region to qualify as a speech fusion area, namely, (1) responsiveness to stimulation in each modality in isolation, (2) a superadditive response to congruent audiovisual speech (AV > A + V), and (3) a subadditive response to incongruent stimuli (AV < A + V). Only the STS met all of these criteria. Moreover, a single sweep EEG study lends further credence to this notion, as two components were found: STS activation peaking from about 150 to 300 ms after stimulus onset, and a distributed component spanning parietal, occipital, sensorimotor, temporal and prefrontal areas (Callan et al. 2001). This second component was attributed to a task-induced effect unrelated to the binding of audiovisual speech. These results are in accordance with the conclusion that the activity of the STS alone, not an anatomically distributed network of brain areas, is responsible for audiovisual speech integration (Calvert et al. 2000; Calvert 2001). If binding auditory and visual speech streams is accomplished largely within a single cortical region the absence of a long-range synchronization effect is unsurprising, as this measure indexes connectivity between multiple task-relevant regions.

An alternative interpretation of our results is that both congruent and incongruent audiovisual speech perception rely upon a common distributed network of brain areas. The topography and time–course of both long-range gamma-band synchronization effects, as well as the distribution of gamma-band current on the scalp, are similar (Figures 6.3a, 6.4b) in the time range of 170 to 250 ms after stimulus onset. Consider, for example, that activity from a single network governing the integration of auditory and visual speech streams produces the effects reported here. Our hypothesis was that stimuli

that were perceived as congruent would be accompanied by increased gamma-band synchronization as a result of the binding of stimulus features across modalities, and because of detection and functional integration within the distributed network of brain areas responsible for audiovisual speech integration. It is possible, however, that it is not whether the stimulus streams are effectively integrated, but rather the amount of processing needed to determine if the streams should be integrated, that determines the level of network activation in this task. Synchronization between neural populations relevant for the performance of a particular task is supposed to enable the effective transfer of information (Fries 2005). Adaptive resonance theory (e.g., Grossberg 1995) would predict that the process of constructing a multisensory perception involves reentrant processing wherein feedforward and feedback neural signals are exchanged between distributed brain regions until these areas have found a "match." In this view, reentrant information exchanges, mediated by neural synchrony, would continue until ambiguity about how the perception should be organized would be resolved. Accordingly, the amount of information exchange, and thus neural synchrony, should be higher in situations where there is greater uncertainty about whether or not stimulus features from temporally-shifted audiovisual streams should be grouped. This predicts that audiovisual streams that clearly correspond, or clearly do not correspond, should produce less synchronization then those for which this is a more difficult determination. A parabolic relationship would thus exist between the amount of temporal mismatch between the auditory and visual streams and the amount of synchronization between relevant brain areas. In light of such a theory, it may be that the incongruent stimuli presented in this study produced increased synchronization between brain areas because

more information exchange between relevant brain areas was required to determine that they were a nonmatch than was required for the determination that congruent stimuli should be grouped. This interpretation is given some credence by our behavioural data, as incongruent speech stimuli (89.8% correct) were correctly identified less frequently than were congruent stimuli (96.1% correct). Further studies, however, with consistent results over more conditions of audiovisual temporal incongruence, would be needed before it could be concluded that this explanation is to be preferred to the idea that the STS alone mediates audiovisual speech fusion.

6.6 Conclusion

We present evidence that a large-scale network of brain areas responsible for detection of temporal mismatch between audio and visual streams of speech stimuli achieves transient functional integration through gamma-band phase-synchronization. Our results provide a striking anatomical and time–course corroboration of previous findings. This work addresses a major theoretical hurdle regarding the mechanism for transient functional integration and provides an important dissociation between phase-synchronization and stimulus coherence, highlighting the functional nature of network-based synchronization.

6.7 Supplementary Material D: Synchronization at Other Frequencies

The current project's data analysis method produces a large data space. The purpose of these supplementary materials is to impress upon the reader that our data set indicates that our main effect is very robust. It can be seen in frequency bands adjacent to those shown in the main article. Since data were bandpass filtered at 1 Hz intervals and then subjected to PLV analysis results in adjacent frequency bands represent independent calculations, yet capture overlapping neural energies (bandwidth = ± 0.05 of the filtered frequency). That this effect is evidenced across multiple adjacent frequencies confirms that it did not occur by chance, but rather reflects the predicted neural response. Synchronization and desynchronization is shown for all pairs 40 – 44 Hz during the period of the burst of gamma synchronization.

44 Hz Incongruent percept

170 180 190 200 210 220 230 240 250 ms

44 Hz Congruent percept

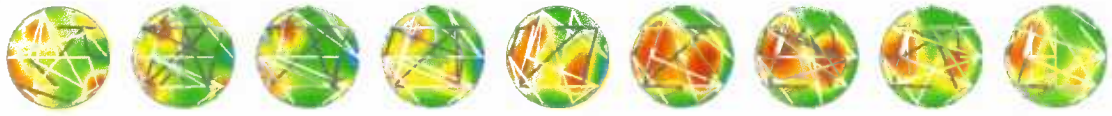

170 180 190 200 210 220 230 240 250 ms

43 Hz Incongruent percept

170 180 190 200 210 220 230 240 250 ms

43 Hz Congruent percept

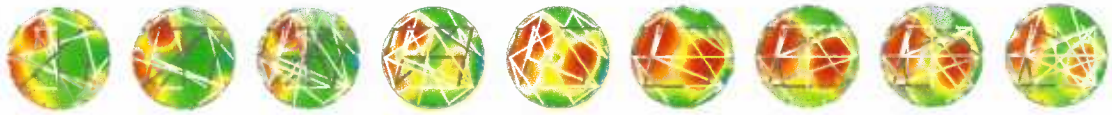

170 180 190 200 210 220 230 240 250 ms

42 Hz Incongruent percept

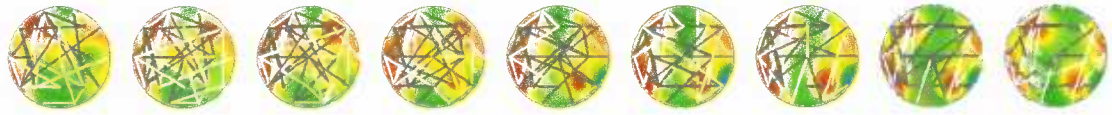

170 180 190 200 210 220 230 240 250 ms

42 Hz Congruent percept

170 180 190 200 210 220 230 240 250 ms

41 Hz Incongruent percept

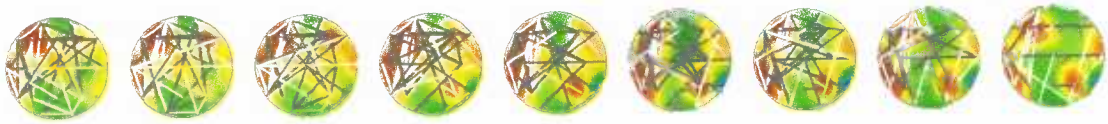

170 180 190 200 210 220 230 240 250 ms

41 Hz Congruent percept

170 180 190 200 210 220 230 240 250 ms

40 Hz Incongruent percept

170 180 190 200 210 220 230 240 250 ms

40 Hz Congruent percept

170 180 190 200 210 220 230 240 250 ms

6.8 References

Bushara KO, Grafman J, Hallet M. Neural correlates of auditory-visual stimulus onset asynchrony. J Neurosci (2001) 21(1):300–304

Callan DE, Callan AM, Kroos C, Vatikiotis-Bateson E. Multimodal contribution to speech perception revealed by independent component analysis: a single-sweep EEG case study. Cog Brain Res (2001) 10:349–353

Calvert GA, Campbell R, Brammer MJ. Evidence from functional magnetic resonance imaging of crossmodal binding in human heteromodal cortex. Curr Biol (2000) 10:649–657

Calvert GA. Crossmodal processing in the human brain: insights from functional neuroimaging studies. Cer Cortex (2001) 11:1110–1123

Canolty RT, Edwards E, Dalal SS, Soltani M, Nagarajan SS, Kirsh HE, Berger MS, Barbaro NM, Knight RT. High gamma power is phase-locked to theta oscillations in the human neocortex. Science (2006) 313:1626–1628

Delorme A, Makeig S. EEGLAB: an open source toolbox for analysis of single-trial EEG dynamics. J Neurosci Methods (2004) 134:9–21

Dixon NF, Spitz L. The detection of auditory visual desynchrony. Perception (1980) 9:719–721

Doesburg SM, Kitajo K, Ward LM. Increased gamma-band synchrony precedes switching of conscious perceptual objects in binocular rivalry. Neuroreport (2005) 16(11):1139–1142.

Eggermont JJ. Sound-induced synchronization of neural activity between and within three cortical areas. J Neurophysiol (2000) 83:2708–2722

Engel AK, Singer W. Temporal binging and the neural correlates of sensory awareness. Trends Cogn Sci (2001) 5:16–25

Fingelkurts AA, Fingelkurts AA, Krause CM, Möttönen R, Sams M. Cortical operational synchrony during audio–visual speech integration. Brain Lang (2003) 85:297–312

Ford JM, Gray M, Faustman WO, Heinks, Mathalon DH. Reduced gamma-band coherence to distorted feedback during speech when what you say is not what you hear. Int J Psychophysiol (2005) 57:143–150

Freeman WJ. Origin, structure, and role of background EEG activity. Part 1. Analytic amplitude. Clin Neurophysiol (2004) 115:2077–2088

Fries P. A mechanism for cognitive dynamics: neuronal communication through neuronal coherence. Trends Cogn Sci (2005) 9:474–479

Grossberg S. The attentive brain. Am Sci (1995) 83:483–449

Jones JA, Callan DE. Brain activity during audiovisual speech perception: an fMRI study of the McGurk effect. Neuroreport (2003) 14(8):1129–1133

Kaiser J, Hertrich I, Ackermann H, Lutzenberger W. Gamma-band activity over early sensory areas predicts detection of changes in audiovisual speech stimuli. Neuroimage (2006) 15:646–653

Kaiser J, Hertrich I, Ackermann H, Mathiak K, Lutzenberger W. Hearing lips: gamma-band activity during audiovisual speech perception. Cer Cortex (2005) 15:646–653

Kanayama N, Sato A, Ohira H. Crossmodal effect with rubber hand illusion and gamma-band activity. Psychophysiol (2007) 44: 392–402

King AJ. Multisensory integration: strategies for synchronization. Curr Biol (2005) 15(9):R339–R341

Lachaux JP, Rodriguez E, Martinerie J, Varela FJ. Measuring phase synchrony in brain signals. Hum Brain Mapp (1999) 8(4):94–208

Lewkowicz DJ. Perception of auditory–visual temporal synchrony in human infants. J Exp Psychol: Hum Percept Perform (1996) 22(5):1194–1106

McGurk H, MacDonald J. Hearing lips and seeing voices. Nature (1975) 264:746–748

Miller LM, D'Esposito M. Perceptual fusion and stimulus coincidence in the cross-modal integration of speech. J Neurosci (2005) 25(25):5884–5893

Perrin F, Bertrand O, Pernier J. Scalp current density mapping: value and estimation from potential data. IEEE Trans Biomed Eng BME (1987) 34:283–288

Pikovski A, Rosenblum M, Kurths J. Synchronization: a universal concept in nonlinear sciences. (2001) Cambridge University Press, Cambridge 432 p

Rodriguez E, George N, Lachaux JP, Martinirie J, Renault B, Varela FJ. Perception's shadow: long-distance synchronization of human brain activity. Nature (1999) 397:430–433

Schroeder E, Foxe J. Multisensory contributions to low-level "unisensory" processing. Curr Opin Neurobiol (2005) 6(4):285–296

Senkowski D, Talsma D, Grigutsch M, Herrmann CS, Woldorff M. Good times for multisensory integration: effects of the precision of temporal synchrony as revealed by gamma-band oscialltions. Neuropsychologia (2007) 45(3):561–571

Senkowski D, Talsma D, Herrmann CS, Woldorff M. Multisensory processing and oscillatory gamma responses: effects of spatial selective attention. Exp Brain Res (2005) 166:411–426

Shadlen MN, Movshon JA. Synchrony unbound: a critical evaluation of the temporal binding hypothesis. Neuron (1999) 24:67–77

Tallon-Baudry C, Bertrand O. Oscillatory gamma activity in human and its role in object representation. Trends Cogn Sci (1999) 3(4):151–162

Varela F, Lachaux JP, Rodriguez E, Martinerie J. The brainweb: phase synchronization and large-scale integration. Nat Rev Neurosci (2001) 2(4):229–239

von Stein A, Sarnthein J. Different frequencies for different scales of cortical integration: from local gamma to long range alpha/theta. (2000) Int J Psychophysiol 38(3):301–313

Ward LM. Synchronous neural oscillations and cognitive processes. Trends Cogn Sci (2003) 17:553–559

Wright TM, Pelphrey KA, Allison T, McKeown MJ, McCarthy G. Polysensory interaction along temporal regions evoked by audiovisual speech. Cer Cortex (2003) 13:1034–1043

Yuval-Greenberg S, Deouell LY. What you see is not (always) what you hear: induced gamma band responses reflect cross-modal interactions in familiar object recognition. J Neurosci (2007) 27(5):1090–1096

CHAPTER 7: CONCLUSION

7.1 A Summary of the Thesis

The works presented in this monograph, taken together, provide an account of how neural oscillations contribute to selective attention and perceptual consciousness. A consistent view of the roles of oscillatory synchronization in particular frequency bands emerges, as well as the relationship between oscillations across various spectral bands, and across local and long distance scales. The hypothesis that long-range phase synchronization between cortical regions is a mechanism for transient functional coupling is supported. Our view of the relationship between neural synchrony, selective attention and perceptual consciousness is now more refined, however, as it is becoming clearer how synchronization at different frequencies and scales act in concert to organize neural activity to support these processes.

The studies presented here provide evidence for the hypothesis that long-distance gamma-band phase synchronization is a mechanism underlying the dynamic assignment of functional connectivity in the human brain. The experiments addressing selective visuospatial attention, the emergence of a new percept on binocular rivalry, and the detection of audiovisual asynchrony in speech stimuli all speak to this point, as well as providing experimental basis for additional important theoretical refinements. First, it is now abundantly clear that although long-distance gamma-band synchronization among a network of task relevant brain areas may be responsible for setting up a large-scale neural assembly, it is certainly not responsible for maintaining such an assembly as long as it is required. This is evidenced by the short-lived nature of such synchronization effects.

Secondly, our analysis of long-distance gamma-band synchronization in audiovisual speech processing reveals a key distinction. Synchronously oscillating neural populations are biased for functional integration, but neural integration does not always entail perceptual integration. This distinction has perhaps been glossed over in previous manifestations of the theory. Since perceptual binding requires integration between select neural populations, this has been interpreted to mean that greater perceptual integration will always be accompanied by greater neural synchronization (for example, Engel and Singer 1991; Varela et al. 1991). The work presented here provides a dissociation between perceptual integration and integration within in a large-scale network of cooperating brain areas.

If long-distance gamma-band neural synchronization is capable of establishing a transient functional assembly of neural populations, but not maintaining it, how can the integration-by-synchronization hypothesis account for situations where a perceptual or attentional state is maintained over a period of time? Our results on selective visuospatial attention and coherent perception in binocular rivalry indicate that long-range theta rhythms are involved in accomplishing this. Specifically, it appears that the transient bursts of long distance synchronization recur at a theta rate. Such results imply that theta waves may be acting as a carrier frequency for gamma oscillations. This is consistent with the theoretical postulation that low frequency carriers will be required to maintain the organization of gamma synchronous assemblies due to the longer conduction delays involved in large-scale gamma-synchronous assemblies (von Stein and Sarnthein 2002). One potential problem with a system that maintains its state using a mechanism with distinct periodic windows in which a new constellation of neural populations can be

organized (ie a new gamma oscillatory complex may only arise once per theta cycle) is that a 'speed limit' is placed upon network dynamics, as are particular intervals in time during which such a cyclical system is not disposed to being reorganized. This may explain the attentional blink phenomenon, wherein the rapid serial presentation of stimuli causes stimuli to not be perceived. In this view, rapid presentation of stimuli at a rate faster than the theta carrier cycle will cause some stimuli to not receive sufficient integration into the next gamma synchronous assembly and consequently not be perceived (see Fell et al. 2002 for review).

It stands to reason that if the theta modulated gamma mechanism has inherent blind spots, or windows in time during which certain stimuli might be missed, that other mechanisms might be required that do not suffer from such drawbacks, at least for certain tasks. The results presented here on the role of long-range alpha band synchronization help to address this. During the time period preceding the appearance of an expected visual target, greater alpha-band synchronization is seen between primary visual cortex and parietal cortex contralateral to the attended visual hemifield. Since alpha oscillations do not appear to be directly involved in a cyclical reorganization of high-frequency oscillations, they are better suited for sustained functional coupling as needed in the anticipatory biasing of the cortex for selective attention. Occipital-parietal alpha synchronization observed here also occurred at a considerably faster rate than theta oscillations, which means that there is less time between one cycle and the next which theoretically entails a much shorter window between cycles of information exchange.

Interestingly, our work shows that long-distance alpha-band synchronization is greater between occipital and parietal cortex *contalateral* to the attended visual hemifield, local alpha activity is greater in visual cortex *ipsilateral* to the locus of visual attention. This result demonstrates a dissociation between the functional role of alpha oscillations at different scales of measurement. Our data are consistent with notions that although local alpha synchronization is relevant for inhibition, synchronization of alpha rhythms across long distance scales indexes functional coupling between brain regions (Palva and Palva 2007; Klimesch et al. 2007). Moreover, observed alpha synchronization effects occur in temporal coordination with changes in frequency bands, suggesting that these mechanisms act in concert during attentional processing.

In summary, the work presented here indicates that long-distance gamma-band phase synchronization is responsible for establishing a new task or percept dependant network of neural populations, and that the maintenance of such a network is governed by the periodic reintegration of those neural populations according to a theta cycle. Long-distance alpha-band synchronization may function to couple attention control areas to primary sensory cortex representing attended locations, accounting for the enhanced processing that targets appearing at attended locations receive. Local alpha oscillations, conversely, appear relevant for inhibition of to-be-ignored information, revealing a functional dissociation between local and long range synchronization in the alpha band. As a whole, these studies provide a sharper view of how synchronous neural oscillations in various frequency bands, and across local and long distance scales, contribute to selective attention and perceptual consciousness.

7.2 Implications, Limitations, and Future Directions

The present work makes inroads into accounting for how neural synchronization between specific cortical regions relates to dynamic cognitive networks. A limitation of data presented here addressing synchronization between localized brain activations, however, is that these sources represent reconstruction of activity within a fairly narrow frequency range (8-15 Hz in Chapter 3B; 4-7 Hz in Chapter 4). A major implication of the results presented in this dissertation is that oscillatory network dynamics involve coordinated activity across multiple frequency ranges and across local and long-distance scales. Calculation of synchronization between narrow-band sources might not reveal all of the relevant sources of neural activation in a particular task (i.e. a theta weighted breamformer analysis might not reveal sources of local power change centred in other frequency ranges). To address this, further studies need to be conducted using source reconstruction techniques which account for a broader bandwidth of brain activity. Event related synthetic aperture magnetometry (erSAM) is an excellent candidate for this (e.g. Herdman et al. 2003). Alternatively, multiple narrowband beamformer source reconstructions could be performed on a single data set in order to image sources of activation in all relevant frequency bands. Application of phase locking analysis to each of these source solutions could more thoroughly illuminate the relationships between oscillatory synchronization at different scales and in various frequency windows.

The work presented here buttresses the view that synchronization of brain rhythms across distant cortical regions promotes information exchange within a task-relevant network of brain regions. This entails that greater long-range synchronization

between brain regions increases the causal influence of one area's activity on the activity of another brain region. Such influence, however, can be bidirectional or unidirectional. For example, it has been shown that when human subjects recognize a familiar object greater local gamma-band EEG activation and long-distance gamma-band EEG synchronization is observed, relative to when an unfamiliar object is perceived (Gruber et al. 2003). Source reconstruction of gamma activation in this paradigm reveals a common, anatomically plausible, network of brain regions in both conditions and that the gamma-band source power, as well as gamma-band phase locking between sources, is greater when a familiar object is recognized (Supp et al. 2007). Furthermore, partial directed coherence analysis indicates that when a familiar object is recognized causal influence between certain brain regions is bidirectional, whereas when an unfamiliar object is perceived causation is unidirectional (Supp et al. 2007). It is important to note that statistically significant phase synchronization is seen between these sources in both experimental conditions, thus phase synchronization can detect causal influence between brain regions but cannot discern its direction. Adaptive Resonance Theory (ART) proposes that during perception and cognition cortical areas representing hierarchically organized processing stages engage in cyclical information exchange between lower and higher areas until a stable representation is achieved through elimination of the 'error signal' between those areas (Grossberg 1999). In the context of ART, it seems plausible that task-dependant neural synchronization between brain regions may in some cases represent unidirectional or feed-forward influence amongst brain regions, while in other instances represent a cyclical exchange of information between areas participating in a task-dependant network. These two possibilities lead to very different interpretations. In

the former case, each area would be acting relatively unilaterally to perform a particular stage of processing and then passing its finished results to the next relevant area. In the latter instance, conversely, processing is much more distributed as resolution at one stage depends on continual feedback from higher areas. To distinguish between these possibilities new experiments need to be conducted in which analysis of causality is used to compliment the calculation of phase synchronization between reconstructed sources of electrical or magnetic brain activation.

Results such as those presented in this monograph entail that long-range synchronization is relevant for the transient reorganization of cortical network dynamics. There is considerable ambiguity, however, regarding how it is that connectivity is being affected in terms of the precise organization of cycles across distant regions. The most widely held understanding of this mechanism is that synchronously oscillating neurons (or neural populations) are able to consistently exchange bursts of action potentials that will be received during the depolarized phase of the target neuron's ongoing membrane potential fluctuation (Fries 2005). When this is occurring across some distance a phase delay between two synchronously oscillating neural populations would be expected due to a conduction delay. Magnetoencephalograpic imaging of task-dependent coherence in the human motor system lends support to this view (Schnitzler et al. 2006). It a study of synchronization between electrodes implanted in cats, however, it was found that task-dependent coherence between visual and motor cortex occurred with zero phase delay (Roelfsema et al. 1997). Interhemispheric zero-phase-lag stimulus-dependent gamma-band coherence has also been observed using electrodes implanted in cat primary visual cortex, and this coherence is destroyed when the corpus callosum is severed (Engel et al.

1991). It is possible that such effects are due to a mechanism wherein the synchronization of these oscillations is being organized by carrier frequency. In such a scenario it could be the case that an observed zero phase lag is actually a 360° phase delay wherein the two oscillating neural populations receive information sent on a previous cycle, possibly being transferred through an intermediary brain region. The resolution of such issues will require future studies focusing on the relationship of phase delays to oscillatory synchronization, and how such phase delays relate to interactions between synchronization in different frequency ranges.

In short, future study of neural synchronization and human brain dynamics will require a combination of phase synchronization with source reconstruction approaches that provide a more complete account of activation across multiple relevant frequency ranges, and application of further analysis techniques, such as those indexing causality and phase delays, to these data sets. The goal of such future work would be the integration of human brain synchronization results into our understanding of the mechanics of the cortex at lower levels of analysis and moving toward unification of our knowledge of large-scale dynamics with our understanding of smaller scale network activity and cellular mechanisms.

7.3 References

Engel AK, König P, Kreiter AK, Singer W. Interhemispheric synchronization of oscillatory neuronal responses in cat visual cortex. Science (1991) 252:1177–1179.

Engel AK and Singer W. Temporal binding and the neural correlates of sensory awareness. Trends Cog Sci (2001) 5:16-25

Fell J, Klaver P, Elger CE, Fernández G. Suppression of EEG gamma activity may cause the attentional blink. Conscious Cogn (2002) 11(1):114–122

Fries P. A mechanism for cognitive dynamics: neuronal communication through neuronal coherence. Trends Cogn Sci (2005) 9:474–479.

Grossberg S. The link between learning, attention, and consciousness. Conscious Cogn (1999) 8(1):1–44

Gruber T, Müller MM, Keil A. Modulation of induced gamma band responses in a perceptual learning task in the human EEG. J Cogn Neurosci (2002) 14(5):732–744.

Herdman AT, Wollbrink A, Chau W, Ishii R, et al. Determination of activation areas in the human auditory cortex by means of synthetic aperture magnetometry. Neuroimage (2003) 20(2):995–1005

Klimesch W, Sauseng P, Hanslmayer S. EEG alpha oscillations: the inhibition timing hypothesis. Brain Res Rev (2007) 53(1):63–88

Palva S, Palva JM. New vistas for alpha-frequency band oscillations. Trends Neurosci (2007) 30(4):150–158

Roelfsema PR, Engel AK, König P, Singer W. Visuomotor integration is associated with zero time-lag synchronization among cotical areas. Nature (1997) 385(6612):157–161.

Schnitzler A, Timmermann L, Gross J. Physiological and pathological oscillatory networks in the human motor system. J Physiol Paris (2006) 99:3–7

Supp GG, Schlögl A, Trujillo-Barreto N, Müller MM, Gruber T. Directed cortical information flow during human object recognition: analyzing induced EEG gamma-band responses in brain's source space. PLoS ONE (2007) 2(1):e684.

Varela F, Lachaux JP, Rodriguez E, Martinierie J. The brainweb: phase synchronization and large-scale integration. Nat Rev Neurosci (2001) 2(4):229–239

von Stein A, Sarnthein J. Different frequencies for different scales of cortical integration: from local gamma to long range alpha/theta synchronization. Int J Psychophysiol (2000) 38:301–313

The University of British Columbia
Office of Research Services and Administration
Behavioural Research Ethics Board

Certificate of Approval

PRINCIPAL INVESTIGATOR	DEPARTMENT	NUMBER
Ward, L.M.	Psychology	**B00-0505**

INSTITUTION(S) WHERE RESEARCH WILL BE CARRIED OUT:
UBC Campus ,

CO-INVESTIGATORS:

SPONSORING AGENCIES:
Natural Science Engineering Research Council

TITLE:
Fundamental Psychophysics and Attention

APPROVAL RENEWED DATE:	TERM (YEARS):	AMENDMENT:	AMENDMENT APPROVED:
[illegible]	1	Sept. 15, 2004, Consent Form	[illegible]

CERTIFICATION:

The protocol describing the above-named project has been reviewed by the Committee and the experimental procedures were found to be acceptable on ethical grounds for research involving human subjects.

Approval of the Behavioural Research Ethics Board by one of the following:
Dr. James Frankish, Chair,
Dr. Cay Holbrook, Associate Chair,
Dr. Susan Rowley, Associate Chair
Dr. Anita Hubley, Associate Chair

This Certificate of Approval is valid for the above term provided there is no change in the experimental procedures

The University of British Columbia
Office of Research Services and Administration
Behavioural Research Ethics Board

Certificate of Approval

PRINCIPAL INVESTIGATOR	DEPARTMENT	NUMBER
Ward, L.M.	Psychology	**B00-0505**

INSTITUTION(S) WHERE RESEARCH WILL BE CARRIED OUT

UBC Campus ,

CO-INVESTIGATORS:

SPONSORING AGENCIES

Natural Science Engineering Research Council

TITLE :

Neural Synchrony and Cognitive Processes

APPROVAL DATE	TERM (YEARS)	AMENDMENT	AMENDMENT APPROVED
04-09-27 (yr/mo/day)	1	April 29, 2005, title	

CERTIFICATION:

The protocol describing the above-named project has been reviewed by the Committee and the experimental procedures were found to be acceptable on ethical grounds for research involving human subjects.

Approval of the Behavioural Research Ethics Board by one of the following:
Dr. James Frankish, Chair,
Dr. Cay Holbrook, Associate Chair,
Dr. Susan Rowley, Associate Chair
Dr. Anita Hubley, Associate Chair

This Certificate of Approval is valid for the above term provided there is no change in the experimental procedures

The University of British Columbia
Office of Research Services and Administration
Behavioural Research Ethics Board

Certificate of Approval

PRINCIPAL INVESTIGATOR	DEPARTMENT	NUMBER
Ward, L.M.	Psychology	**B00-0505**

INSTITUTION(S) WHERE RESEARCH WILL BE CARRIED OUT

UBC Campus ,

CO-INVESTIGATORS:

SPONSORING AGENCIES

Natural Science Engineering Research Council

TITLE :

Neural Synchrony and Cognitive Processes

APPROVAL RENEWED DATE	TERM (YEARS)	
SEP 15 2005	1	

CERTIFICATION:

The protocol describing the above-named project has been reviewed by the Committee and the experimental procedures were found to be acceptable on ethical grounds for research involving human subjects.

Approval of the Behavioural Research Ethics Board by one of the following:
Dr. Peter Suedfeld, Chair,
Dr. Susan Rowley, Associate Chair

This Certificate of Approval is valid for the above term provided there is no change in the experimental procedures